EXHIBIT 28

Analyses and Historical Reconstruction of Groundwater Flow, Contaminant Fate and Transport, and Distribution of Drinking Water Within the Service Areas of the Hadnot Point and Holcomb Boulevard Water Treatment Plants and Vicinities, U.S. Marine Corps Base Camp Lejeune, North Carolina

Chapter A–Supplement 6
Characterization and Simulation of Fate and Transport of Selected Volatile Organic Compounds in the Vicinities of the Hadnot Point Industrial Area and Landfill

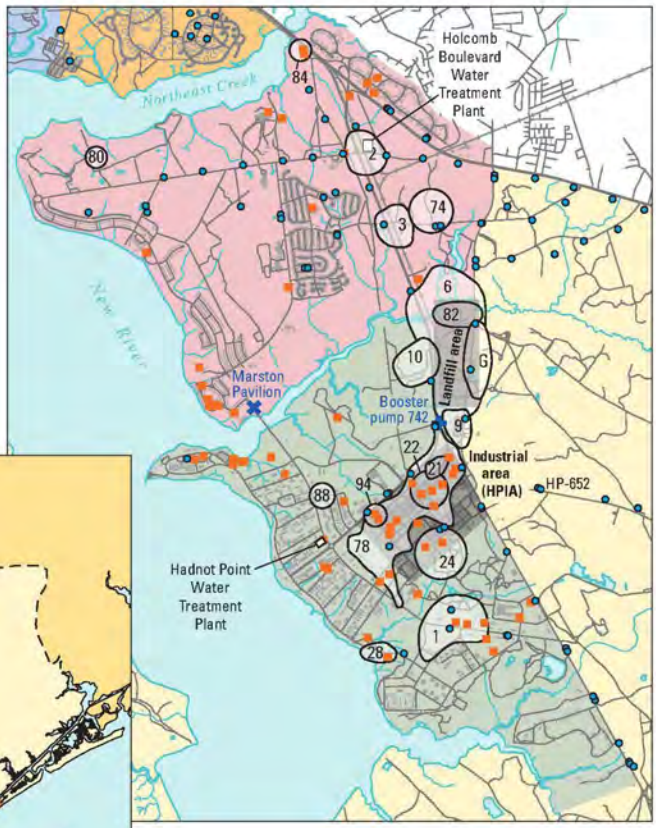

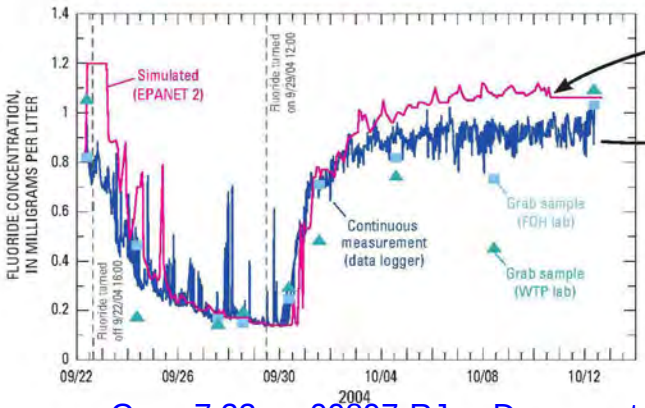

ATSDR
AGENCY FOR TOXIC SUBSTANCES AND DISEASE REGISTRY

Atlanta, Georgia – March 2013

Front cover: Historical reconstruction process using data, information sources, and water-modeling techniques to estimate historical contaminant concentrations.

Maps: U.S. Marine Corps Base Camp Lejeune, North Carolina; Holcomb Boulevard and Hadnot Point areas showing extent of sampling at Installation Restoration Program sites (white numbered areas), above-ground and underground storage tank sites (orange squares), and water-supply wells (blue circles).

Photograph (upper): Hadnot Point water treatment plant (Building 20).

Photograph (lower): Well house building for water-supply well HP-652.

Graph: Measured fluoride data and simulation results for Paradise Point elevated storage tank (S-2323) for tracer test of the Holcomb Boulevard water-distribution system, September 22–October 12, 2004; simulation results obtained using EPANET 2 water-distribution system model assuming last-in first-out plug flow (LIFO) storage tank mixing model. [WTP lab, water treatment plant water-quality laboratory; FOH lab, Federal Occupational Health Laboratory]

Analyses and Historical Reconstruction of Groundwater Flow, Contaminant Fate and Transport, and Distribution of Drinking Water Within the Service Areas of the Hadnot Point and Holcomb Boulevard Water Treatment Plants and Vicinities, U.S. Marine Corps Base Camp Lejeune, North Carolina

Chapter A–Supplement 6
Characterization and Simulation of Fate and Transport of Selected Volatile Organic Compounds in the Vicinities of the Hadnot Point Industrial Area and Landfill

By L. Elliott Jones, René J. Suárez-Soto, Barbara A. Anderson, and Morris L. Maslia

Agency for Toxic Substances and Disease Registry
U.S. Department of Health and Human Services
Atlanta, Georgia

March 2013

Authors

L. Elliott Jones, MS, PE
Hydrologist and Groundwater Specialist
U.S. Geological Survey
Georgia Water Science Center
Norcross, Georgia

René J. Suárez-Soto, MSEnvE, EIT
Environmental Health Scientist
Agency for Toxic Substances and Disease Registry
Division of Community Health Investigations
Atlanta, Georgia

Barbara A. Anderson, MSEnvE, PE
Environmental Health Scientist
Agency for Toxic Substances and Disease Registry
Division of Community Health Investigations
Atlanta, Georgia

Morris L. Maslia, MSCE, PE, D.WRE, DEE
Research Environmental Engineer and Project Officer
Agency for Toxic Substances and Disease Registry
Division of Community Health Investigations
Exposure-Dose Reconstruction Project
Atlanta, Georgia

For additional information write to:

Project Officer
Exposure-Dose Reconstruction Project
Division of Community Health Investigations
Agency for Toxic Substances and Disease Registry
4770 Buford Highway, Mail Stop F-59
Atlanta, Georgia 30341-3717

Suggested citation

Jones LE, Suárez-Soto RJ, Anderson BA, and Maslia ML. Characterization and Simulation of Fate and Transport of Selected Volatile Organic Compounds in the Vicinities of the Hadnot Point Industrial Area and Landfill—Supplement 6. In: Maslia ML, Suárez-Soto RJ, Sautner JB, Anderson BA, Jones LE, Faye RE, Aral MM, Guan J, Jang W, Telci IT, Grayman WM, Bove FJ, Ruckart PZ, and Moore SM. Analyses and Historical Reconstruction of Groundwater Flow, Contaminant Fate and Transport, and Distribution of Drinking Water Within the Service Areas of the Hadnot Point and Holcomb Boulevard Water Treatment Plants and Vicinities, U.S. Marine Corps Base Camp Lejeune, North Carolina—Chapter A: Summary and Findings. Atlanta, GA: Agency for Toxic Substances and Disease Registry; 2013.

Contents

Figures

Appendix Figures Graphs showing—

Tables

Appendix Table

Conversion factors and definitions of common terms and abbreviations used throughout the Chapter A report series are listed in the front of the Chapter A report.

Use of trade names and commercial sources is for identification only and does not imply endorsement by the Agency for Toxic Substances and Disease Registry, the U.S. Department of Health and Human Services, or the U.S. Geological Survey.

Analyses and Historical Reconstruction of Groundwater Flow, Contaminant Fate and Transport, and Distribution of Drinking Water Within the Service Areas of the Hadnot Point and Holcomb Boulevard Water Treatment Plants and Vicinities, U.S. Marine Corps Base Camp Lejeune, North Carolina

Chapter A–Supplement 6

Characterization and Simulation of Fate and Transport of Selected Volatile Organic Compounds in the Vicinities of the Hadnot Point Industrial Area and Landfill

By L. Elliott Jones,[1] René J. Suárez-Soto,[2] Barbara A. Anderson,[2] and Morris L. Maslia[2]

Introduction

This supplement of Chapter A (Supplement 6) describes the reconstruction (i.e., simulation) of historical concentrations of tetrachloroethylene (PCE), trichloroethylene (TCE), and benzene[3] in production wells supplying water to the Hadnot Point water treatment plant (HPWTP) at U.S. Marine Corps Base (USMCB) Camp Lejeune, North Carolina (Figure S6.1). A fate and transport model (i.e., MT3DMS [Zheng and Wang 1999]) was used to simulate contaminant migration from source locations through the groundwater system and to estimate monthly mean contaminant concentrations in water withdrawn from water-supply wells in the vicinity of the Hadnot Point Industrial Area (HPIA) and the Hadnot Point landfill (HPLF) area.[4] The reconstructed contaminant concentrations were subsequently input into a flow-weighted, materials mass balance (mixing) model (Masters 1998) to estimate monthly mean concentrations of the contaminants in finished water[5] at the HPWTP (Maslia et al. 2013). The calibrated fate and transport models described herein were based on and used groundwater velocities derived from groundwater-flow models that are described in Suárez-Soto et al. (2013). Information and data pertinent to historical operations of water-supply wells are described in Sautner et al. (2013) and Telci et al. (2013).

---

[1] U.S. Geological Survey, Georgia Water Science Center, Norcross, Georgia.

[2] Agency for Toxic Substances and Disease Registry, Atlanta, Georgia.

[3] Chapter A–Supplement 6 (this supplement) focuses solely on analyses and simulation of benzene dissolved in groundwater. For analyses and simulation of benzene characterized as a light nonaqueous phase liquid (LNAPL), refer to Jang et al. (2013).

[4] The Hadnot Point Industrial Area (HPIA) is a formally designated name and acronym used in many Camp Lejeune references (e.g., Baker Environmental, Inc. [1994], CH2M HILL [2006]), and the ATSDR Hadnot Point–Holcomb Boulevard Chapter reports and Chapter A supplements follow this naming convention. The acronym HPLF is used in the ATSDR Hadnot Point–Holcomb Boulevard report series for brevity and convenience to identify the Hadnot Point landfill.

[5] For this study, finished water is defined as groundwater that has undergone treatment at a water treatment plant and was subsequently delivered to a family housing unit or other facility. Throughout this report and the Hadnot Point–Holcomb Boulevard report series, the term finished water is used in place of terms such as finished drinking water, drinking water, treated water, or tap water.

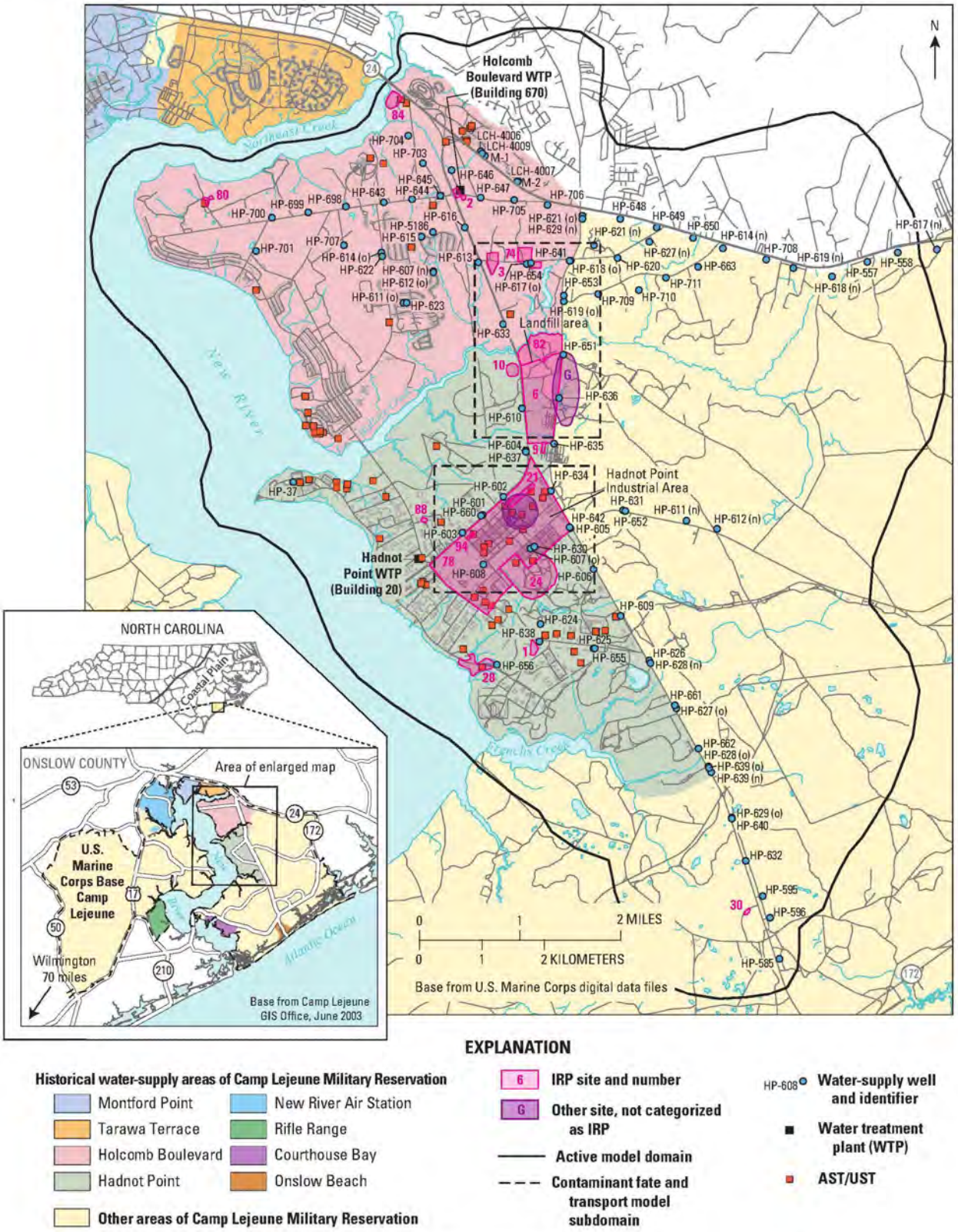

Figure S6.1. Groundwater-flow model domain, contaminant fate and transport model subdomains, Installation Restoration Program (IRP) and above-ground and underground storage tank (AST/UST) sites, and water-supply wells, Hadnot Point–Holcomb Boulevard study area, U.S. Marine Corps Base Camp Lejeune, North Carolina.

Background

USMCB Camp Lejeune is located in the Coastal Plain of North Carolina, in Onslow County, south of the City of Jacksonville and about 70 miles northeast of the City of Wilmington, North Carolina (Figure S6.1). The area of investigations is inclusive of the HPWTP and Holcomb Boulevard water treatment plant (HBWTP) service areas, hereafter called the study area or the Hadnot Point–Holcomb Boulevard (HPHB) study area. In general, the study area is bordered on the north by Northeast Creek and North Carolina Highway 24 (SR24), to the west by New River, to the south by Frenchs Creek, and generally to the east by the drainage divides of the upstream tributaries of Wallace Creek and Frenchs Creek. Total study area is approximately 50 square miles (mi^2).

Eight water-distribution systems have supplied or currently (2013) are supplying finished water to family housing and other facilities at USMCB Camp Lejeune, North Carolina. The three water-distribution systems of interest to this study—Tarawa Terrace (TT), Hadnot Point (HP), and Holcomb Boulevard (HB)—historically supplied finished water to a majority of family housing at USMCB Camp Lejeune. Two of the three water-distribution systems were contaminated with volatile organic compounds (VOCs). Groundwater supplied to the Tarawa Terrace water treatment plant (TTWTP), and subsequently to TT housing areas and other facilities, was contaminated with PCE and related degradation products such as TCE and vinyl chloride (VC). Similarly, groundwater supplied to the HPWTP was contaminated with TCE, as well as PCE and refined petroleum products such as benzene, toluene, ethylbenzene, and xylenes (BTEX). Groundwater supplied to the HBWTP was mostly uncontaminated (Faye et al. 2010, Tables C11–C12), except for the intermittent transfers of contaminated Hadnot Point finished water to the Holcomb Boulevard water-distribution system during 1972–1985 (Maslia et al. 2013).

The HPWTP was constructed probably during 1941 and 1942, along with much of the original infrastructure of USMCB Camp Lejeune. Construction of the HBWTP was completed during the summer of 1972 (Scott A. Brewer, USMCB Camp Lejeune, written communication, September 29, 2005).[6] For the period of interest to this study (1942–2008), 96 water-supply wells have historically or are currently (2013) providing groundwater to the HPWTP and HBWTP (Sautner et al. 2013; Telci et al. 2013). The operational chronology of water-supply wells during the period of interest to the study (1942–2008) is shown in Figure A5[7] (Maslia et al. 2013) and is discussed in detail in Sautner et al. (2013).

Conceptual Models

Conceptual models for groundwater flow and contaminant migration are used as the bases to develop, apply, and calibrate complex numerical models that simulate groundwater flow and contaminant fate and transport within the HPHB study area. For groundwater flow, the conceptual model is described in detail in Faye et al. (2013); a related numerical model is described in detail in Suárez-Soto et al. (2013) and is briefly summarized below. Following that summary, a detailed description of the conceptual model of contaminant migration, which includes a discussion of contaminant sources and histories is presented.

Groundwater Flow

Conceptualization, development and calibration of a three-dimensional groundwater-flow model, used as the basis for the fate and transport model is described by Suárez-Soto et al. (2013). Briefly, the groundwater-flow model simulates the flow of groundwater from its source as recharge from precipitation, into the uppermost aquifer—the Brewster Boulevard upper aquifer—through the underlying aquifers—including the Tarawa Terrace and the Upper and Middle Castle Hayne aquifers (Table S6.1)—to discharge locations at water-supply or remediation wells, New River, or various tributaries of New River. The model area is bounded to the north, east, and south by topographic divides at the headwaters of the drainage areas of the north flowing tributaries of Northeast Creek, Wallace Creek, and Frenchs Creek, and to the west by New River (Figure S6.1).

Contaminant Migration

Contaminant migration is limited to PCE, TCE, and benzene within the HPIA and the HPLF area (Figure S6.1). Conceptually, it is assumed that hydraulic-head gradients are the only mechanism for fluid flow and that Darcy's law is valid, chemical reactions do not affect fluid or aquifer properties, and a contaminant dissolves in groundwater such that there are no density effects.

Using site and building history, contaminant data, and remediation efforts described in Faye et al. (2010, 2012), contaminant sources that potentially affected water-supply wells were identified and are listed in Table S6.2. Sources with sufficient supporting documentation were included in the conceptual and numerical models and are described hereafter.

[6] Based on information contained in the written communication from USMCB Camp Lejeune, the start of continuous operations at the HBWTP is estimated to be about June 1972.

[7] References to figures, tables, or appendixes in the Chapter A report (e.g., Figure A1) are found in Maslia et al. (2013).

Table S6.1. Correlation between geologic and hydrogeologic units and model layers, Hadnot Point–Holcomb Boulevard study area, U.S. Marine Corps Base Camp Lejeune, North Carolina.

[—, not applicable]

[1]Geologic units			[1]Hydrogeologic units	[1]Thickness	[2]Model layer number
System	Series	Formation	Aquifer and confining unit	Range, in feet	
Quaternary	Holocene Pleistocene	Undifferentiated	Brewster Boulevard upper aquifer	4 to 42	1
Tertiary	Pliocene	Absent	Absent	Absent	
	Miocene	Pungo River Formation, undifferentiated	Brewster Boulevard upper confining unit	1 to 22	
			Brewster Boulevard lower aquifer	4 to 48	
		Belgrade Formation, undifferentiated	Brewster Boulevard lower confining unit	2 to 30	2
			Tarawa Terrace aquifer (upper part)	8 to 86	3
	Oligocene	River Bend Formation, undifferentiated	Tarawa Terrace aquifer (middle and lower parts)		
			Upper Castle Hayne confining unit (previously designated the Tarawa Terrace confining unit in Faye [2007])	4 to 40	4
	Late Eocene	Unnamed	Upper Castle Hayne aquifer–River Bend unit	16 to 70	5
		Castle Hayne Formation	Local confining unit	8 to 23	
			Upper Castle Hayne aquifer–Lower unit	10 to 48	
	Middle Eocene		Middle Castle Hayne confining unit	12 to 27	6
			Middle Castle Hayne aquifer	62 to 122	7
			Lower Castle Hayne confining unit	18 to 38	Base of model
			Lower Castle Hayne aquifer	64 to 86	
	Paleocene	Beaufort Formation, undifferentiated	Beaufort confining unit (generally occurs at top of Beaufort Formation)	—	

[1] From Faye (2012)

[2] From Suárez-Soto et al. (2013)

Table S6.2. Inventory of potential contaminant-source areas in the vicinity of historically contaminated water-supply wells, Hadnot Point–Holcomb Boulevard study area, U.S. Marine Corps Base Camp Lejeune, North Carolina.

[AST/UST, above-ground storage tank/underground storage tank; IRP, Installation Restoration Program; PCE, tetrachloroethylene; TCE, trichloroethylene; HPFF, Hadnot Point fuel farm; Bldg, Building; J, laboratory qualifier indicating concentration was estimated]

[1]Historically contaminated water-supply wells	Sample dates	Contaminants detected	Number of detections/ number of analyses	Statistics for detected concentrations, in micrograms per liter					Potential source locations	
				Minimum	25th percentile	50th percentile	75th percentile	Maximum	[2]AST/UST sites	[3]IRP sites (source areas)
Hadnot Point Industrial Area (HPIA)										
HP-602	7/1984–1/1991	Benzene PCE TCE	6/8 3/8 7/8	17 1.5 0.7J	67.5 2.4 20.1	175 3.2 300	342.5 13.6 440	720 24 1,600	HPFF, Bldg 1115, Bldg 1101	Site 78 (Bldg 901/902 area), Site 21
HP-603	12/1994–9/1995	TCE	3/7	1.0J	2.0	3.0	3.8	4.6J	Bldg 1613, Bldg 61, Bldg 1502, Bldg 1601, Bldg 1607	Site 78 (Bldg 1601), Site 94
HP-608	12/1984–11/1986	Benzene TCE	3/4 4/4	1.6 9.0	2.7 12	3.7 39.5	3.9 77	4 110	Bldg 1601, Bldg 1502, Bldg 1607, Bldg S1856	Site 78 (Bldg 1601), Site 24
HP-634	12/1984–1/1991	PCE TCE	1/5 1/5	10 1,300	10 1,300	10 1,300	10 1,300	10 1,300	Bldg 738, Bldg 900, Bldg 903	Site 78 (Bldg 901/902 area), Site 21
HP-660	12/1984–1/1991	PCE TCE	2/5 4/5	4.4 1.0J	4.6 19.8	4.7 118	4.9 215	5.0 230	Bldg 1115, Bldg 1401, Bldg 1502, Bldg 1601, Bldg 1613	Site 78 (Bldg 1601), Site 94
Hadnot Point landfill area (HPLF)										
HP-651	1/1985–1/1991	PCE TCE	5/5 5/5	45 13	53 32	307 3,200	386 17,600	400 18,900	Unknown	Site 6, Site 82
HP-653	1/1985–1/1991	TCE	2/3	2.6	3.3	4.1	4.8	5.5	Unknown	Unknown
HP-610	2/1985–10/1992	TCE	1/2	37	37	37	37	37	Unknown	Site 6
HP-645 area										
HP-645	11/1986–2/1987	Benzene	2/3	20	87.5	155	222.5	290	Bldg 645, Bldg 40	Site 2
Other areas										
HP-637	12/1984–8/1992	TCE	1/5	0.9J	0.9J	0.9J	0.9J	0.9J	Unknown	Site 6, Site 9, Site 78
HP-652	1/1985–12/2001	TCE	1/5	9.0	9.0	9.0	9.0	9.0	Unknown	Unknown
HP-706	9/1995–1/1998	Benzene	2/2	0.6	2.0	3.4	4.7	6.1	Unknown	Unknown

[1]See Figure A8 (Maslia et al. 2013) for locations

[2]Sites managed under the AST/UST program at Camp Lejeune. At these sites, an environmental release has occurred and subsequent investigations and/or remediation activities are conducted under the auspices of the Resource Conservation and Recovery Act (RCRA) and within the North Carolina Department of Environment and Natural Resources underground storage tank regulatory framework; refer to Faye et al. (2012) for additional details on selected AST/UST sites at Camp Lejeune

[3]Sites managed under the IRP at Camp Lejeune. At these sites, an environmental release has occurred and subsequent investigations and/or remediation activities are conducted within the Comprehensive Environmental Response, Compensation, and Liability Act of 1980 (CERCLA) regulatory framework. Within Site 78, specific local source areas are listed parenthetically; refer to Faye et al. (2010) for additional details on IRP sites at Camp Lejeune

Hadnot Point Industrial Area (HPIA) Contaminant Sources

HPIA contaminant source areas include (1) TCE and benzene releases around Building 1601, (2) TCE releases around Buildings 901, 902, and 903, (3) benzene releases in the Hadnot Point fuel farm (HPFF) area, (4) benzene releases in Building 1613, (5) TCE releases around Building 1115, and (6) TCE releases around Building 1401 (Figure S6.2). With the exception of benzene releases in the HPFF area and Building 1613, all sources mentioned above are included in the numerical models described in this supplement. Benzene releases as light nonaqueous phase liquid (LNAPL) from sources in the HPFF and Building 1613 areas and the simulation of the fate and transport of benzene as an LNAPL are described in Jang et al. (2013).

Building 1601 was constructed during the 1940s and was originally used as a garage for motor vehicles and a vehicle maintenance facility (Faye et al. 2010). Disposal of waste oil and other chemicals in a 1,600-gallon[8] (gal) underground storage tank (UST 1601) was probably the source for detections of TCE—and possibly benzene—in well HP-608 (Figure S6.2).

The steel tank (UST 1601) was installed in 1942 according to Geraghty and Miller (1990) and removed during remediation activities performed during June 29, 1993 (Peele's Pump and Tank Company 1993). Two additional tanks and fuel dispenser islands located southeast from Building 1601 could have also contributed to the contamination of benzene detected in HP-608. These tanks were connected to the HPFF by a 4-inch diameter underground pipeline that ran along East Street (Catlin Engineers & Scientists 1996, OHM Remediation Services Corporation 2001).The content from these tanks probably leaked through joints, valves, or other weak points and entered the subsurface. Over time, the contaminants migrated through the subsurface and entered the groundwater system. The predevelopment groundwater-flow direction was south and southwest of Building 1601 toward well HP-608; therefore, a plume probably formed in a southwest direction. Water-supply well HP-608 started pumping around 1942 and probably did not change the direction of the plume substantially but did increase the horizontal migration of contaminants toward the water-supply well (HP-608).

TCE releases around Buildings 901, 902, and 903 probably occurred from the leaking of two USTs and the degreasing activities around this area (Figure S6.2). A 440-gal UST located east of Building 901 could have possibly contributed to the contamination of TCE in the area (Environmental Science and Engineering, Inc. 1988). Similarly, a UST of unknown capacity located between Buildings 902 and 903 could have contributed to the TCE contamination in the area. The installation dates of these tanks are unknown; however, the buildings surrounding this area were constructed around 1948, and presumably the tanks were installed at the same time. The highest concentration of TCE around this area (13,000 micrograms per liter [µg/L]) corresponds to an unpaved area southeast of Building 901 where contaminants could have entered the subsurface due to degreasing activities near Building 901. The contaminants probably entered the groundwater system near the sources identified previously and migrated west and northwest in the direction of groundwater flow. About 1963, with the onset of pumping in well HP-634, the groundwater flow in this area was affected, causing the TCE plume to migrate somewhat backward toward the water-supply well (HP-634). Sources around Buildings 901–903 were probably removed during remediation efforts that began about January 1995 (Sovereign Consulting Inc. 2007).

TCE releases around Buildings 1115 and 1401 have been documented to a lesser degree. The presence of chlorinated alkenes around Building 1115 is documented by Faye et al. (2012, Table D5), and the concentrations varied from below detection limits to maximum values of 160 µg/L for TCE, 11 µg/L for PCE, 110 µg/L for total DCE, and 6 µg/L for VC. The chlorinated alkenes found around Building 1115 are presumably the result of natural attenuation of TCE.

[8]UST 1601 tank capacity is reported as 1,600 gallons in Richard Catlin & Associates (1996) and as 1,500 gallons in Geraghty and Miller (1990). The capacity reported by Richard Catlin & Associates (1996) is used in this report.

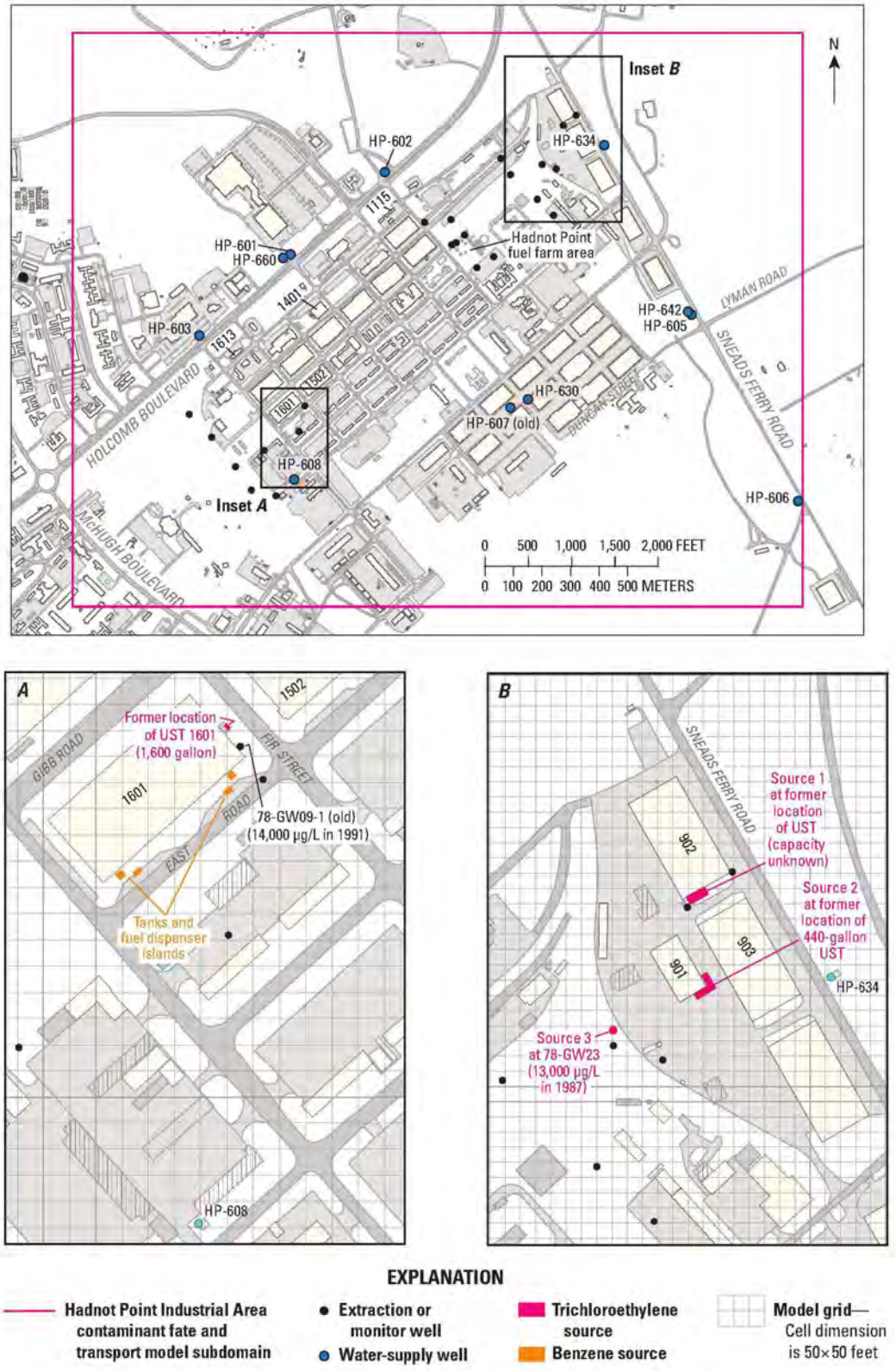

Figure S6.2. Contaminant fate and transport model source areas, selected water-supply wells, model features, water-supply wells, and source locations and enlarged maps for *(A)* Building 1601 area and *(B)* Building 901 area for the Hadnot Point Industrial Area model, Hadnot Point–Holcomb Boulevard study area, U.S. Marine Corps Base Camp Lejeune, North Carolina. [See Table S6.5 for contaminant source location; µg/L, micrograms per liter]

Hadnot Point Landfill (HPLF) Area Contaminant Sources

In the HPLF area, disposal of TCE and PCE at storage lot 203 and possibly at Installation Restoration Program (IRP) Site 82 probably first occurred during the early operation of the landfill in the 1940s (Figure S6.3). It is not known whether the materials were disposed directly to the ground surface or leaked from disposal drums or other containers. The PCE and TCE concentrations in soil and groundwater samples were used as evidence for the location of the sources.

Elevated concentrations of TCE (up to 180,000 µg/L) and PCE (up to 6,500 µg/L) were detected in a deep monitoring well (06-GW01D) that was constructed in the Upper Castle Hayne aquifer during October 1992 (Figure S6.3). At the location of monitoring well 06-GW01D, near the eastern end of the boundary between storage lot 203 and IRP Site 82, the contaminants migrated from the ground surface downward through a sequence of hydrogeologic units (the Brewster Boulevard aquifer system, the Brewster Boulevard lower confining unit, the Tarawa Terrace aquifer, and the Tarawa Terrace confining unit) before reaching the Upper Castle Hayne aquifer (Table S6.1). The Upper Castle Hayne aquifer is more permeable than the overlying units, and TCE and PCE were dissolved into the groundwater of the aquifer and were transported in a north-northwesterly direction by groundwater flowing toward Wallace Creek. Because there are few monitoring wells constructed in the hydrogeologic units below the Upper Castle Hayne aquifer, and none downgradient of monitoring well 06-GW01D, it is unknown if a pool of DNAPL formed at the base of the Upper Castle Hayne aquifer or if the DNAPL continued a downward migration to underlying units.

Eventually, a plume of TCE- and PCE-contaminated groundwater in the Upper Castle Hayne aquifer extended from the source location(s) north-northwestward to Wallace Creek, which is a local groundwater drain. Near the source locations, the vertical groundwater gradient is downward. The vertical gradient is reversed near Wallace Creek, however, and groundwater flows upward from the Castle Hayne aquifer through the overlying hydrologic units and discharges to Wallace Creek. Near Wallace Creek, the TCE- and PCE-contaminated groundwater follows the groundwater flow upward and into the creek.

Water-supply well HP-651, located east of the northeastern corner of storage lot 203 (Figure S6.3), was put in service in July 1972 and pumped water from the Upper Castle Hayne aquifer. The long-term average pumping rate from water-supply well HP-651 was about 130 gallons per minute (gpm) for the next 12 years and 7 months, until the well was taken out of service during January 1985.[9] The radius of influence of water-supply well HP-651 extended to the presumed TCE and PCE source location near monitoring well 06-GW01D within a few months after July 1972. During the time HP-651 operated, the groundwater-flow direction in the Upper Castle Hayne aquifer changed from north-northwestward to eastward toward water-supply well HP-651, and part of the TCE- and PCE-contaminated groundwater also began to flow toward water-supply well HP-651. After well HP-651 was taken out of service, the original north-northwestward groundwater-flow direction was restored, and the TCE- and PCE-contaminated groundwater that had been drawn toward water-supply well HP-651 began to migrate toward Wallace Creek.

[9] For water-supply well capacities, histories, and monthly pumping rates, refer to Sautner et al. (2013) and Telci et al. (2013).

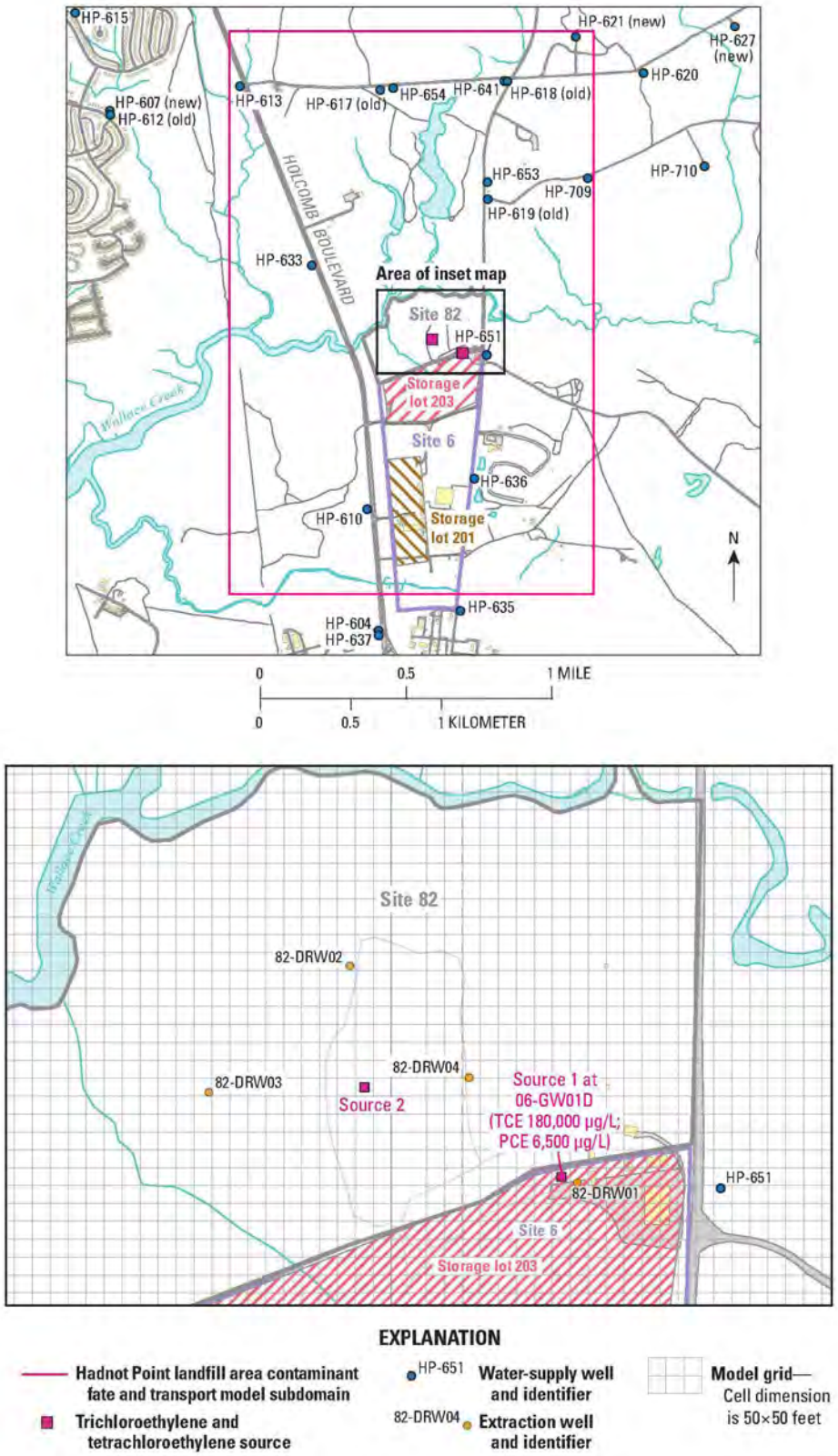

Figure S6.3. Contaminant fate and transport model source locations, selected water-supply wells, model features, water-supply wells, and source locations and enlarged map for Installation Restoration Program Site 82 area for the Hadnot Point landfill model, Hadnot Point–Holcomb Boulevard Study area, U.S. Marine Corps Base Camp Lejeune, North Carolina. [See Table S6.5 for contaminant source location; µg/L, micrograms per liter]

Mathematics of Contaminant Fate and Transport

The partial differential equation describing the fate and transport of contaminants dissolved in a three-dimensional groundwater system, under a local equilibrium assumption,[10] can be written as follows (Zheng and Wang 1999):

$$Rn_E \frac{\partial C}{\partial t} = \frac{\partial}{\partial x_i}\left(n_E \boldsymbol{D}_{ij} \frac{\partial C}{\partial x_j} \right) - \frac{\partial}{\partial x_i}\left(n_E V_i C\right) + q_s C_s - q'_s C - \lambda_1 n_E C - \lambda_2 \rho_b \bar{C} \quad , \tag{S6.1}$$

where[11]:

R is retardation factor, dimensionless;[12]
n_E is effective porosity, dimensionless;
C is dissolved concentration $[ML^{-3}]$;
t is time $[T]$;
$x_{i,j}$ is distance along the respective Cartesian coordinate axis $[L]$;
$\boldsymbol{D}_{ij}$ is the hydrodynamic dispersion tensor $[L^2T^{-1}]$;
V_i is groundwater or linear pore velocity, $[LT^{-1}]$, which is related to the specific discharge (q_i) or Darcy velocity vector through the relation, $V_i = \boldsymbol{q}_i / n_E$;
q_s is volumetric flow rate per unit volume of aquifer representing fluid sources (positive) and sinks (negative) $[T^{-1}]$;
C_s is concentration of the source or sink flux $[ML^{-3}]$;
q'_s $\partial n_E / \partial t$ is the rate of change in transient groundwater storage $[T^{-1}]$;
λ_1 is the first-order reaction rate for the dissolved phase $[T^{-1}]$;
λ_2 is the first-order reaction rate for the sorbed (solid) phase—λ_2 is zero for this study $[T^{-1}]$;
ρ_b is bulk density of the subsurface medium $[ML^{-3}]$; and
$\bar{C}$ is concentration of contaminant sorbed in the subsurface solids $[MM^{-1}]$.

Boundary Conditions

Equation S6.1 is subject to the following three types of boundary conditions:

- **Type 1:** Specified concentration boundary (Dirichlet condition), in which the concentration is specified along a boundary. A specified concentration boundary in a transport model is a source that provides contaminant mass to the model domain or is a sink that removes mass from the model domain. Contaminant sources for PCE, TCE, and benzene in the HPIA or HPLF models were simulated using a Type 1 boundary and are further described in subsequent sections.
- **Type 2:** A specified concentration gradient (Neumann condition) normal to the boundary. A special case of a Neumann or Type 2 boundary condition is a no-dispersive mass flux boundary condition, in which case, the value of the boundary condition is set to zero.
- **Type 3:** A combination of a Type 1 and Type 2 boundary condition (Cauchy condition), in which the concentration value and the concentration gradient are specified. The Type 3 or Cauchy boundary condition represents the total flux (dispersive and advective) normal to the boundary. If it can be assumed that the advective flux dominates the dispersive flux, then the Type 3 boundary condition can be handled by using the source/sink term in Equation S6.1.

[10] Local equilibrium is assumed for various sorption processes to indicate that sorption is sufficiently rapid compared to the transport time scale.

[11] In the notation throughout this report, M = mass units, L = length units, and T = time units.

[12] Refer to section on Sorption for a detailed definition of retardation factor.

Initial Conditions

The mathematical equation of contaminant fate and transport (Equation S6.1) describes the transient changes of contaminant concentration in groundwater. To obtain a solution to Equation S6.1, initial conditions must be specified that require the specification of the value of the contaminant concentration throughout the model domain. The initial condition for the model is a concentration of zero for all contaminants (e.g., PCE, TCE, and benzene) at simulation time equal to zero (i.e., January 1942).

Review of Assumptions

A number of assumptions have been made in developing the mathematical equation for contaminant fate and transport described by Equation S6.1. The main assumptions are listed below and follow those described by Konikow et al. (1996).

1. Darcy's law is valid in the solution domain, and hydraulic-head gradients are the only mechanism for fluid flow.
2. Aquifer hydraulic conductivity is independent of time (constant). If an aquifer is anisotropic, it is assumed that the principal axes of the hydraulic conductivity tensor are aligned with the modeling grid coordinate system, so that the cross-terms of the hydraulic conductivity tensor are eliminated.
3. Gradients of fluid density, viscosity, and temperature do not affect the velocity distribution.
4. Chemical reactions do not affect fluid or aquifer properties.
5. Dispersivity coefficients are constant with time, and the aquifer is isotropic with respect to longitudinal dispersivity.
6. The contaminant's solubility is such that it dissolves in groundwater and does not affect groundwater density.

The implication of assumption 6, above, is that contaminants such as TCE and PCE, which are denser than water, are characterized as DNAPLs, and benzene, which is less dense than water, is characterized as an LNAPL and cannot be simulated using Equation S6.1. With respect to TCE and PCE, available field data (Faye et al. 2012) indicate that observed groundwater concentrations are less than respective saturation limits; therefore, these contaminants were dissolved in groundwater, and Equation S6.1 is applicable. With respect to benzene in the fuel farm area, field data indicate substantial "floating" product (Faye et al. 2012); therefore, a mathematical equation describing benzene by different fluid phases and densities (relative to groundwater) was applied. This specific situation, dissolution of benzene from an LNAPL and migration in groundwater, is described in Jang et al. (2013). For conditions in the vicinity of Building 1601, where field data indicated benzene concentration in a dissolved phase (Faye et al. 2012), Equation S6.1 is appropriate and was used to simulate the migration of benzene in groundwater.

Three-Dimensional Contaminant Fate and Transport Model

The finite-difference, groundwater-flow model of the HPHB study area of USMCB Camp Lejeune, described in Suárez-Soto et al. (2013), was used as the basis for simulating contaminant transport in the HPIA and the HPLF area. Contaminant fate and transport simulations were conducted by using two variably spaced grid models that were refined in the HPIA and HPLF area to comply with numerical discretization requirements for simulating contaminant migration using 50-foot (ft)×50-ft finite-difference cells. Groundwater flow was simulated by using the numerical code MODFLOW-2005 (Harbaugh 2005), originally developed by McDonald and Harbaugh (1984). MT3DMS[13] (Modular 3-Dimensional Transport, Multi-Species) version 5.3, developed by Zheng and Wang (1999), was the numerical code used to simulate contaminant fate and transport for the variably spaced grid models representing the HPIA and HPLF area.[14]

The HPIA model has the same boundaries as the variably spaced grid model that is described in Suárez-Soto et al. (2013). The HPIA model domain consists of 288 rows, 298 columns, and 7 layers; the active model area is about 50 mi^2 and has 453,654 active cells. The more finely discretized (50×50-ft grid) area of the model domain is bounded by the Holcomb Boulevard–Sneads Ferry Road intersection in the north, McHugh Boulevard in the west, the McHugh Boulevard–Duncan Street intersection in the south, and Lyman Road in the east (Figure S6.2). The 50×50-ft area of the model is 8,400 ft (1.59 miles [mi]) from west to east, is 6,600 ft (1.25 mi) from north to south, and consists of 132 rows and 168 columns.

The HPLF model also has the same boundaries as the variably spaced grid model that is described in Suárez-Soto et al. (2013). The HPLF model domain consists of 348 rows, 268 columns, and 7 layers; the active model area is about 50 mi^2 and has 532,287 active cells. The more finely discretized (50×50-ft grid) area of the HPLF model domain is in a less developed area of USMCB Camp Lejeune than the HPIA model and is bisected west to east roughly through the middle by Wallace Creek (Figure S6.3). The 50×50-ft-grid area of the HPLF model is 6,600 ft (1.25 mi) from west to east and extends almost a mile south of Wallace Creek to Bearhead Creek and almost a mile north of Wallace Creek. The area of the grid is 10,200 ft (1.93 mi) from north to south and consists of 204 rows and 132 columns.

Vertical discretization for both models consists of seven layers. Model layers 1, 3, 5, and 7 represent water-bearing units, and model layers 2, 4, and 6 explicitly represent confining units. Several hydrogeologic units were combined in layers 1 and 5. Model layers and corresponding hydrogeologic units are listed in Table S6.1. Details and information pertaining to the hydrogeologic framework used to derive groundwater-flow and contaminant fate and transport model layers are described by Faye (2012).

Monthly water-supply-well pumping model arrays are based on time-series output from the analysis of well operations discussed in Sautner et al. (2013) and Telci et al. (2013). The only exception is that in addition to pumping from water-supply wells, the HPLF model also included pumping from six shallow and four deep extraction (remediation) wells that began operation at IRP Site 82 during October 1996. Some monthly and some quarterly pumping rates for extraction wells were tabulated by Engineering and Environment, Inc. and Michael Baker Jr., Inc. (2004). During months of missing record, quarterly rates were distributed evenly for each of the 3 months in the quarter.

Initial conditions of hydraulic head corresponded to simulated predevelopment (steady-state) hydraulic heads obtained from the calibrated model described in Suárez-Soto et al. (2013). For contaminant concentrations, the initial conditions were set to a concentration of zero for all contaminants (e.g., PCE, TCE, and benzene) at simulation time equal to zero (i.e., January 1942).

Time discretization for the HPIA and HPLF models consists of 798 monthly stress periods (January 1942–June 2008) and 1 time step per stress period.[15] Horizontal hydraulic conductivity, horizontal anisotropy, vertical anisotropy, specific yield, specific storage, and recharge are identical to the 300×300-ft regional model described in Suárez-Soto et al. (2013). Therefore the 50×50-ft-grid area of the model has blocks of 36 cells (6×6) with properties that identically correspond to one 300×300-ft cell of the regional model.

In the HPIA and HPLF models, pumping from water-supply wells is the same as for the HPHB study area model described in Suárez-Soto et al. (2013). Water-supply wells that are within the 50×50-ft grid of the HPIA and HPLF models were assigned to the appropriate cell according to their location (using North Carolina State Plane coordinates), although that location may not coincide with the closest cell to the center of the corresponding 300×300-ft grid cell to which it was assigned in the HPHB model. The refinement of well locations within the more finely discretized areas of the HPIA and HPLF models results in some slight differences in the simulated locations of pumping stresses.

[13] MT3DMS—three-dimensional mass transport, multispecies model developed on behalf of the U.S. Army Engineer Research and Development Center. MT3DMS-5.3 (Zheng and Wang 1999) is the specific version of MT3DMS code used for the HPHB study area analyses; references to MT3DMS in text, figures, tables, and appendixes refer to MT3DMS-5.3.

[14] Henceforth, the contaminant fate and transport model applied to the Hadnot Point Industrial Area will be referred to as the HPIA model; the contaminant fate and transport model applied to the Hadnot Point landfill area will be referred to as the HPLF model.

[15] Refer to Suárez-Soto et al. (2013, Appendix S4.6) for a sequential list of stress periods and corresponding month and year.

Solute sources of TCE, PCE, and benzene were placed at locations within model layers based on information of contaminant releases and spills and measured contaminant concentrations in water-supply, monitor, and extraction wells (Faye et al. 2012). Locations of the aforementioned modeled contaminant sources are shown in Figures S6.2 and S6.3 and are listed in Table S6.2. Transport model parameter values for contaminant-source concentrations, retardation factors, and biochemical degradation rates were adjusted by using manual trial-and-error means to achieve reasonable matches between historical measured concentrations and simulated values at selected water-supply, monitor, and extraction wells. Calibrated parameter values are within reasonable and acceptable parameter-value limits found in the literature and also applied to the TT study area (Faye 2008). Specific comparisons between measured and simulated concentrations are described in the Historical Reconstruction Results section.

Hydrodynamic Dispersion

To compute values of hydrodynamic dispersion coefficients, MT3DMS requires the cell-by-cell assignment of the effective molecular diffusion coefficient (D^*) for the simulated chemical in groundwater, longitudinal dispersivity (α_L), and the ratios of transverse horizontal and vertical dispersivity (α_T and α_V, respectively) to α_L. All of these dispersion parameters for the HPIA and HPLF models are the calibrated values derived by Faye (2008) for migration of PCE within the TT study area. Longitudinal dispersivity was assigned a value of 25 ft to all cells in all layers (Table S6.3). Ratios of α_T/α_L and α_V/α_L of 0.1 and 0.01, respectively, were assigned to all cells in all layers. D^* was assigned a value of 1.0×10^{-3} square feet per day (ft^2/d) throughout the model. These parameter values were not modified during model calibration.

Table S6.3. Calibrated model parameter values used to simulate contaminant fate and transport, Hadnot Point–Holcomb Boulevard study area, U.S. Marine Corps Base Camp Lejeune, North Carolina.

[—, not applicable; ft, foot; ft^3, cubic foot; d, day; g, gram; mg, milligram; L/kg, liter per kilogram; PCE, tetrachloroethylene; TCE, trichloroethylene; HPIA, Hadnot Point Industrial Area; HPLF, Hadnot Point landfill]

[1]Model parameter	[2]Model layer number						
	1	2	3	4	5	6	7
[3]Contaminant fate and transport models, January 1942–June 2008—Subdomain area (50-ft×50-ft cells)							
Distribution coefficient, K_d (ft^3/mg):							
PCE	1.1×10^{-8}	1.1×10^{-8}	1.1×10^{-8}	1.1×10^{-8}	1.1×10^{-8}	1.1×10^{-8}	1.1×10^{-8}
TCE	5.3×10^{-9}	5.3×10^{-9}	5.3×10^{-9}	5.3×10^{-9}	5.3×10^{-9}	5.3×10^{-9}	5.3×10^{-9}
Benzene	4.0×10^{-9}	4.0×10^{-9}	4.0×10^{-9}	4.0×10^{-9}	4.0×10^{-9}	4.0×10^{-9}	4.0×10^{-9}
Bulk density, ρ_b (g/ft^3)	46,700	46,700	46,700	46,700	46,700	46,700	46,700
Effective porosity, n_E	0.2	0.2	0.2	0.2	0.2	0.2	0.2
Biodegradation, λ (d^{-1}):							
HPIA (TCE)	2.0×10^{-3}	2.0×10^{-3}	2.0×10^{-3}	2.0×10^{-3}	2.0×10^{-3}	2.0×10^{-3}	2.0×10^{-3}
HPIA (benzene)	1.0×10^{-4}	1.0×10^{-4}	1.0×10^{-4}	1.0×10^{-4}	1.0×10^{-4}	1.0×10^{-4}	1.0×10^{-4}
HPLF (PCE and TCE)	1.4×10^{-4}	1.4×10^{-4}	1.4×10^{-4}	1.4×10^{-4}	1.4×10^{-4}	1.4×10^{-4}	1.4×10^{-4}
Effective molecular diffusion coefficient, D^*(ft^2/d)	1.0×10^{-3}	1.0×10^{-3}	1.0×10^{-3}	1.0×10^{-3}	1.0×10^{-3}	1.0×10^{-3}	1.0×10^{-3}
Dispersivity (ft):							
Longitudinal, α_L	25	25	25	25	25	25	25
Transverse, α_T	2.5	2.5	2.5	2.5	2.5	2.5	2.5
Vertical, α_V	0.25	0.25	0.25	0.25	0.25	0.25	0.25
Source concentration, C (mg/L):							
HPIA (TCE)	640	640	640	0	0	0	0
HPIA (benzene—dissolved)	1.7	—	—	—	—	—	—
HPLF (PCE)	42–105	33–83	27–66	18–46	6–16	0	0
HPLF (TCE)	256–384	256–384	256–384	256–384	256–384	256–384	256–384

[1] Symbolic notation used to describe model parameters obtained from Harbaugh (2005), Zheng and Wang (1999)

[2] See Table S6.1 for correlation between geologic and hydrogeologic units and model layers for the HPHB study area; refer to Faye (2012) and Suárez-Soto et al. (2013) for details: aquifers are designated as model layers 1, 3, 5, and 7; confining units are designated as model layers 2, 4, and 6

[3] See Figures S6.1–S6.3 for groundwater-flow model domain and contaminant fate and transport model subdomains

Sorption

Sorption in the HPHB study area is assumed to be similar to sorption in the TT study area of USMCB Camp Lejeune described in Faye (2008). Sorption processes (i.e., adsorption and absorption) for the HPIA and HPLF models were represented in MT3DMS by using a linear isotherm sorption model. The input data required to simulate sorption include porosity, distribution coefficient, and soil bulk density. Constant values were assigned to the aforementioned model parameters throughout the model owing to the lack of site-specific field data. MT3DMS uses values assigned to porosity, distribution coefficient, and soil bulk density to compute a retardation factor. The retardation factor is related to the linear equilibrium isotherm by the following formula (Freeze and Cherry 1979; Zheng and Wang 1999):

$$R = V_w / V_c = 1 + K_d \rho_b / n_E, \qquad \text{(S6.2)}$$

where

R is retardation factor, dimensionless;
K_d is distribution coefficient $[L^3M^{-1}]$;
ρ_b is bulk density of the porous media $[ML^{-3}]$;
n_E is effective porosity of the porous media, dimensionless;
V_w is linear groundwater velocity $[LT^{-1}]$; and
V_c is solute velocity $[LT^{-1}]$.

The distribution coefficient, K_d, is a chemical- and soil-specific parameter used to quantify how a chemical partitions between an aqueous phase and a soil or sediment phase. Typically, K_d values are calculated based on laboratory-scale experimental data that quantify partitioning behavior for a chemical in simple systems (e.g., octanol water) and field data or estimates for the amount of organic material present in the soil or aquifer material of interest (USEPA 1996). Model-specific K_d values for benzene (0.11 liter per kilogram [L/kg]), TCE (0.15 L/kg), and PCE (0.30 L/kg) were derived by using partitioning data for each chemical (Mackay et al. 2006; USEPA 1996), an assumed value of 0.002 for the site-specific organic carbon fraction of aquifer material, and refinement during the model calibration process. Final model-specific K_d values are well within the range of values calculated from multiple sources of partitioning data (Table S6.4). When using consistent model units of feet and milligrams,[16] the input K_d values for benzene, TCE, and PCE are 4.0×10^{-9}, 5.30×10^{-9}, and 1.06×10^{-8} cubic feet per milligram (ft^3/mg), respectively (Table S6.3).

The value of bulk density, ρ_b, is based on default parameter values published by the USEPA (1996) for soil specific gravity—1.65 grams per cubic centimeter (g/cm^3) or 4.67×10^6 milligrams per cubic foot (mg/ft^3) in consistent model units. Effective porosity, n_E, was assumed to be 20 percent (0.2) for all model layers (Faye 2008). Both parameters—ρ_b and n_E—were not adjusted during model calibration. Applying the aforementioned parameter values to Equation S6.2, the resulting dimensionless retardation factors (R) for benzene, TCE, and PCE, are 1.9, 2.2, and 3.5, respectively.

[16] All model parameter values must be supplied to MT3DMS in model consistent units. For the HPHB study area models, MT3DMS units are as follows: Length units are in feet (ft), Time units are in days (d), and Mass units are in milligrams (mg).

Table S6.4. Chemical-specific distribution coefficients and retardation factors calculated from multiple sources of partition coefficient data, Hadnot Point–Holcomb Boulevard study area, U.S. Marine Corps Base Camp Lejeune, North Carolina.

[USEPA, U.S. Environmental Protection Agency; TCE, trichloroethylene; PCE, tetrachloroethylene; g/cm^3, gram per cubic centimeter]

Contaminant	Distribution coefficient, K_d, in liters per kilogram (L/kg)			Retardation factor[1]
	Minimum	Maximum	Basis for calculation	
Benzene	0.028	0.946	Range of K_d values calculated by using fraction organic carbon (f_{OC}) value of 0.002 and 63 different soil organic carbon/water partition coefficient (K_{OC}) and octanol/water partition coefficient (K_{OW}) values compiled in Mackay et al. (2006) and USEPA (1996)	1.2–8.8
TCE	0.03	0.99	Range of K_d values calculated by using fraction organic carbon (f_{OC}) value of 0.002 and 64 different soil organic carbon/water partition coefficient (K_{OC}) and octanol/water partition coefficient (K_{OW}) values compiled in Mackay et al. (2006) and USEPA (1996)	1.2–9.2
PCE	0.03	21.43	Range of K_d values calculated by using fraction organic carbon (f_{OC}) value of 0.002 and 53 different soil organic carbon/water partition coefficient (K_{OC}) and octanol/water partition coefficient (K_{OW}) values compiled in Mackay et al. (2006) and USEPA (1996)	1.2–177.8

[1] Retardation factor calculated using Equation S6.2; porosity equals 0.2, and bulk density equals 1.65 g/cm^3

Biochemical Reactions

Contaminants of interest to this study (i.e., PCE, TCE, and benzene) were probably degraded due to microbial activity as indicated by the presence of degradation by-products (e.g., *cis*-1,2-dichloroethylene [1,2-cDCE], *trans*-1,2-dichloroethylene [1,2-tDCE], and VC) (Faye et al. 2010, 2012). Biodegradation of PCE and TCE probably occurred through reductive dechlorination, and benzene was probably degraded under anaerobic conditions. Biodegradation pathways and biochemical reactions are complex and further explained by Lawrence (2007). In general, the presence of certain elements, such as an electron acceptor, an electron donor, a carbon source, nitrogen, macronutrients, and micronutrients, are required for bacteria to grow and to achieve biodegradation (Madigan et al. 2003). Biodegradation rates are further controlled by temperature, pH, and other environmental factors. Biological reaction kinetics are poorly understood in uncontrolled systems (e.g., groundwater-flow systems), and typically they have been modeled using simple models such as first-order or Michaelis-Menten kinetics (Yu and Semprini 2004). For the HPHB study area, biodegradation of dissolved contaminants was simulated using a first-order degradation rate, which is expressed by the relation

$$C = C_0 e^{-\lambda_1 t}, \qquad \text{(S6.3)}$$

where

C is contaminant concentration [ML^{-3}];

C_0 is initial contaminant concentration [ML^{-3}];

e is base of Naperian or natural logarithms, dimensionless;

λ_1 is the biochemical degradation rate constant for the dissolved phase, [T^{-1}]; and

t is elapsed time, [T].

Degradation rates are calculated by using multiple approaches, including laboratory methods, field experiments, and modeling analyses. It is important to understand that degradation kinetics vary spatially and temporally and represent an estimate under very specific conditions; therefore, degradation rates represent conditions of a dynamic process. For example, laboratory methods, such as a microcosm test (USGS 2013), are able to separate the effects of degradation from other processes such as dispersion. However, microcosm tests are closed systems in which chemical properties can change substantially over time and may not represent conditions present in an open system (e.g., aquifer). Field experiments may adequately represent aquifer conditions; however, field experiments seldom measure degradation rates, and attenuation rates are usually calculated instead. Attenuation rates are typically a combination of multiple processes such as degradation, sorption, and dispersion. In practice, it is typical to compute attenuation rates if possible because they can provide some insight about degradation.

Attenuation rates were computed for multiple chlorinated solvents using site-specific field data and are described in detail in Appendix S6.1. Attenuation rates for PCE range from about 1.5×10^{-4} to 9.8×10^{-4} per day (d^{-1}), which in terms of half-life correspond to about 4,500 to 700 d, respectively. TCE attenuation rates range from about 3.6×10^{-4} to 1.5×10^{-3} d^{-1}, which in terms of half-life correspond to about 1,900 to 460 d, respectively. CH2M HILL (2010) reported low levels of total organic carbon, which could impede degradation.

Aronson and Howard (1997) reported mean first-order degradation rates for TCE and PCE for multiple sites across the United States. The mean rates reported for TCE and PCE are 2.5×10^{-3} d^{-1} and 2.9×10^{-3} d^{-1}, respectively. Benzene rates reported by Cozzarelli et al. (2010), USEPA (1999), Wiedemeier (1995), and Wilson et al. (1994) were reviewed and further described by Jang et al. (2013), and a value of 1×10^{-4} d^{-1} was selected. Because degradation rates vary widely, the values were adjusted during the calibration process. Mean values for TCE and PCE, previously described, were initially used in contaminant fate and transport simulations and were adjusted to history-match (reconstruct) the concentrations at certain water-supply and monitor wells (Figures S6.4 and S6.6). For example, a low reaction rate was required for the contaminants to migrate to the locations of and at the concentrations detected in the six downgradient extraction wells in the Brewster Boulevard aquifer (shallow wells 82-SRW01–82-SRW06, model layer 1) and the four downgradient extraction wells in the Upper Castle Hayne aquifer (deep wells 82-SWR01–82-SWR04, model layer 5). The final calibrated degradation rate values at the HPIA are 2.0×10^{-3} d^{-1} for TCE and 1.0×10^{-4} d^{-1} for benzene. At the HPLF, the final calibrated values are 1.4×10^{-4} d^{-1} for TCE and PCE (Table S6.3).

Source Concentrations

Sources in the HPIA and HPLF models were simulated using a specified concentration (Type 1) boundary condition. Source locations and durations were estimated by using the information previously described in the Conceptual Models section of this report and in Faye et al. (2010, 2012). Source location, concentration, and duration are summarized in Table S6.5. The sources were placed in the nearest cell to the physical feature representing the source. For example, the nearest cell to the center of the leaking storage tank was used in Building 1601 to represent a TCE source. In the landfill area, the cell containing the monitor well with the highest concentrations was used to represent a TCE and PCE source. Source duration varied for each of the locations. Historical records delineating the start date of fuel spills or releases from the UST systems were not available. Consequently, a rationale for the source start date was formulated based on the installation date of UST systems and empirical data on the cause and timing of fuel leaks and releases from UST systems. In 1987, the USEPA published a report indicating that fuel delivery piping and spills/overfills accounted for more fuel releases (in terms of number of releases, not volume of release) than the associated storage tanks themselves (USEPA 1987). In fact, fuel piping and fittings were implicated in 80–85 percent of all releases from UST systems (USEPA 1987). In a separate study containing an analysis of 1,244 leak incident reports across the United States, the USEPA reported mean and median age for UST system piping leaks as 11 and 9 years, respectively (USEPA 1986). Therefore, for this analysis, the median age of 9 years was used.

The maximum concentration used in the model did not exceed the respective solubility limit for the corresponding contaminant—1,280 milligrams per liter (mg/L) for TCE, 210 mg/L for PCE, and 17 mg/L for benzene in a fuel mixture (Lawrence 2007; USEPA 2011). Sources in the HPIA area are TCE and benzene; sources in HPLF area are PCE and TCE. Contaminant fate and transport for source chemicals in the HPIA (TCE and benzene) and the HPLF area (PCE and TCE) were modeled concurrently using the MT3DMS model code.[17]

[17] MT3DMS identifies species by numbers. In the HPIA model input files, TCE and benzene are species 1 and 2, respectively. In the HPLF model input files, TCE and PCE are species 1 and 2, respectively.

Table S6.5. Calibrated contaminant fate and transport model parameter values used to describe contaminant sources in the Hadnot Point Industrial Area (HPIA) and Hadnot Point landfill (HPLF) area, Hadnot Point–Holcomb Boulevard study area, U.S. Marine Corps Base Camp Lejeune, North Carolina.

Source area[1]	Cell location (row, column, layer)[2]	Concentration, in milligrams per liter	Source duration
Trichloroethylene (TCE)			
Building 1601	165, 116, 1–3	640	January 1951–June 1993
Building 900 area			
Source 1	102, 178, 1–3	640	January 1957–December 1994
Source 2	108, 179, 1–3		
Source 3	113, 173, 1–3		
Building 1401	122, 138, 1–3	640	January 1951–June 1993
Building 1115	145, 121, 1–3	640	January 1951–June 1993
Landfill area			
Source 1	159, 156, 1–7	256–384	January 1948–June 2008
Source 2	154, 145, 1–7		
Tetrachloroethylene (PCE)			
Landfill area			
Source 1	159, 156, 1–5	16–105	January 1948–June 2008
Source 2	154, 145, 1–5	6–42	
Benzene			
Building 1601			
Source 1	168, 117, 1	1.7	January 1951–June 1993
Source 2	171, 113, 1		

[1] Refer to Figures S6.2 and S6.3 for maps showing location

[2] Cell location corresponds to their respective models (i.e., HPIA or HPLF). Cell location with coordinates row 1, column 1 and layer 1 corresponds to the northwest corner and uppermost cell of the total model domain

Four source areas of TCE were identified and included in the HPIA model.

1. A 1,600-gal waste-solvent storage tank between Buildings 1601 and 1502 (row 165, column 116, layers 1–3) (Figure S6.2).
2. Building 900 area (Figure S6.2):
   a. Source 1: An underground storage tank in the area between Buildings 902 and 903 (row 102, column 178, layers 1–3), which was used for engine degreasing.
   b. Source 2: A 440-gal underground storage tank east of Building 901 used to store TCE (row 108, column 179, layers 1–3), and
   c. Source 3: High concentrations of TCE southwest of Building 901 (row 113, column 173, layers 1–3) probably associated with degreasing activities in the area,
3. Building 1115 (row 122, column 138, layers 1–3).
4. Building 1401 (row 145, column 121, layers 1–3).

All TCE sources in the HPIA were assigned a concentration of 640 mg/L, which corresponds to 50 percent of the TCE solubility limit.[18]

Benzene was simulated in the HPIA model to account for the benzene source resulting from two storage tanks related to a fuel dispensing island on the south side of Building 1601 (Figure S6.2). The sources are located in two cells (row 168, column 117, layer 1, and row 171, column 113, layer 1). The specified concentration is 1.7 mg/L, which corresponds to 10 percent of the effective solubility limit.[19]

In the HPLF model, a single source of TCE was initially placed near monitor well 06-GW01D (row 159, column 156, layers 1–7) in all model layers where the maximum concentrations of TCE were detected, beginning in January 1948 (Figure S6.3). The dominant groundwater-flow path from that location to Wallace Creek caused the TCE migration to bypass the area of monitor well 06-GW27DW and extraction well 82-DRW03 to the northeast, where groundwater samples from the early 1990s through the early 2000s had concentrations of TCE as great as 22,000 µg/L. A second source of TCE roughly midway between extraction wells 82-DRW03 and 82-DRW04 (row 154, column 145, layers 1–7) was added during the calibration process to approximate the historical TCE concentrations detected in the two wells 06-GW27DW and 82-DRW03. The two TCE source locations in the HPLF model are shown in Figure S6.3.

Because the highest concentration of TCE was detected in well 06-GW01D, which is completed in model layer 5 (Upper Castle Hayne aquifer–River Bend and Lower units—Table S6.1), it was assumed that TCE migrated vertically from the source, presumed to be at or near ground surface, downward through confining layers into the Castle Hayne aquifer system quickly compared to the length of time that the contaminants have had to migrate laterally through the aquifer layers (from the late 1940s until first detected in groundwater samples in the mid-1980s). Thus, TCE was applied as a constant-concentration source of equal concentration in each model layer (1–7). Based on adjustments made during the calibration process, the concentration of TCE at the first HPLF source was 384 mg/L (30 percent of the solubility limit of TCE in water), and the concentration of TCE at the second HPLF source was 256 mg/L (20 percent of the solubility limit).

Adjustment in the PCE source concentration in layer 1 during the calibration process resulted in PCE concentrations of 105 mg/L at the first source (row 159, column 156) and 42 mg/L at the second source (row 154, column 145). The layer 1 PCE source concentrations correspond to 50 percent and 20 percent, respectively, of the solubility limit of PCE in water, which is 210 mg/L (Lawrence 2007). Initial simulations using constant PCE-concentration sources through all layers indicate that the simulated PCE concentration was either too high in layer 5 or too low in layer 1 to match measured PCE concentrations. To achieve closer agreement with observed PCE data, the PCE source concentration was reduced linearly in successive layers at increasing depths to layer 5, where the PCE concentration was 15 percent of the layer 1 concentration (Tables S6.2 and S6.3). An analytical model simulating vertical migration of PCE, the analytical contaminant transport analysis system or ACTS (Maslia and Aral 2004), was used to evaluate and estimate the decrease in PCE concentration in successive layers of greater depth for different values of half-life ($t_{1/2}$) of PCE and retardation factor (R).[20] Results of the analytical model provided estimates that were reasonable based on tested ranges of PCE $t_{1/2}$ and R. PCE source concentration was decreased about 85 percent between model layers 1 and 5 based on results from the analytical model.

[18] The water solubility of TCE is reported as 1,280 mg/L at 25 degrees Celsius (°C) (Lawrence 2007).

[19] Effective solubility means the solubility of a compound that will dissolve from a chemical mixture (e.g., gasoline). The effective solubility of a compound from a chemical mixture is less than its aqueous solubility (Mississippi Department of Environmental Quality 2007). Benzene solubility in water at 25 °C is 1,780 mg/L (ATSDR 2007). The source of benzene is fuel and its effective solubility is 17 mg/L (USEPA 2011).

[20] The half-life ($t_{1/2}$) is the elapsed time when half of the initial concentration remains and is related to the biochemical degradation rate (r) by Equation S6.3: $t_{1/2} = ln(2)/r$.

Historical Reconstruction Results

This section presents and discusses details pertinent to simulation results of TCE, PCE, and benzene concentrations in groundwater and at selected water-supply wells determined through the historical reconstruction process. Readers interested in a detailed discussion of the historical reconstruction process should refer to Maslia et al. (2013).

Hadnot Point Industrial Area

The discussion and presentation of HPIA historical reconstruction (model) results presented herein focus on water-supply wells HP-601, HP-602, HP-608, and HP-634—the only wells with reconstructed (simulated) concentrations that exceeded 1 µg/L. Among the aforementioned water-supply wells, well HP-634 has the maximum reconstructed TCE concentration (659 µg/L), and well HP-608 has the maximum reconstructed benzene concentration (11 µg/L).

Figure S6.4 shows the reconstructed (simulated) TCE concentrations for selected water-supply wells in the HPIA (wells HP-601, HP-602, HP-634, and HP-660).[21,22] Monthly reconstructed TCE concentrations derived using the aforementioned analyses for selected water-supply wells are tabulated and listed in Appendix A3. These results should be interpreted as monthly mean concentrations of TCE (occurring on the last day of each month) dissolved in groundwater at the aforementioned water-supply wells (locations shown on Figure S6.2). The reconstructed concentrations at water-supply wells are flow-weighted concentration values for supply wells that are open to multiple water-bearing units. The flow ratios for each model layer are listed in Suárez-Soto et al. (2013, Table S4.7). As can be seen in the graphs of Figure S6.4, observation data in water-supply wells are limited. For example, well HP-634 only has one measured concentration data point that exceeds the detection limit for comparison to reconstructed TCE concentrations. For water-supply wells HP-602 and HP-608, measurements were taken on the same day or within a time span of 1 month or less (Table A4), whereas model results represent a mean concentration over an entire month. Not only does this make it difficult to calibrate a numerical model that at best only approximates the physics, chemistry, and biology of "real-world" conditions, but it calls into question which observation data and data values should be used for comparisons with simulated concentrations. Given the aforementioned limitations and constraints, the reconstructed (simulated) TCE concentrations reasonably agree with measured data and "real-world" conditions.

Areal distributions of reconstructed TCE concentrations for model layers 1, 3, and 5 for four periods—January 1951, January 1968, November 1984, and June 2008—are shown in Figure S6.5. Model layers 1, 3, and 5 represent major water-bearing units in the study area and are correlated with the Brewster Boulevard aquifer system, the Tarawa Terrace aquifer, and the Upper Castle Hayne aquifer, respectively (Table S6.1). The specific simulation dates noted above were selected to show typical historical reconstruction results because (1) January 1951 represents an early time period after the onset of pumping, (2) January 1968 represents the start of the epidemiological health study, (3) November 1984 represents the month prior to the shutdown of many of the contaminated water-supply wells, and (4) June 2008 represents the end of the historical reconstruction simulation and a time when all contaminated water-supply wells had been removed from service for more than 20 years. Viewed synoptically, the maps in Figure S6.5 illustrate a progression in the areal distribution of TCE by model layer at the HPIA from the early onset of pumping (January 1951) to substantial effect of TCE at water-supply wells (January 1968 and November 1984), to dilution and reduction in the TCE concentration at the end of the historical reconstruction simulation (June 2008) because of the cessation of pumping of historically contaminated HPIA water-supply wells. Larger scale maps showing additional HPIA details such as building identification are provided in Appendix A4.

Benzene sources around Building 1601 resulted in a maximum reconstructed concentration of 11 µg/L at water-supply well HP-608 during September 1979 (Appendix A3). The simulated concentration first exceeded the current maximum contaminant level (MCL)[23] for benzene (5 µg/L) during September 1967. A summary of historical reconstruction results for TCE and benzene in the HPIA is listed in Table A14.

[21] Water-supply well HP-660 replaced HP-601 and probably operated from July 1984 to November 1984—see Figure A5 and Sautner et al. 2013.

[22] Results for benzene concentrations in water-supply well HP-602 (Figure S6.4 and Appendix A3) were derived by simulating benzene as an LNAPL—details provided in Jang et al. (2013).

[23] Values of MCL referenced in HPHB study area reports and supplements refer to current values of MCLs—see Table A3.

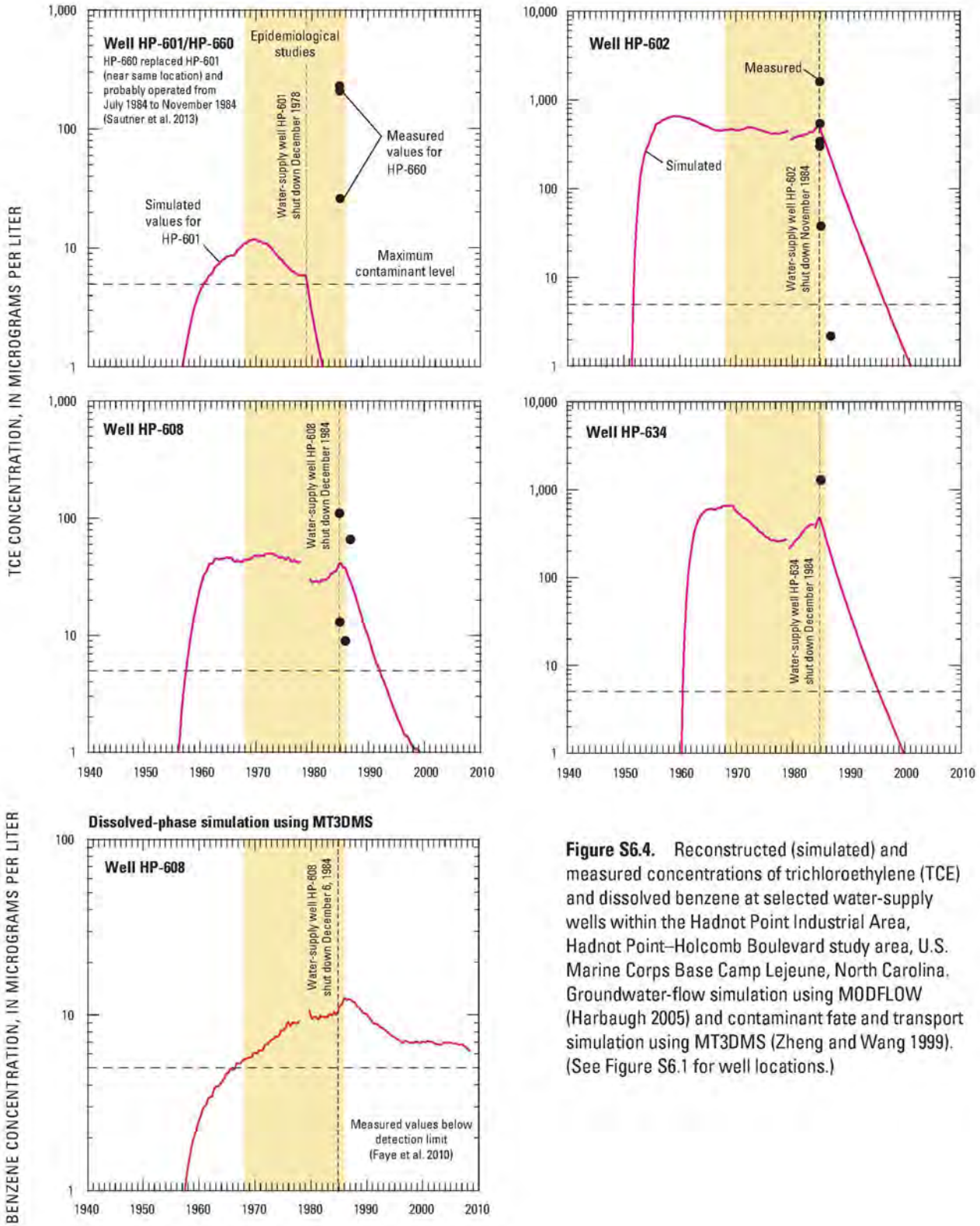

Figure S6.4. Reconstructed (simulated) and measured concentrations of trichloroethylene (TCE) and dissolved benzene at selected water-supply wells within the Hadnot Point Industrial Area, Hadnot Point–Holcomb Boulevard study area, U.S. Marine Corps Base Camp Lejeune, North Carolina. Groundwater-flow simulation using MODFLOW (Harbaugh 2005) and contaminant fate and transport simulation using MT3DMS (Zheng and Wang 1999). (See Figure S6.1 for well locations.)

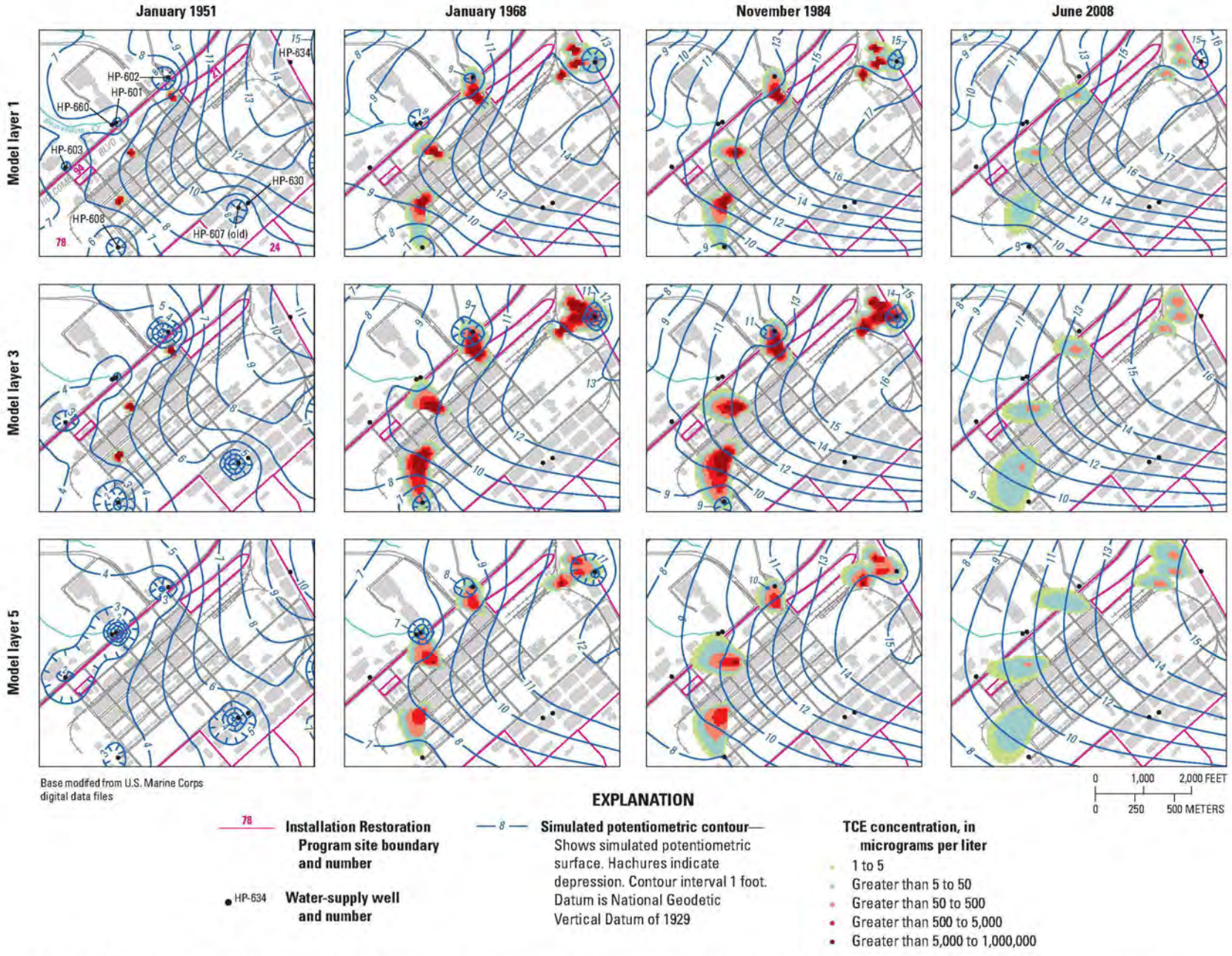

Figure S6.5. Reconstructed (simulated) water levels and distribution of trichloroethylene (TCE) within the Hadnot Point Industrial Area fate and transport model subdomain, model layers 1, 3, and 5, Hadnot Point–Holcomb Boulevard study area, U.S. Marine Corps Base Camp Lejeune, North Carolina, January 1951, January 1968, November 1984, and June 2008. (See Figure A11 for location and building numbers; see Appendix A6 for more detailed maps and results.)

Hadnot Point Landfill Area

For the HPLF model, the primary result is the reconstructed (simulated) monthly mean concentrations of PCE and TCE at water-supply well HP-651 (Figure S6.6), which was the only water-supply well in the HPLF area where water-quality samples indicated measured concentrations of PCE and TCE greater than the MCL (5 µg/L). The reconstructed concentration of PCE first exceeded the MCL during April 1973; the reconstructed concentration of TCE first exceeded the MCL during August 1972. The maximum reconstructed concentration of PCE was 353 µg/L during December 1982, and the maximum reconstructed concentration for TCE was 7,135 µg/L during December 1978.

After pumping ceased at water-supply well HP-651 during February 1985, the reconstructed concentrations of PCE and TCE at well HP-651 declined for the remainder of the simulation period, ending during June 2008. Reconstructed contaminant concentrations of both PCE and TCE at well HP-651 exceeded measured concentrations after pumping ceased. A plausible explanation for this observation is that the calibrated PCE and TCE source concentrations were constant in time and were not varied temporally. Most likely, contaminant-source concentrations diminished during the HP-651 post-production period. However, data were not available to justify introducing time-varying contaminant-source concentrations.

To evaluate the effect of the remediation extraction-well system that began operating during January 1996, the source concentration in the model most likely would have to be reduced to calibrate to measured concentration data at extraction and monitor wells subsequent to January 1996—this type of analysis is beyond the scope of this study. However, measured PCE and TCE concentration data obtained from extraction wells were used to assist with fate and transport model calibration for the HPLF area. Reconstructed and observed concentrations of PCE and TCE for four deep extraction wells, 82-DRW01–82-DRW04, are shown in Figure S6.6.

Reconstructed PCE and TCE concentration trends in extraction well 82-DRW01 show substantial variability (Figure S6.6). A plausible explanation for this variability is that extraction well 82-DRW01 is located near water-supply well HP-651 and is represented in the model by the cell directly adjacent to the first specified-concentration source cell for PCE and TCE. Because extraction well 82-DRW01 is located between the contaminant source and water-supply well HP-651, the reconstructed PCE and TCE concentrations increased sharply when well HP-651 began operating during July 1972. The reconstructed PCE and TCE concentrations began to decrease during February 1985 when production from water-supply well HP-651 ceased. A subsequent increase in PCE and TCE concentrations occurs when the extraction-well system began operating during January 1996, and another decrease in PCE and TCE concentrations occurs when production from extraction well 82-DRW01 ceased during January 2006. The close proximity of extraction well 82-DRW01 to the specified-concentration source model cell also is a likely reason for reconstructed PCE and TCE concentrations exceeded measured PCE and TCE concentrations.

PCE and TCE concentrations in the other three extraction wells (82-DRW02, 82-DRW03, and 82-DRW04) exhibit similar but less variable trends. The reconstructed concentrations in wells 82-DRW03 and 82-DRW04 begin to decrease slightly when water-supply well HP-651 began operating during July 1972 (Figure S6.6) due to the migration of contaminant plumes eastward toward well HP-651. Because extraction well 82-DRW02 is located beyond the radius of influence of water-supply well HP-651, the PCE and TCE concentrations continue to rise when water-supply well HP-651 began operating. The PCE and TCE concentrations in extraction wells 82-DRW03 and 82-DRW04 increase when the extraction-well system began operating during January 1996 because the contaminant plume migrates toward these extraction wells. However, concentrations in downgradient extraction well 82-DRW02 decrease due to the reversal of plume migration caused by the relatively high rate of extraction at well 82-DRW04.

Historical reconstruction results for PCE and TCE in the IRP Site 82 area are shown in areal plots (Figures S6.7–S6.14) of reconstructed contaminant concentrations at the following different times:

1. January 1958: 10 years after introduction of contaminant sources during January 1948 in the HPLF area model (Figure S6.7).
2. January 1968: 20 years after introduction of contaminant sources in the HPLF model (Figure S6.8).
3. June 1972: 24.5 years after introduction of contaminant sources in the HPLF model and just prior to the start of pumping at water-supply well HP-651 (Figure S6.9).
4. June 1978: 6 years after the start of pumping at water-supply well HP-651 (Figure S6.10).
5. November 1984: 12.5 years after the start of pumping at water-supply well HP-651 and 2 months prior to cessation of operations at the well (Figure S6.11).
6. December 1995: Nearly 11 years after pumping operations at water-supply well HP-651 ceased and prior to beginning of pumping at extraction wells (Figure S6.12).
7. December 2005: 10 years after the start of pumping at extraction wells, just prior to the end of pumping at extraction well 82-DRW01 (Figure S6.13).
8. June 2008: End of historical reconstruction simulation, 12.5 years after the start of pumping at extraction wells and 2.5 years after pumping at extraction well 82-DRW01 ceased (Figure S6.14).

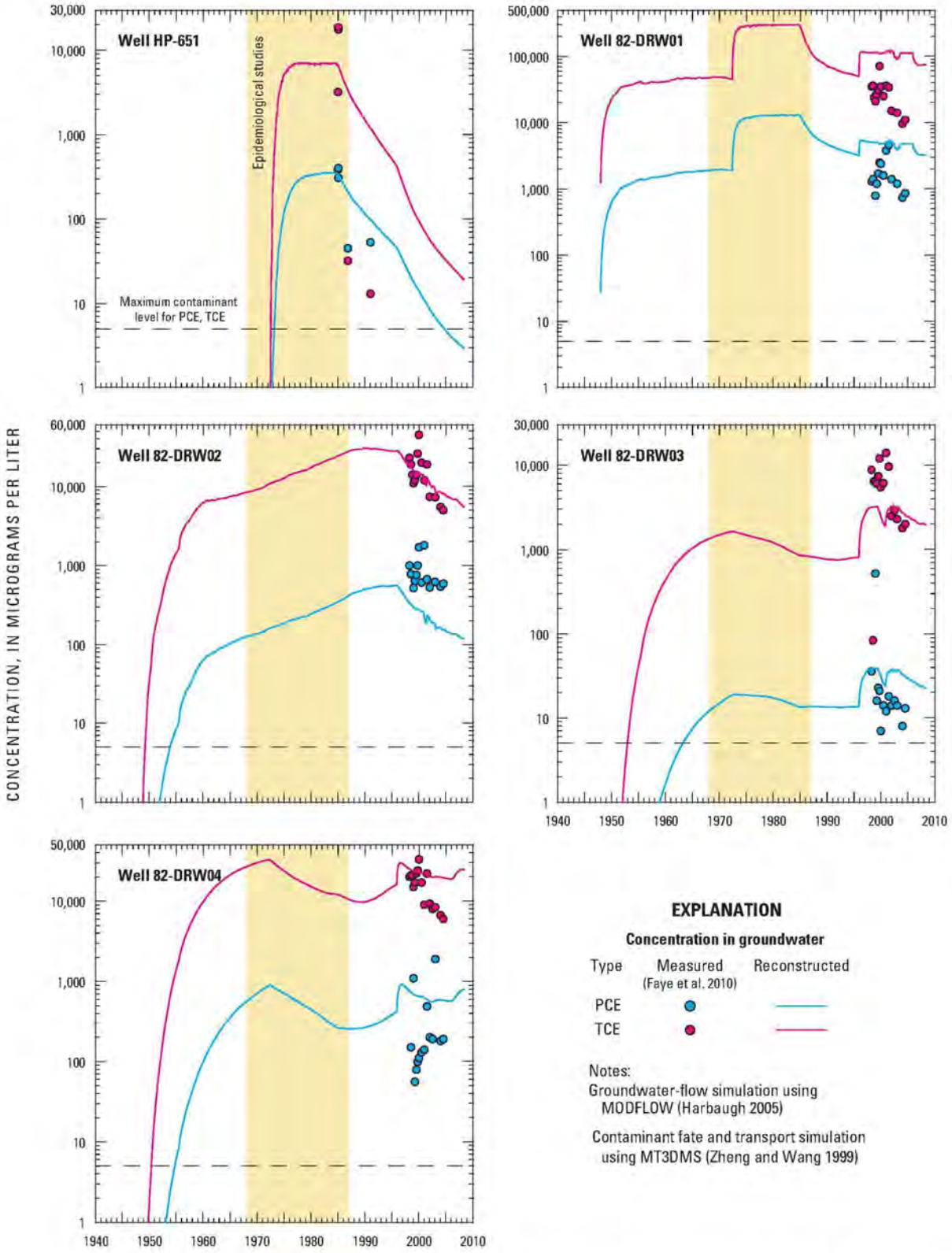

Figure S6.6. Reconstructed (simulated) and measured concentrations of trichloroethylene (TCE) and tetrachloroethylene (PCE) at water-supply well HP-651 and extraction wells 82-DRW01, 82-DRW02, 82-DRW03, and 82-DRW04, model layer 5, Hadnot Point landfill area, Hadnot Point–Holcomb Boulevard study area, U.S. Marine Corps Base Camp Lejeune, North Carolina.

Historical reconstruction results for each of the aforementioned eight monthly times are presented for the PCE and TCE contaminant plumes in Figures S6.7–S6.14. Collectively these results show the spatial distribution of PCE and TCE over time. All results are for model layer 5, the Upper Castle Hayne aquifer, which supplied water to well HP-651 and deep extraction wells 82-DRW01–82-DRW04. The PCE and TCE plumes are similar in shape for each of the eight monthly simulation results presented. Note, however, that the TCE plume has substantially greater reconstructed concentrations than the PCE plume.

During January 1958, after 10 years of simulated contaminant migration to the northwest along the hydraulic gradient, the forward edge of the PCE plume has not reached Wallace Creek (Figure S6.7*A*). The TCE plume, characterized by higher concentrations that are a consequence of greater contaminant mass and resulting source concentrations, has reached Wallace Creek by January 1958 (Figure S6.7*B*). By January 1968, after 20 years of simulated contaminant migration, the westernmost edge of the PCE plume has reached Wallace Creek (Figure S6.8*A*), and the TCE plume reached Wallace Creek all along the forward margin (Figure S6.8*B*). By June 1972, the month before the beginning of pumping at well HP-651 and after 24.5 years of contaminant migration, the PCE and TCE plumes have migrated only marginally further than during January 1968 (Figure S6.9).

During June 1978, 6 years after the start of pumping at water-supply well HP-651, the upstream margins of the PCE and TCE plumes had migrated eastward from near the location of the first source (at monitor well 06-GW01D) and were captured by pumping at well HP-651 (Figure S6.10). A deep cone of depression developed in the potentiometric surface of the Upper Castle Hayne aquifer due to a relatively high pumping rate at well HP-651—about 23,000 cubic feet per day (ft^3/d). The direction of groundwater flow near well 06-GW01D shifted from northwestward toward Wallace Creek to eastward toward well HP-651. The same basic plume shape persisted from June 1978 through November 1984, which was about 2 months before the end of pumping at water-supply well HP-651. However, during November 1984, due to a higher monthly pumping rate (about 37,000 ft^3/d), the cone of depression in the potentiometric surface was deeper than during June 1978 (Figures S6.11 and S6.10, respectively), probably causing contaminants to migrate at a faster rate.

During December 1995, about 11 years after the end of pumping at water-supply well HP-651, the hydraulic gradient and groundwater-flow direction reverted to a north-northwesterly direction. The PCE and TCE plumes slowly migrated away from well HP-651 toward Wallace Creek (Figure S6.12).

During December 2005, the effect of pumping from the four deep extraction wells 82-DRW01–82-DRW04 was apparent in the water-level contours characterized by the deep cone of depression at extraction well 82-DRW04 and shallower cones of depression at the other three extraction wells (Figure S6.13). Since January 1995 and during the operation of the extraction-well system, the average pumping rate at well 82-DRW04 was about 28,400 ft^3/d, compared with the average pumping rates at extraction wells 82-DRW01–82-DRW03 of 5,900 ft^3/d, 4,800 ft^3/d, and 7,100 ft^3/d, respectively. Pumping at extraction well 82-DRW01 ended during January 2006; by June 2008, the shallow cone of depression associated with extraction well 82-DRW01 had recovered (Figure S6.14). Both the PCE and TCE plumes had a smaller areal extent during December 2005 (Figure S6.13) and June 2008 (Figure S6.14) as a result of the operation of the extraction-well system.

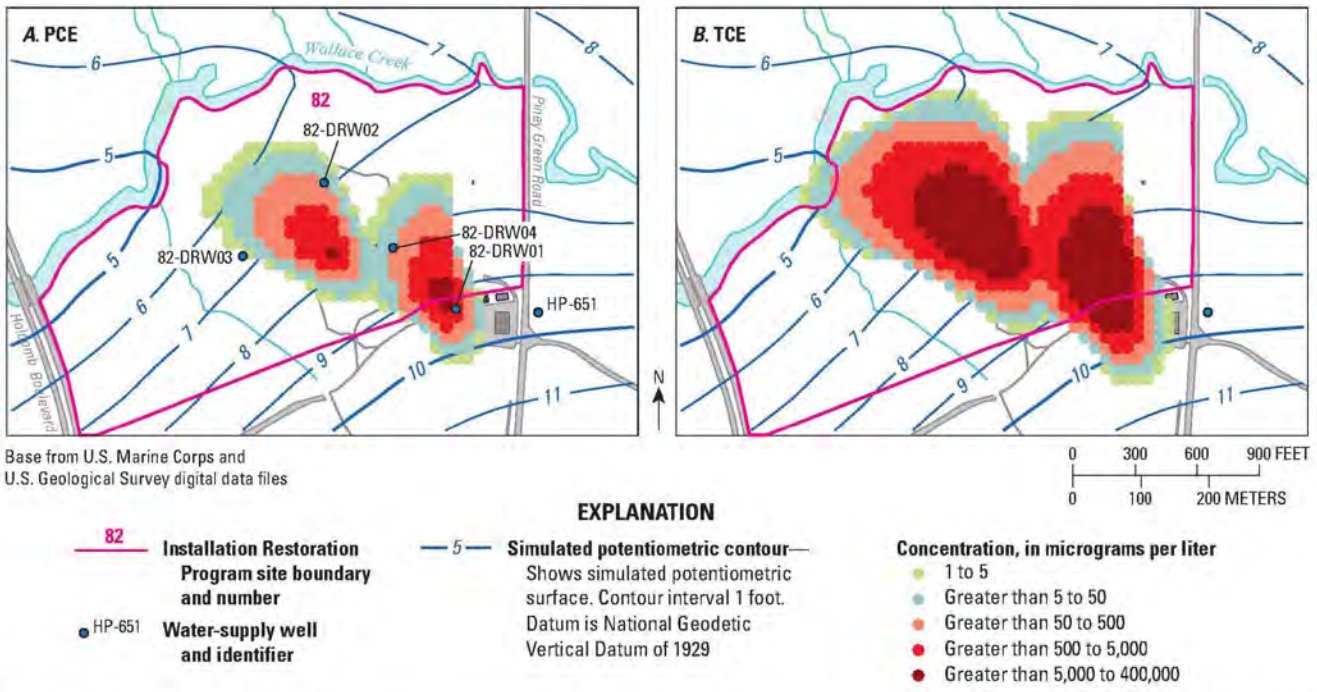

Figure S6.7. Reconstructed (simulated) water levels and distribution of *(A)* tetrachloroethylene (PCE) and *(B)* trichloroethylene (TCE) within the Hadnot Point landfill area fate and transport model subdomain, model layer 5, Hadnot Point–Holcomb Boulevard study area, U.S. Marine Corps Base Camp Lejeune, North Carolina, January 1958.

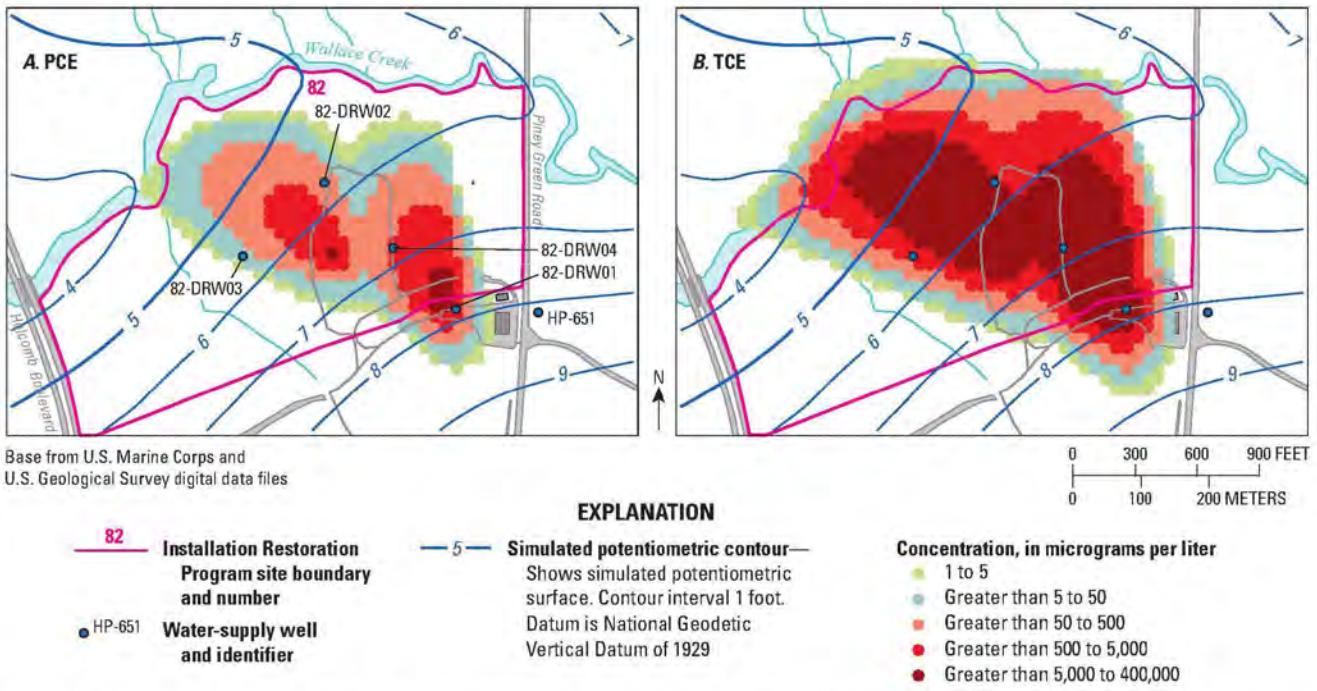

Figure S6.8. Reconstructed (simulated) water levels and distribution of *(A)* tetrachloroethylene (PCE) and *(B)* trichloroethylene (TCE) within the Hadnot Point landfill area fate and transport model subdomain, model layer 5, Hadnot Point–Holcomb Boulevard study area, U.S. Marine Corps Base Camp Lejeune, North Carolina, January 1968.

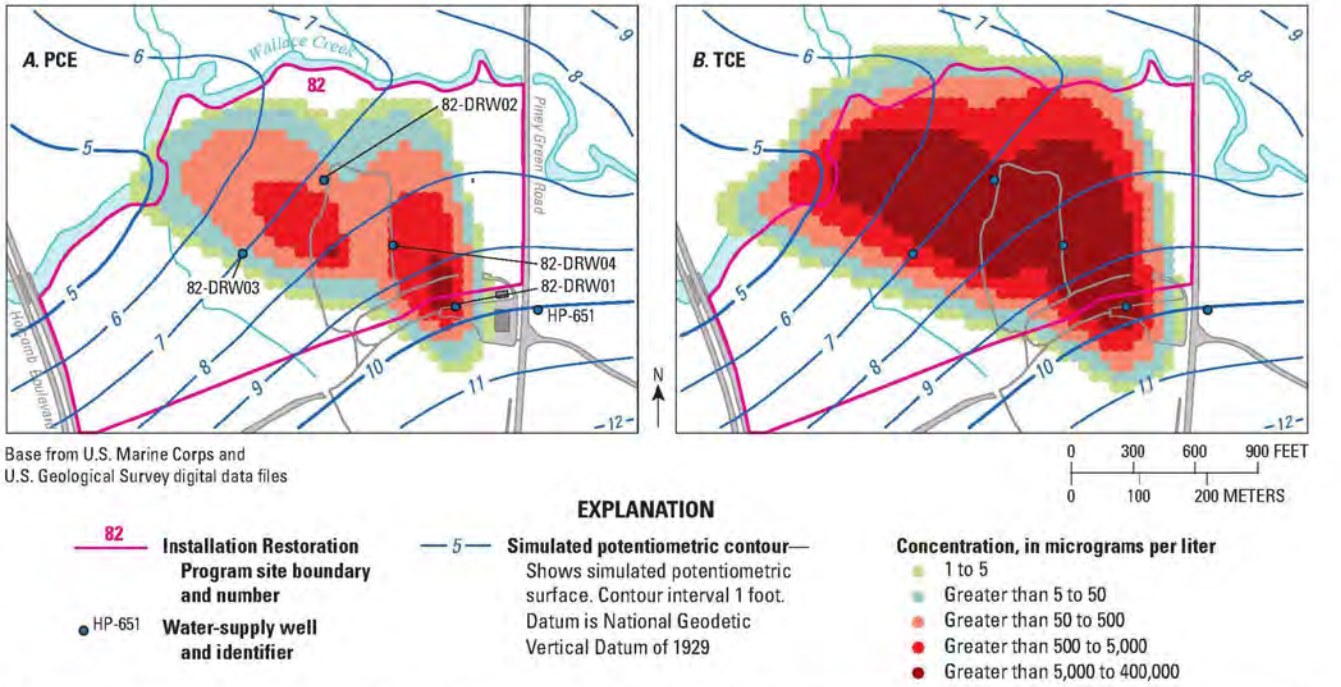

Figure S6.9. Reconstructed (simulated) water levels and distribution of *(A)* tetrachloroethylene (PCE) and *(B)* trichloroethylene (TCE) within the Hadnot Point landfill area fate and transport model subdomain, model layer 5, Hadnot Point–Holcomb Boulevard study area, U.S. Marine Corps Base Camp Lejeune, North Carolina, June 1972.

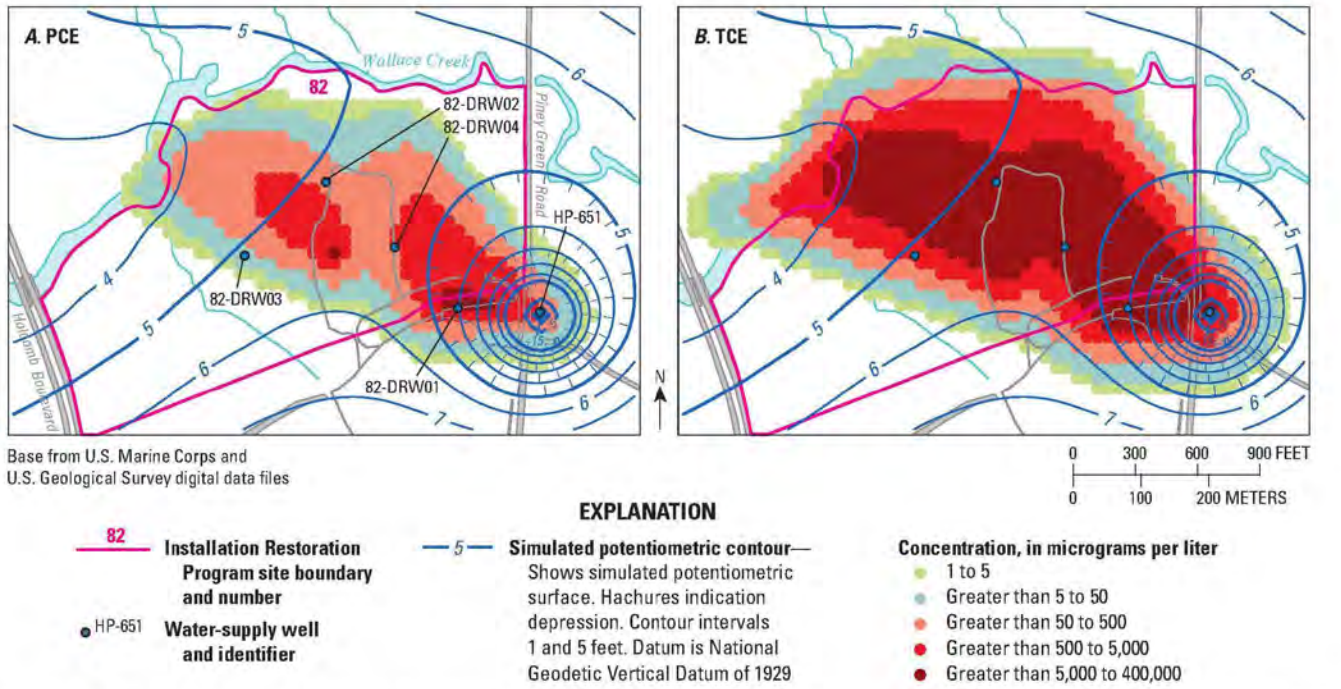

Figure S6.10. Reconstructed (simulated) water levels and distribution of *(A)* tetrachloroethylene (PCE) and *(B)* trichloroethylene (TCE) within the Hadnot Point landfill area fate and transport model subdomain, model layer 5, Hadnot Point–Holcomb Boulevard study area, U.S. Marine Corps Base Camp Lejeune, North Carolina, June 1978.

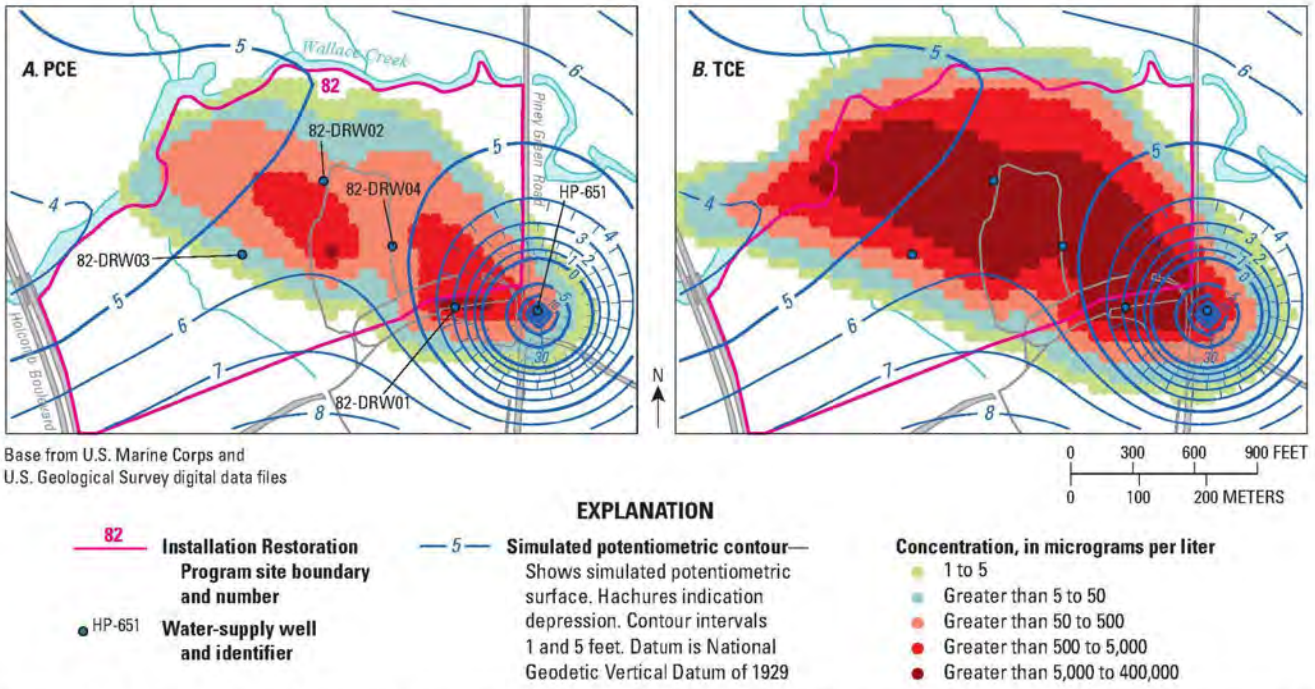

Figure S6.11. Reconstructed (simulated) water levels and distribution of *(A)* tetrachloroethylene (PCE) and *(B)* trichloroethylene (TCE) within the Hadnot Point landfill area fate and transport model subdomain, model layer 5, Hadnot Point–Holcomb Boulevard study area, U.S. Marine Corps Base Camp Lejeune, North Carolina, November 1984.

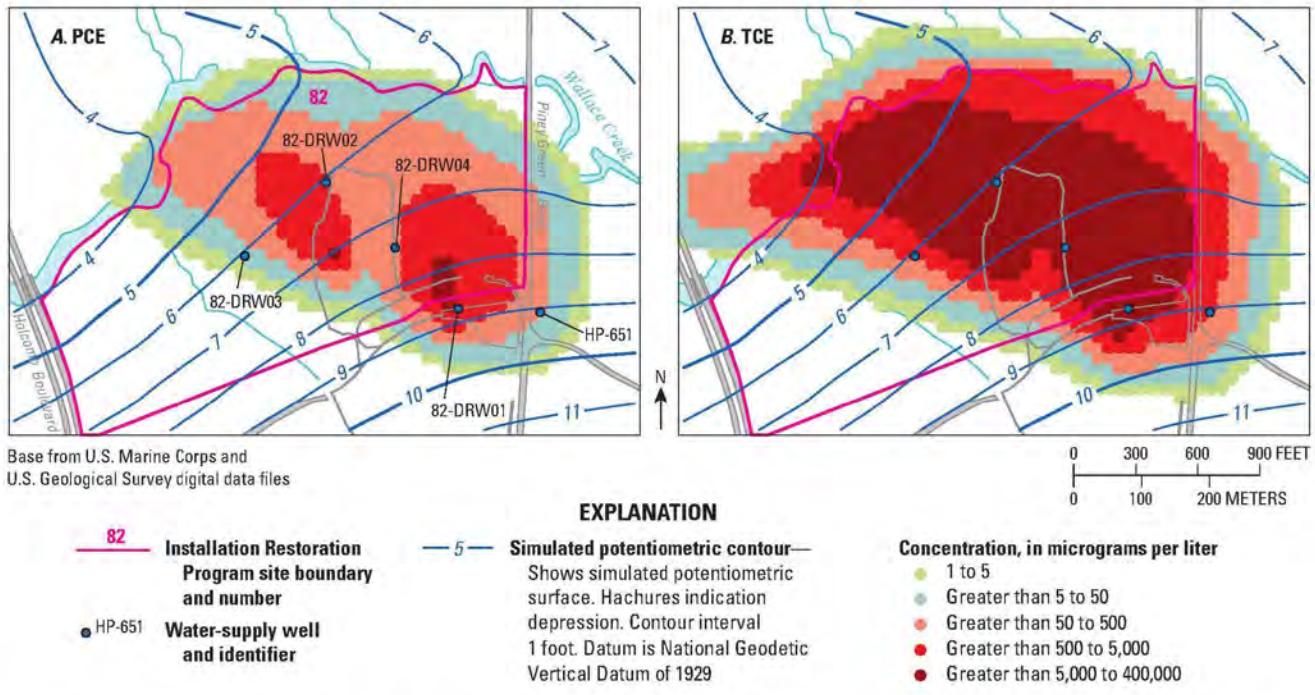

Figure S6.12. Reconstructed (simulated) water levels and distribution of *(A)* tetrachloroethylene (PCE) and *(B)* trichloroethylene (TCE) within the Hadnot Point landfill area fate and transport model subdomain, model layer 5, Hadnot Point–Holcomb Boulevard study area, U.S. Marine Corps Base Camp Lejeune, North Carolina, December 1995.

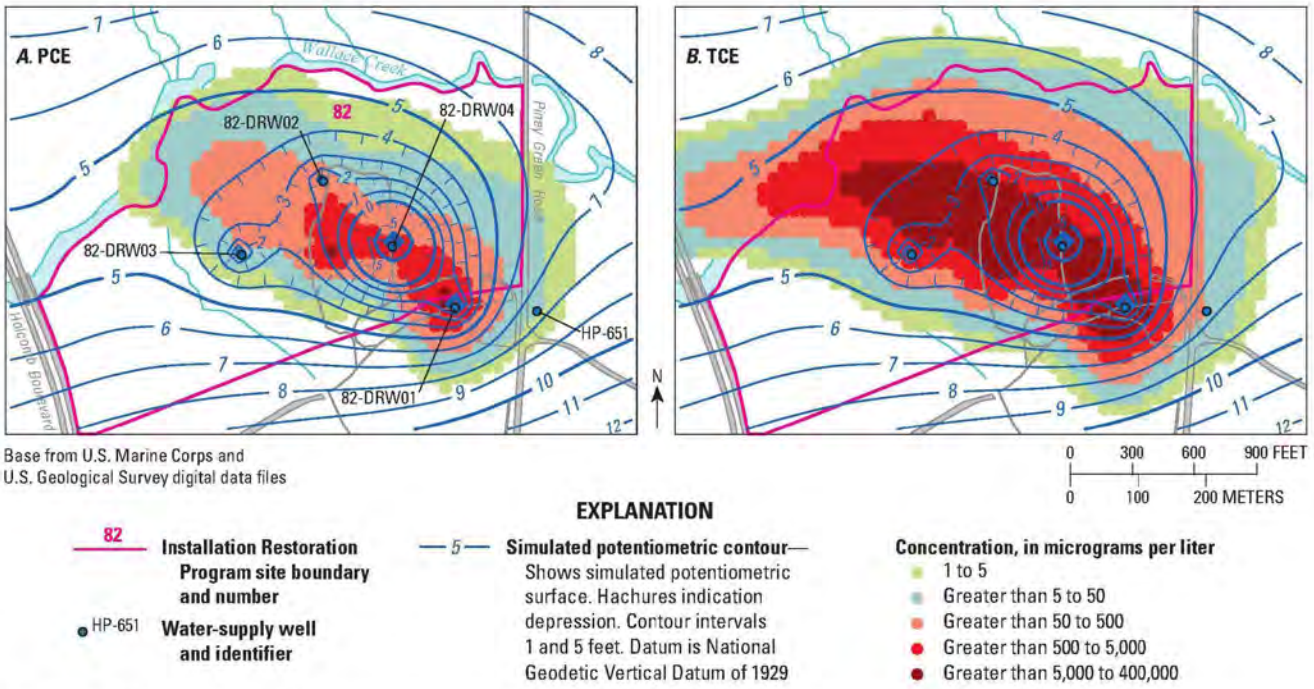

Figure S6.13. Reconstructed (simulated) water levels and distribution of *(A)* tetrachloroethylene (PCE) and *(B)* trichloroethylene (TCE) within the Hadnot Point landfill area fate and transport model subdomain, model layer 5, Hadnot Point–Holcomb Boulevard study area, U.S. Marine Corps Base Camp Lejeune, North Carolina, December 2005.

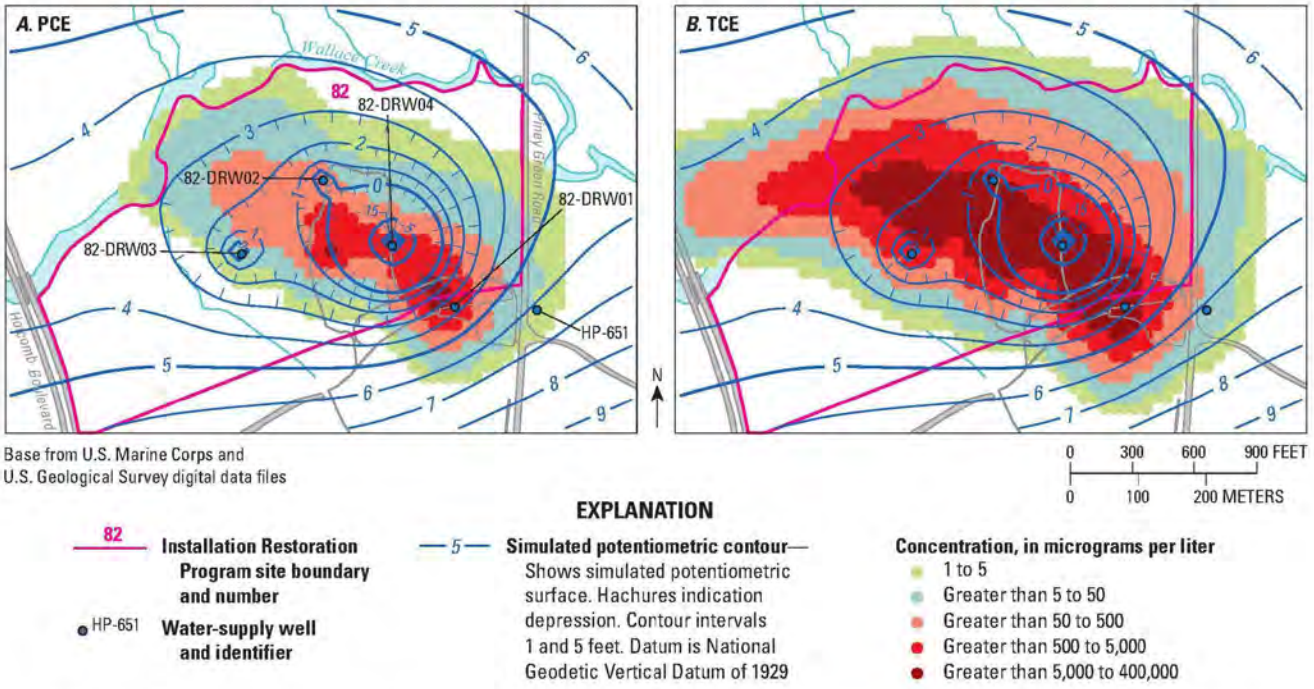

Figure S6.14. Reconstructed (simulated) water levels and distribution of *(A)* tetrachloroethylene (PCE) and *(B)* trichloroethylene (TCE) within the Hadnot Point landfill area fate and transport model subdomain, model layer 5, Hadnot Point–Holcomb Boulevard study area, U.S. Marine Corps Base Camp Lejeune, North Carolina, June 2008.

Historical Reconstruction Results

For the HPLF model, historical reconstruction results from model layer 5—corresponding to the Upper Castle Hayne aquifer system (Table S6.1)—have been presented and discussed in detail. This is because water-supply well HP-651—the only contaminated water-supply well in the area—is open solely to the Upper Castle Hayne aquifer system. Areal distributions of reconstructed PCE and TCE concentrations for model layers 1, 3, and 5 for four periods—January 1968, June 1978, November 1984, and June 2008—are shown in Figures S6.15 and S6.16, respectively. Model layers 1, 3, and 5 represent major water-bearing units in the study area and are correlated with the Brewster Boulevard aquifer system, the Tarawa Terrace aquifer, and the Upper Castle Hayne aquifer, respectively (Table S6.1). The sizes and shapes of the PCE and TCE plumes are similar for each of the three model layers; the contaminant plumes originated at each of the two specified concentration nodes and migrated in a northwesterly direction toward Wallace Creek. After pumping started at water-supply well HP-651 during July 1972, the PCE and TCE plumes in model layer 5 migrated toward well HP-651 by June 1978 (Figures S6.9 and S6.10, respectively). By contrast, in model layers 1 and 3, PCE and TCE plumes migrated more slowly toward well HP-651. The prominent differences among the layers in the configuration of reconstructed water levels are due to variations in the input pumping rates for the model layers and the presence of the simulated groundwater drain representing Wallace Creek in model layer 1. Steep cones of depression are present in model layer 5 at well HP-651 during June 1978 and November 1984 (Figures S6.10 and S6.11, respectively) and at extraction well 82-DRW04 during June 2008 (Figure S6.14). However, the cones of depression are progressively shallower and less prominent in model layers 3 and 1 for these monthly results, indicating that contaminant migration in layer 5 is faster than in layers 1 and 3 because of higher velocities in model layer 5 induced by the operation of water-supply well HP-651. In model layer 1, Wallace Creek is apparent as a groundwater drain as indicated by water-level contours pointing sharply upstream.

To illustrate the relative effect of pumping water-supply well HP-651 and the subsequent operation of the extraction system, a section line (A–A') was constructed from a point upgradient (southeast) of water-supply well HP-651, to well HP-651, to three of the four extraction wells (82-DRW01, 82-DRW04, and 82-DRW02), then continuing northwestward across Wallace Creek, to a point beyond Wallace Creek (Figure S6.17). The model cells coincident with section line A–A' are shown in Figure S6.17*A*, and the water levels for the previously discussed eight monthly historical reconstruction results are shown in Figure S6.17*B*. For results for 4 months—January 1958, January 1968, June 1972, and December 1995—there was no pumping from any of the wells along the section. Thus, water levels reflect the unstressed gradient from the southeast end of section line A–A' to Wallace Creek. The small differences in water levels for the unstressed monthly results are due to differences in simulated recharge.

During June 1978, more than 25 ft of drawdown (water-level decline from unstressed periods) are apparent at water-supply well HP-651 as a consequence of pumping the well at a rate of about 120 gpm. The higher rate of pumping at well HP-651 during November 1984 (about 190 gpm) produces a drawdown of almost 40 ft. By December 2005, the cones of depression due to pumping at three extraction wells are apparent. Extraction well 82-DRW04, which had the highest average pumping rate of all of the extraction wells (about 150 gpm), causes a drawdown of more than 20 ft, whereas the other two extraction wells, 82-DRW02 and 82-DRW01 (average pumping rates of about 25 gpm and 30 gpm, respectively), cause a drawdown of less than 5 ft. By June 2008, pumping at extraction well 82-DRW01 has ended, and the water level has recovered.

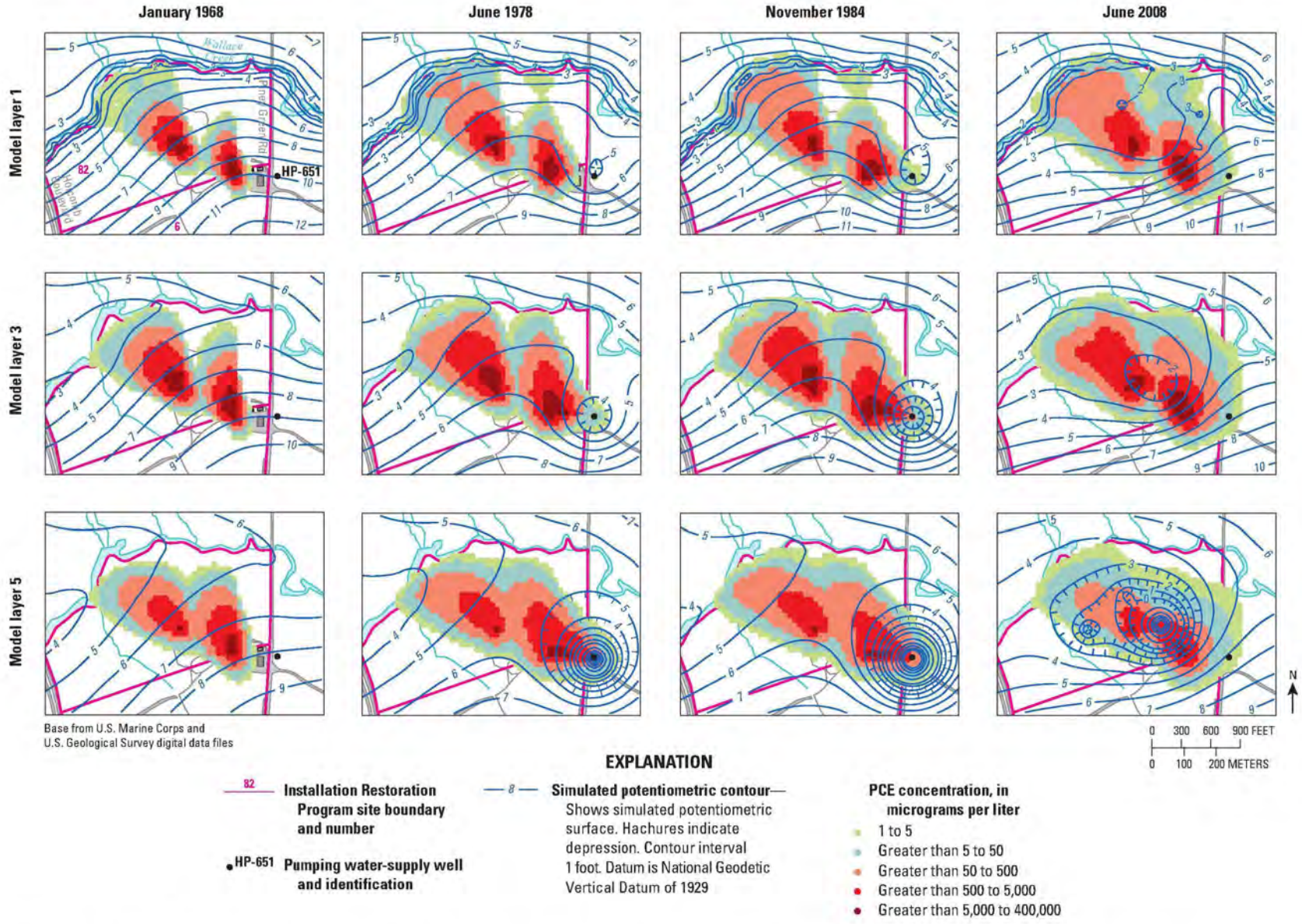

Figure S6.15. Reconstructed (simulated) water levels and distribution of tetrachloroethylene (PCE) within the Hadnot Point landfill area fate and transport model subdomain, model layers 1, 3, and 5, Hadnot Point–Holcomb Boulevard study area, U.S. Marine Corps Base Camp Lejeune, North Carolina, January 1968, June 1978, November 1984, and June 2008. (See Figure A14 for location; see Appendix A6 for more detailed maps and results.)

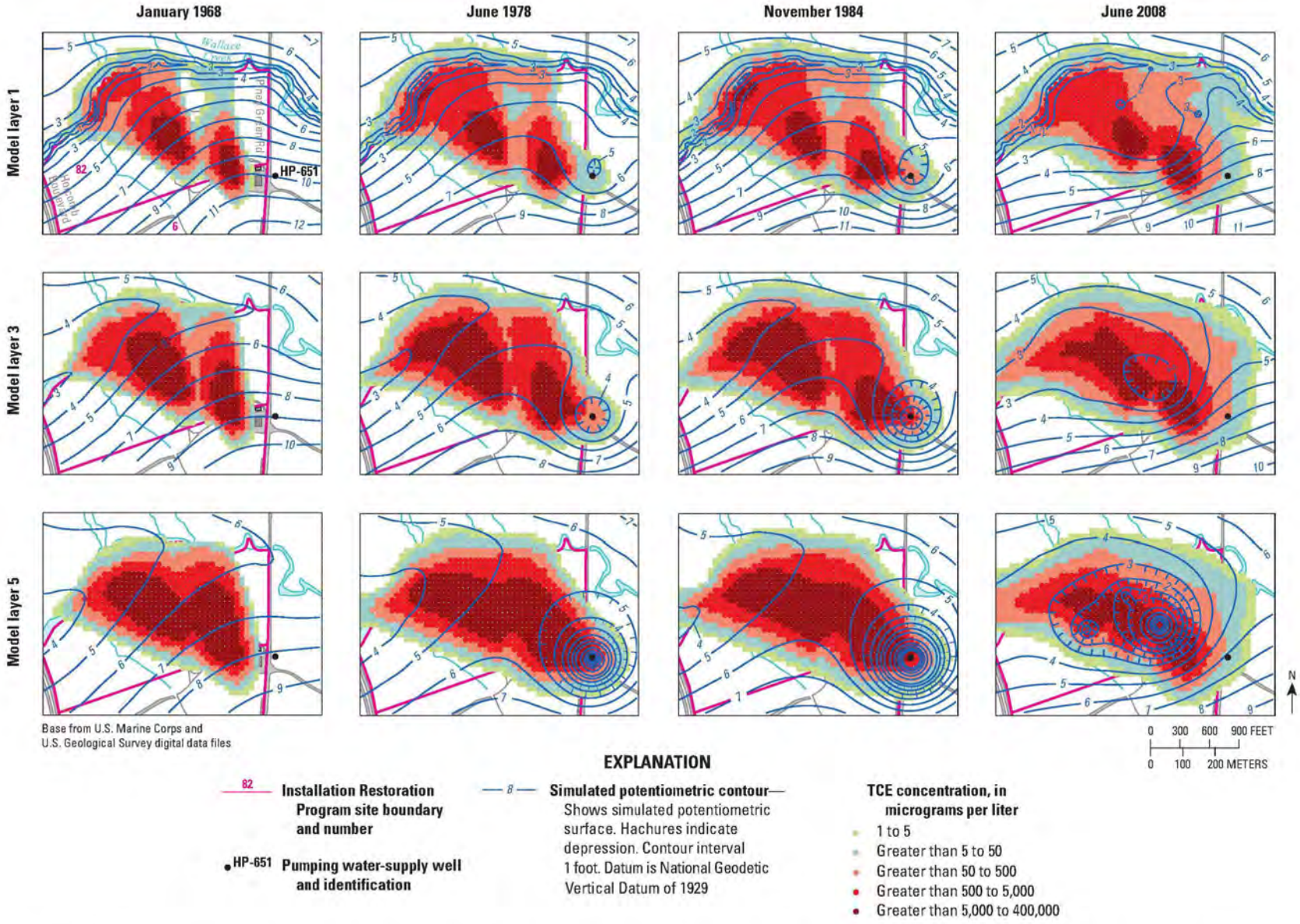

Figure S6.16. Reconstructed (simulated) water levels and distribution of trichloroethylene (TCE) within the Hadnot Point landfill area fate and transport model subdomain, model layers 1, 3, and 5, Hadnot Point–Holcomb Boulevard study area, U.S. Marine Corps Base Camp Lejeune, North Carolina, January 1968, June 1978, November 1984, and June 2008. (See Figure A13 for location; see Appendix A4 for more detailed maps and results.)

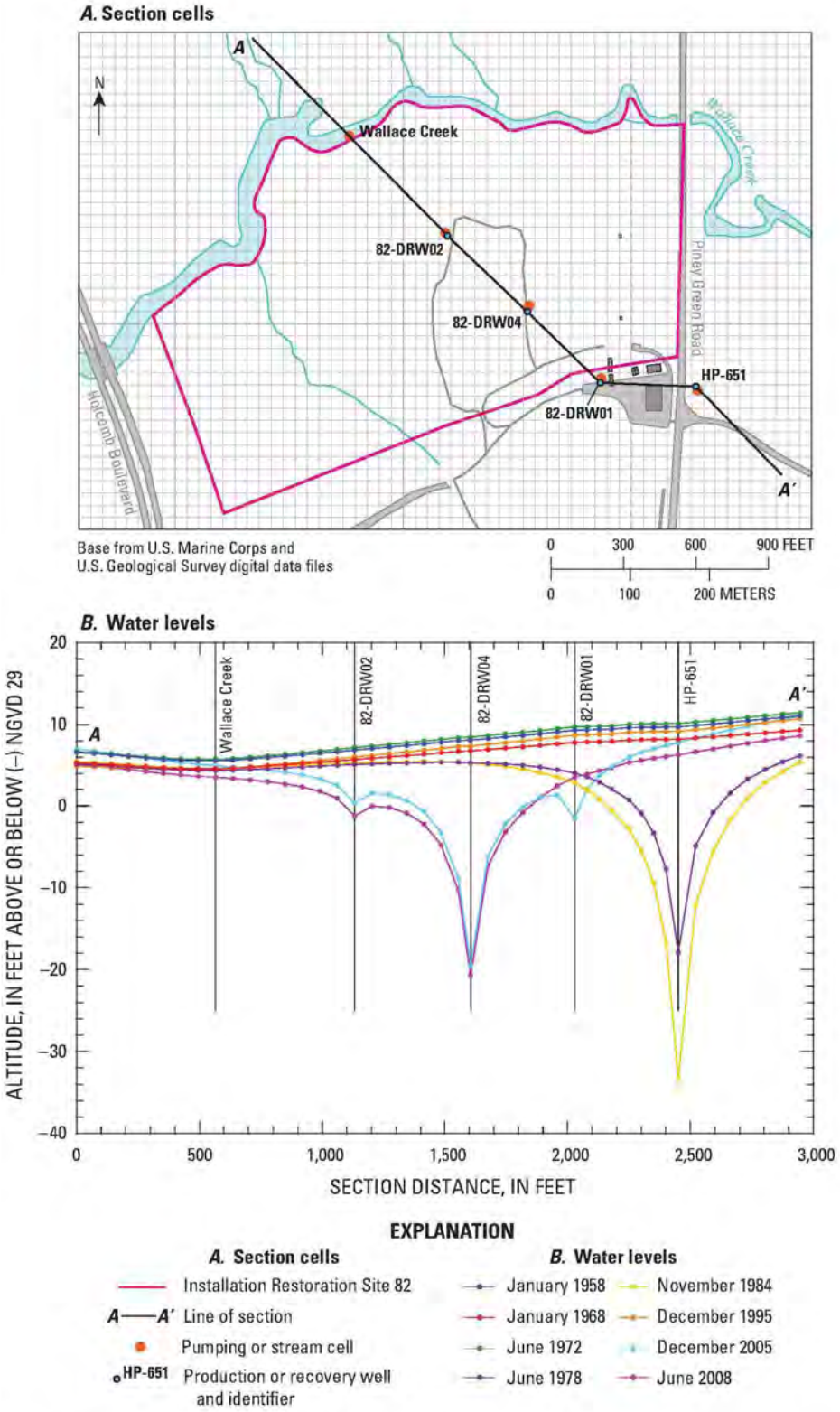

Figure S6.17. *(A)* Line of section *A–A′* and *(B)* simulated water levels within the Hadnot Point landfill area fate and transport model subdomain, model layer 5, Hadnot Point–Holcomb Boulevard study area, U.S. Marine Corps Base Camp Lejeune, North Carolina.

Sensitivity Analyses

Sensitivity analyses were conducted by using ranges of values of selected parameters associated with the MODFLOW model input (flow parameters) and the MT3DMS model input (fate and transport parameters). Simply stated, sensitivity analysis is a method for evaluating the effect of variation of model input parameter values (e.g., recharge, dispersivity), within physically realistic ranges of values, on resulting model output parameter values (e.g., potentiometric levels, contaminant concentrations). The results from all sensitivity analyses were used to define a range of finished-water concentrations at the HPWTP. Details of the sensitivity analyses conducted on groundwater-flow model parameter values that were used to evaluate parameter variation effects on groundwater levels are described in Suárez-Soto et al. (2013).

Flow Parameters

Flow parameters that were selected for the sensitivity analysis included the hydraulic conductivity, K_h, of each model layer, hydraulic conductivity of all layers, and recharge. Each parameter was decreased and increased by one order of magnitude from its calibrated value (Figure S6.18) in three steps in successive steady-state simulations by using parameter multipliers of 0.1, 0.2, 0.5, 2.0, 5.0, and 10.0.[24] The resulting root-mean-square (RMS) of water-level residuals defines a sensitivity curve or line for each of the aforementioned parameters of variation (Figure S6.18). For each parameter, minimum and maximum values of the multiplier (shown in the lower and upper tails of the sensitivity curve, respectively) that have an RMS residual of 5 ft were determined through additional simulations and interpolation. If a tail of a sensitivity curve did not exceed an RMS residual of 5 ft when varying

[24] A multiplier of 1.0 indicates a calibrated parameter value.

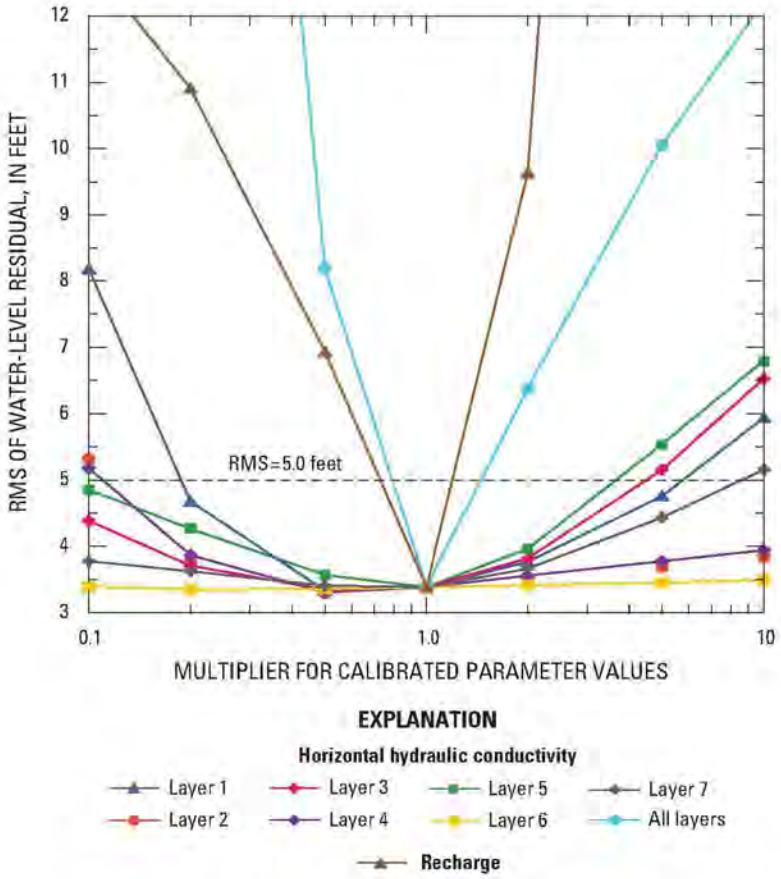

Figure S6.18. Sensitivity of steady-state (predevelopment) simulation results to changes in groundwater-flow model parameter values based on change in root-mean-square (RMS) of water-level residuals, Hadnot Point–Holcomb Boulevard study area, U.S. Marine Corps Base Camp Lejeune, North Carolina (from Suárez-Soto et al. 2013).

a parameter value by plus or minus one order of magnitude (multiplier less than 0.1 or greater than 10), the parameter being varied was interpreted and rated as insensitive. Otherwise, the multipliers resulting in RMS residuals of 5 ft were rated as low in sensitivity (multiplier of 0.1–0.2 or 5–10), moderate in sensitivity (multiplier of 0.2–0.5 or 2–5), or high in sensitivity (multiplier of 0.5–1 or 1–2) (Table S6.6). The values of the flow parameters corresponding to the minimum and maximum parameter multipliers determined in this manner are identified in this report as the *calibration-constrained* values of the flow parameter.

Interpretation of sensitivity analyses results shown in Figure S6.18 indicates that the steady-state (predevelopment) groundwater-flow potentiometric levels are most sensitive to changes in the hydraulic conductivity of all layers and to recharge; the least sensitive groundwater-flow model parameters are the hydraulic conductivities of layers 6 and 7. The rated sensitivities for hydraulic conductivities of the other model layers are a mixture of sensitivities ranging from insensitive, to low sensitivity, to moderate sensitivity (Table S6.6).

By using the calibration-constrained values of the aforementioned flow parameters, contaminant fate-and-transport simulations were conducted to determine the ranges of simulated PCE and TCE concentrations at historically contaminated water-supply wells that result from varying each of the flow parameters. PCE and TCE concentrations at water-supply well HP-651 (in the HPLF subdomain) that were simulated by using the calibrated and the calibration-constrained values of each flow parameter are shown in Appendix S6.2 (Figures S6.2.1– S6.2.4). TCE concentrations at water-supply well HP-634 (in the HPIA subdomain) that were simulated by using the calibrated and the calibration-constrained values of each flow parameter also are shown in Appendix S6.2 (Figures S6.2.5–S6.2.6).

Pumping rates of water-supply wells were varied by using an analysis similar to that described by Maslia et al. (2009). Resulting monthly pumping rate variation factors (or multipliers) derived by using the analysis described in Maslia et al. (2009) are listed in Table S6.7. Calibrated monthly pumping rates were multiplied by variation factors listed in Table S6.7. The corresponding PCE and TCE concentrations at well HP-651 and TCE concentrations at well HP-634 were simulated by using the calibrated and extreme values of water-supply well pumping (Appendix S6.2, Figures S6.2.3, S6.2.5, and S6.2.7).

Table S6.6. Minimum and maximum model flow-parameter multipliers and rated sensitivity of steady-state (predevelopment) simulation results to changes in flow parameters based on change in root-mean-square of water-level residuals, Hadnot Point–Holcomb Boulevard study area, U.S. Marine Corps Base Camp Lejeune, North Carolina.

[K_h, Hydraulic conductivity; <0.1, multiplier less than 0.1; >10.0, multiplier greater than 10.0]

Model parameter	Minimum	Maximum
K_h layer 1	0.18	5.87
K_h layer 2	0.11	>10.00
K_h layer 3	<0.10	4.59
K_h layer 4	0.11	>10.00
K_h layer 5	<0.10	3.74
K_h layer 6	<0.10	>10.00
K_h layer 7	<0.10	8.66
K_h all layers	0.66	1.51
Recharge	0.70	1.43

EXPLANATION

Sensitivity rating	Minimum	Maximum
Insensitive	<0.10	>10
Low	0.10 to 0.20	5 to 10
Moderate	0.20 to 0.50	2 to 5
High	0.50 to 1	1 to 2

Table S6.7. Minimum and maximum water-supply well pumping multipliers for Hadnot Point and Holcomb Boulevard water treatment plant service areas, Hadnot Point–Holcomb Boulevard study area, U.S. Marine Corps Base Camp Lejeune, North Carolina.

Month	Hadnot Point		Holcomb Boulevard	
	Minimum	Maximum	Minimum	Maximum
January	0.909	1.210	0.785	1.136
February	0.920	1.209	0.847	1.167
March	0.940	1.070	0.822	1.074
April	0.899	1.033	0.874	1.182
May	0.901	1.046	0.916	1.127
June	0.927	1.105	0.984	1.326
July	0.948	1.093	0.970	1.170
August	0.935	1.125	0.970	1.323
September	0.921	1.061	0.878	1.285
October	0.859	1.026	0.823	1.249
November	0.882	1.042	0.795	1.044
December	0.909	1.070	0.753	1.002

Fate and Transport Parameters

Transport parameters for a contaminant fate and transport model applied to the TT study area are described in Maslia et al. (2007) and were the subject of an uncertainty analysis using pseudo-random number generation and Monte Carlo simulation. These transport parameters included distribution coefficient (K_d), bulk density (ρ), effective porosity (n_E), reaction rate (r), contaminant concentration (C), and longitudinal dispersivity (α_L). Because field data describing contaminant fate and transport parameters is lacking for the HPHB study area and the TT study area is adjacent to the HPHB study area, the probability density functions described by Maslia et al. (2009) were used to generate a range of transport parameters values for the analyses reported herein. The mean values listed in Table S6.8 correspond to the calibrated parameter values for the HPIA and HPLF models. The standard deviation listed in Table S6.8 are based on the standard deviations presented by Maslia et al. (2009). See Table S6.8 for details. The ranges of values—minimum and maximum—were used as input for the fate-and-transport models developed for the HPIA and HPLF models. Minimum and maximum values of the transport model parameters (Table S6.8) were derived by using the 2.5 and 97.5 percentiles (the mean ±1.96 times the standard deviation). However, α_L was assumed by Maslia et al. (2009) to be log-normally distributed. To obtain the 2.5 and 97.5 percentiles for α_L, the results of Maslia et al. (2009) were used to adjust the standard deviation of α_L, which was then transformed by the natural logarithm. Then, the 2.5 and 97.5 percentiles of $\ln(\alpha_L)$ were calculated and transformed back to an arithmetic scale.

PCE and TCE concentrations at water-supply well HP-651 and TCE concentrations at water-supply well HP-634 were simulated by using calibrated and 2.5 and 97.5 percentiles of each transport model parameter (Appendix S6.2). Except for longitudinal dispersivity, as discussed below, model results were generally most sensitive to variations in partition coefficient, porosity, and concentration. For the period of operation for well HP-651, contaminant concentrations were higher for minimum values of partition coefficient and porosity and maximum values of concentration.

It should be noted that the graphs showing PCE and TCE concentrations at water-supply well HP-651 using the 97.5 percentile of dispersivity increase the concentrations of PCE and TCE significantly more than changes in the other parameter values (Figures S6.2.7 and S6.2.8). The excessive increase in concentrations is related to increased contaminant mass entering the fate and transport subdomain area at the constant-concentration source cells. The higher value of α_L causes solute mass to move away from cells adjacent to the source cells more rapidly, increasing the local concentration gradient, which causes more contaminant mass to enter the system. In subsequent simulations, the constant-concentration sources for TCE were transformed into equivalent mass-loading rates based on an analysis of the average mass of TCE entering the system. The model was much less sensitive to increases in α_L when using the equivalent mass-loading boundary condition (Figure S6.19).

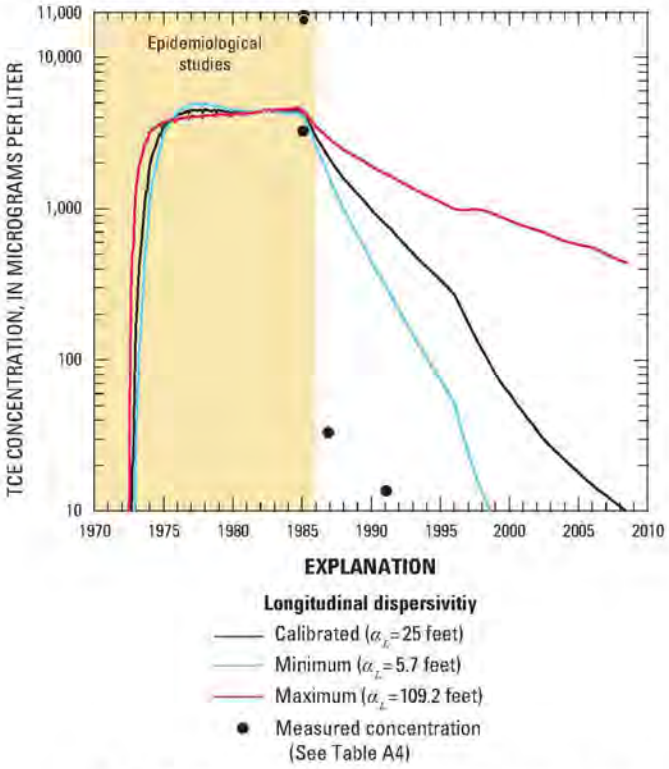

Figure S6.19. Trichloroethylene (TCE) concentrations at water-supply well HP-651 for calibrated value and minimum and maximum values of longitudinal dispersivitiy (α_L) for an equivalent mass-loading rate, Hadnot Point landfill area fate and transport model, layer 5, Hadnot Point–Holcomb Boulevard study area, U.S. Marine Corps Base Camp Lejeune, North Carolina.

Table S6.8. Minimum and maximum transport model parameter values obtained by using normal statistics, Hadnot Point–Holcomb Boulevard study area, U.S. Marine Corps Base Camp Lejeune, North Carolina.

[TCE, trichloroethylene; PCE, tetrachloroethylene; HPLF, Hadnot Point landfill; HPIA, Hadnot Point Industrial Area; ft³/g, cubic feet per gram; g/ft³, grams per cubic foot; [–], dimensionless; d⁻¹, per day; mg/L, milligrams per liter; ft, feet]

[1]Model input parameter	Unit	Normal statistics		2.5–97.5 percentile range	
		[2]Mean, $\bar{X}$	[3]Standard deviation, σ	Minimum ($\bar{X}$–1.96 σ)	Maximum ($\bar{X}$+1.96 σ)
Distribution coefficient, K_d					
TCE	ft³/g	5.3×10^{-6}	1.3×10^{-6}	2.7×10^{-6}	7.9×10^{-6}
PCE	ft³/g	1.1×10^{-5}	2.7×10^{-6}	5.4×10^{-6}	1.6×10^{-5}
Bulk density, ρ_B	g/ft³	47,000	610	46,000	48,000
Effective porosity, n_E	[–]	0.20	4.5×10^{-2}	0.11	0.29
Reaction rate, r	d⁻¹				
PCE and TCE (HPLF)	d⁻¹	1.4×10^{-4}	3.4×10^{-5}	7.4×10^{-5}	2.1×10^{-4}
TCE (HPIA)	d⁻¹	2.0×10^{-3}	4.8×10^{-4}	1.1×10^{-3}	2.9×10^{-3}
Benzene (HPIA)	d⁻¹	1.0×10^{-4}	2.4×10^{-5}	5.3×10^{-5}	1.5×10^{-4}
Contaminant concentration, C					
Hadnot Point Industrial Area					
TCE	mg/L	640	52	540	740
Benzene	mg/L	1.7	0.14	1.4	2.0
Landfill					
TCE					
Source 1, layers 1–7	mg/L	380	31	320	450
Source 2, layers 1–7	mg/L	260	21	220	300
PCE					
Source 1					
Layer 1	mg/L	110	8.5	88	120
Layer 2	mg/L	83	6.8	70	96
Layer 3	mg/L	66	5.4	56	77
Layer 4	mg/L	46	3.7	39	53
Layer 5	mg/L	16	1.3	13	19
Source 2					
Layer 1	mg/L	42	3.4	35	49
Layer 2	mg/L	33	2.7	28	38
Layer 3	mg/L	27	2.2	23	31
Layer 4	mg/L	18	1.5	15	21
Layer 5	mg/L	6.0	0.49	5.0	7.0
[4]Longitudinal dispersivity, α_L	ft	3.2	0.75	5.7	109

[1] All parameters are assumed to be normally distributed except longitudinal dispersivity which is assumed to be lognormally distributed

[2] Mean values correspond to the calibrated values for the HPIA and HPLF models

[3] Standard deviation were obtained based on the standard deviations described by Maslia et al. (2009). For parameter calibrated values used in the HPIA and HPLF models that differed from the corresponding parameter values used in the TT study area model, the standard deviation was adjusted using the following formula:

$$\sigma_{HPHB} = \frac{\bar{X}_{HPHB}}{\bar{X}_{TT}} \sigma_{TT}$$

where

σ_{HPHB} is the standard deviation statistic used in the current study

$\bar{X}_{HPHB}$ is the mean statistic used in the current study. This value corresponds to the calibrated parameter value for the HPIA and HPLF models

$\bar{X}_{TT}$ is the mean statistic used in the Tarawa Terrace study described by Maslia et al (2009)

σ_{TT} is the standard deviation statistic used in the Tarawa Terrace study described by Maslia et al (2009)

[4] Longitudinal dispersivity is assumed to be log normally distributed. Mean and standard deviation values shown are log-transformed using the natural log before they were used to calculate the 2.5 and 97.5 percentile

Cell-Size Sensitivity Analysis

Contaminant fate and transport simulations can exhibit numerical instabilities related to spatial discretization (finite difference grid cell size), which in turn can affect simulated concentrations and computed contaminant mass. The Peclet number (P_e) provides a criterion for controlling numerical oscillations due to spatial discretization when its value is less than or equal to 2 (Daus and Frind 1985; Zheng and Bennett 2002). The Peclet number is physically interpreted as the ratio of advective (V) to dispersive (D) transport terms and is defined as

$$P_e = \frac{V\Delta l}{D}, \tag{S6.4}$$

where

P_e is Peclet number, dimensionless;
V is simulated groundwater-flow velocity $[LT^{-1}]$;
Δl is a characteristic length $[L]$; and
D is dispersion coefficient $[L^2T^{-1}]$.[25]

In a one-dimensional, uniform flow field, Equation S6.4 reduces to

$$P_e = \frac{\Delta l}{\alpha_L}, \tag{S6.5}$$

where α_L is the aquifer dispersivity, $[L]$. By substituting into Equation S6.5 the finite difference cell dimension assigned to the HPIA and HPLF fate and transport model subdomains of 50 ft and the calibrated α_L value of 25 ft (Table S6.3), a P_e value of 2 is obtained, thereby satisfying the aforementioned criterion for controlling oscillations due to spatial discretization. Because of aquifer heterogeneity and water-supply well operations, the flow field in the HPHB study area is not uniform and is three-dimensional. Therefore, a more robust analysis for evaluating P_e (Equation S6.4) is presented.

In a three-dimensional groundwater-flow system, the dispersion coefficient (D) in Equation S6.4 is represented by a dispersion tensor and contains nine terms (Zheng and Bennett 2002):

$$\boldsymbol{D} = \begin{bmatrix} D_{xx} & D_{xy} & D_{xz} \\ D_{yx} & D_{yy} & D_{yz} \\ D_{zx} & D_{zy} & D_{zz} \end{bmatrix}, \tag{S6.6}$$

where $\boldsymbol{D}$ is the dispersion tensor. The dispersion tensor components (e.g., D_{xx}, D_{xy}) are defined in terms of groundwater velocity ($\boldsymbol{V}$) and its directional components (V_x, V_y, and V_z), horizontal, transverse, and vertical dispersivity (α_L, α_T, and α_V; e.g., Table S6.3), and the effective molecular diffusion coefficient (D^*, Table S6.3). If the axes of the computational grid are aligned with the principal directions of groundwater velocity or the cross-terms of $\boldsymbol{D}$ are assumed to be negligible (and approaching zero), then Equation S6.6 reduces to a diagonal matrix containing only the diagonal terms of $\boldsymbol{D}$ such that (Zheng and Bennett 2002)

$$\boldsymbol{D} = \begin{bmatrix} D_{xx} & 0 & 0 \\ 0 & D_{yy} & 0 \\ 0 & 0 & D_{zz} \end{bmatrix}, \tag{S6.7}$$

where:

$$D_{xx} = \alpha_L \frac{V_x^2}{|\boldsymbol{V}|} + \alpha_T \frac{V_y^2}{|\boldsymbol{V}|} + \alpha_V \frac{V_z^2}{|\boldsymbol{V}|} + D^*, \tag{S6.8a}$$

$$D_{yy} = \alpha_L \frac{V_y^2}{|\boldsymbol{V}|} + \alpha_T \frac{V_x^2}{|\boldsymbol{V}|} + \alpha_V \frac{V_z^2}{|\boldsymbol{V}|} + D^*, \tag{S6.8b}$$

$$D_{zz} = \alpha_L \frac{V_z^2}{|\boldsymbol{V}|} + \alpha_T \frac{V_x^2}{|\boldsymbol{V}|} + \alpha_V \frac{V_y^2}{|\boldsymbol{V}|} + D^*, \text{ and} \tag{S6.8c}$$

$$|\boldsymbol{V}| = \sqrt{\left(V_x^2 + V_y^2 + V_z^2\right)}. \tag{S6.8d}$$

Equation S6.4 can now be solved using the diagonal term of the dispersivity tensor (Equation S6.7) to define a Peclet number corresponding to each directional axis, as follows:

$$P_{ex} = \frac{V_x \Delta x}{D_{xx}}, \tag{S6.9a}$$

$$P_{ey} = \frac{V_y \Delta y}{D_{yy}}, \text{ and} \tag{S6.9b}$$

$$P_{ez} = \frac{V_z \Delta z}{D_{zz}}. \tag{S6.9c}$$

In Equations S6.9a–c, Δx, Δy, and Δz correspond to the finite-difference cell dimensions along rows, columns, and model layers, respectively, for the HPIA and HPLF contaminant fate and transport model subdomain areas.

[25] L represents length units; T represents time units; L^0 indicates a dimensionless variable.

To compute the Peclet numbers defined in Equations S6.9a–c, the directional values of velocity and the diagonal terms of the dispersion tensor were extracted from the MT3DMS contaminant fate and transport model code for specific finite-difference cells and simulation months of interest to the ATSDR epidemiological studies. For the HPIA, the cell nearest water-supply well HP-608 (Figure S6.2) was used to compute Equation S6.9 terms for conditions during January 1968 (start of health studies) and November 1984 (month prior to cessation of pumping of water-supply well HP-608). For the HPLF area, the cell nearest water-supply well HP-651 (Figure S6.3) was used to compute Equation S6.9 terms for conditions during June 1972 (start of operations of the well) and November 1984. Peclet number calculations for the calibrated HPIA and HPLF contaminant fate and transport subdomain model locations are listed in Table S6.9 along with values for components of velocity and the dispersion tensor.

For water-supply well HP-608 (HPIA subdomain model), results indicate that the computed Peclet numbers are below or somewhat higher than 2, the criterion indicated by Daus and Frind (1985) for controlling numerical oscillations. However, because the Peclet numbers were computed for a cell directly affected by water-supply well HP-608, cells further distant from the well would have substantially lower velocities, thereby meeting the Peclet criterion. For water-supply well HP-651 (HPLF subdomain model), results indicate that the computed Peclet numbers are greater than 6 for the horizontal Peclet number component (P_{ex}) and less than 1 for the transverse and vertical Peclet number components (P_{ey} and P_{ez}, respectively). These results indicate that the flow field near water-supply well HP-651 is an advective-dominated flow field, principally because well HP-651 was the only major water-supply well in the area and it was withdrawing groundwater solely from one zone—model layer 5. If the finite difference grid is refined whereby cell dimensions are reduced to 25 ft per side or 12.5 ft per side in the areal discretization (Δx and Δy), the resulting Peclet numbers in the vicinity of the aforementioned water-supply wells would approximately be reduced by corresponding factors of 2 and 4, respectively.

To further assess the propensity for numerical oscillations because of inappropriate spatial discretization (resulting in Peclet numbers greater than 2 in the vicinity of water-supply well HP-651), descriptions of model simulations conducted by using the aforementioned refined cell dimensions (25 ft and 12.5 ft per side) for the HPLF contaminant fate and transport subdomain model are presented below.

Table S6.9. Results of Peclet number calculations for the Hadnot Point Industrial Area (HPIA) and Hadnot Point landfill (HPLF) area contaminant fate and transport subdomain models, Hadnot Point–Holcomb Boulevard study area, U.S. Marine Corps Base Camp Lejeune, North Carolina.

Simulation month and year (Stress period)	Cell dimensions (ft)			Velocity (ft/d)			Dispersion (ft²/d)			Peclet number (Equation A8)		
	Δx	Δy	Δz	V_x	V_y	V_z	D_{xx}	D_{yy}	D_{zz}	P_{ex}	P_{ey}	P_{ez}
Hadnot Point Industrial Area, water-supply well HP-608[1]												
Jan. 1968 (313)	50.0	50.0	33.6	12.9	0.7	–0.7	223	37.5	0.7	2.9	0.1	3.5
Nov. 1984 (515)	50.0	50.0	33.6	5.1	–0.1	–0.04	133	20.4	0.4	1.9	0.3	2.9
Hadnot Point landfill (HPLF) area, water-supply well HP-651[2]												
June 1972 (367)	50.0	50.0	57.2	–16.5	–0.05	0.0	126	47.6	1.1	6.6	0.1	0.0
Nov. 1984 (515)	50.0	50.0	57.2	–23.0	–0.3	0.02	176	64.5	1.6	6.6	0.2	0.8

[1]See Figure A13 for well location; HPIA subdomain model cell location: row 184, column 114, layer 3

[2]See Figure A14 for well location; HPLF subdomain model cell location: row160, column 166, layer 5

Sensitivity Analyses

Contaminant fate and transport simulations were conducted by using reduced finite-difference grid cell sizes of 25 ft and 12.5 ft per side. This grid refinement would effectively yield a reduction in the Peclet number by a factor of 2 to 4. Results of the contaminant fate and transport simulations for the HPLF subdomain area for TCE concentrations in water-supply well HP-651 are shown in Figure S6.20. The three concentration plots in the graph represent simulated TCE concentrations in well HP-651 that result from using finite-difference grid cell sizes of 50, 25, and 12.5 ft per side; the 50-ft cell size represents the calibrated model. These results indicate approximately the same results from the onset of pumping during July 1972 to cessation of pumping during February 1985, a period of interest to the ATSDR health studies. Additionally, simulated concentrations at water-supply well HP-651 are similar when using the three different cell sizes (50 ft, 25 ft, and 12.5 ft per side) and range from about 7,100 µg/L to 9,200 µg/L (Figure S6.20). By comparison, measured data range in value from 3,200 µg/L to 18,900 µg/L for the period January 16–February 4, 1985 (Table A4). Thus, sensitivity analysis results for variations in finite-difference cell sizes demonstrate that concentrations simulated by the HPHB study area contaminant fate and transport models were most likely unaffected by numerical oscillations caused by inappropriate (too large) spatial (cell size) discretization.

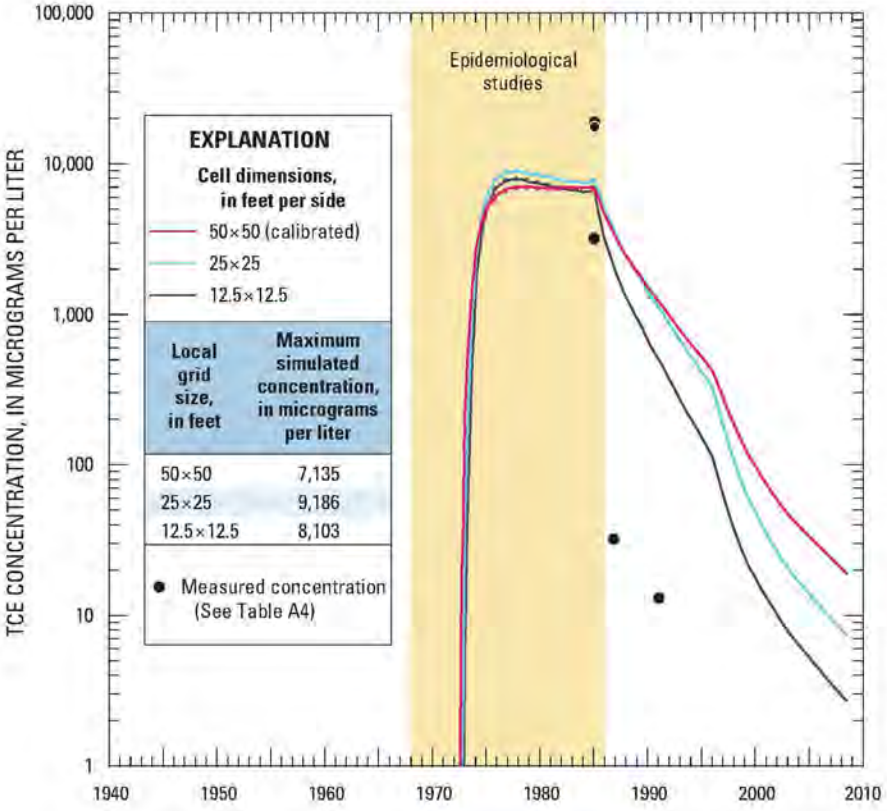

Figure S6.20. Simulated concentrations of trichloroethylene (TCE) in water-supply well HP-651 using finite-difference cell dimensions of 50, 25, and 12.5 feet per side, Hadnot Point–Holcomb Boulevard study area, U.S. Marine Corps Base Camp Lejeune, North Carolina. (See Figure S6.1 for well location.)

Time-Step Size

When conducting fate and transport simulations, numerical instability related to inappropriate temporal discretization (i.e., time-step size) is minimized when the Courant number (C_N) equals 1 or less. For the models described in this supplement, the Courant condition was set to a maximum of 1.[26] The Courant number is defined as

$$C_N = \frac{V\Delta t}{\Delta l} \qquad \text{(S6.10)}$$

where

C_N = Courant number [L^0];
V = simulated groundwater-flow velocity [LT^{-1}];
Δt = stress-period length or time-step size [T]; and
Δl = a characteristic length [L].

The characteristic length of finite-difference numerical models is typically related to grid cell dimensions. The MODFLOW and MT3DMS models applied to the HPHB study area fate and transport model subdomains are uniform at 50 ft per side. Therefore, the characteristic length, Δl, becomes the length of the cell side or the distance between two adjacent cell centroids (50 ft). To minimize and control oscillations of the numerical solution resulting from the temporal discretization, Daus and Frind (1985) indicate that the Courant number (C_N) should be less than or equal to 1. For the HPHB study area groundwater-flow and contaminant fate and transport models, the stress periods were equal to the number of days in a month (i.e., 28, 29, 30, or 31). Except in the immediate vicinity of water-supply wells, groundwater-flow velocities ranged between 0.01 and 0.6 foot per day (ft/d) for the HPIA model subdomain area and between 0.01 and 1 ft/d for the HPLF model subdomain area. Thus, applying Equation S6.10—assuming Δt is the length of the stress period—to each subdomain area yields the following values for Courant numbers:

HPIA subdomain area (Figure S6.2):

$$\frac{0.01\times 28}{50} \le C_N \le \frac{0.6\times 31}{50}$$

$$0.006 \le C_N \le 0.4\,, \qquad \text{(S6.11)}$$

and for the HPLF subdomain area (Figure S6.3):

$$\frac{0.01\times 28}{50} \le C_N \le \frac{1.0\times 31}{50}$$

$$0.006 \le C_N \le 0.6\,. \qquad \text{(S6.12)}$$

This demonstrates that for the HPHB study area, the Courant number was less than 1 throughout the subdomain model areas except in the immediate vicinity of operating water-supply wells.

In the immediate vicinity of operating water-supply wells, simulated velocities were as great as 18 ft/d near well HP-608 in the HPIA area and as great as 10 ft/d near well HP-651 in the HPLF area. Substituting these values of velocity into Equation S6.10—again, Δt is the length of the stress period—results in maximum-value Courant numbers of about 11 and 6 for the HPIA and HPLF fate and transport model subdomain areas, respectively. These Courant numbers—exceeding a value of 1—could be indicative of numerical oscillations leading to inaccurate simulated concentrations. Although the number of time steps (e.g., additional transport steps) was increased to maintain a Courant number of less than 1, an analysis was completed to assess the effect of time discretization into the concentrations at the wells. To assess the effect of numerical oscillations caused by an inappropriate time discretization (that is, too large of a time step), contaminant fate and transport simulations were conducted by assigning 1-day stress periods ($\Delta t = 1$) to the calibrated contaminant fate and transport model for the HPLF subdomain area from November 1, 1984, to January 31, 1985. Pumpage assigned to these months in the calibrated model was assigned to every day of each respective month for the time-step sensitivity analysis. Comparisons of calibrated (30- and 31-day time steps) and simulated (1-day time step) concentrations of PCE and TCE for the days of November 30, 1984, December 31, 1984, and January 31, 1985, for water-supply well HP-651 are listed in Table S6.10. These results indicate that the relative absolute difference in simulated PCE and TCE concentrations at water-supply well HP-651 between the 1-day time step and the 30- and 31-day time steps is typically less than 0.2 percent and never exceeds 0.25 percent. Thus, PCE and TCE concentrations simulated by the HPHB study area contaminant fate and transport models were most likely unaffected by numerical oscillations caused by inappropriate temporal discretization.

[26] The Courant condition is automatically checked for every cell in the computational grid by the MT3DMS code to assure that $C_N \le 1$ for every stress period. If the Courant condition is not met, MT3DMS increases the number of transport time steps within a stress period, thus reducing the value of Δt in Equation 6.10. In most cases, the stress period was discretized by MT3DMS into about 2–5 transport time steps to comply with a Courant condition of less than 1.

Table S6.10. Simulated tetrachloroethylene and trichloroethylene concentrations at water-supply well HP-651, November 1984–January 1985, using 1-day stress periods and 30- or 31-day stress periods (calibrated model), Hadnot Point–Holcomb Boulevard study area, U.S. Marine Corps Base Camp Lejeune, North Carolina.

[µg/L, microgram per liter; Δt, time of stress period]

Contaminant	Simulated elapsed time, in days	Date	[1]Simulated concentration, in µg/L		[2]Absolute relative difference, in percent
			Δt=1 day	Δt=30 or 31 days	
Tetrachloroethylene (PCE)	15,675	Nov. 30, 1984	348.557	347.777	0.22
	15,706	Dec. 31, 1984	337.01	336.601	0.12
	15,737	Jan. 31, 1985	343.498	343.105	0.11
Trichloroethylene (TCE)	15,675	Nov. 30, 1984	6,910.40	6,894.63	0.23
	15,706	Dec. 31, 1984	6,589.20	6,582.72	0.10
	15,737	Jan. 31, 1985	6,779.30	6,772.31	0.10

[1]Simulated PCE and TCE concentrations for $\Delta t = 30$ or $\Delta t = 31$ days are from the calibrated fate and transport model for the Hadnot Point landfill (HPLF) subdomain area.

[2]Absolute relative difference ($|R_C|$) of simulated PCE and TCE concentrations are water-supply wells defined as:

$$|R_C| = \frac{C_{cal} - C_{\Delta t=1}}{C_{\Delta t=1}} \times 100\%,$$

where

C_{cal} is the calibrated PCE or TCE concentration simulated using a time-step size of 30 or 31 days, and

$C_{\Delta t=1}$ is the PCE or TCE concentration simulated using a time-step size of 1 day

Numerical Solver

During the process of calibrating both the HPIA and HPLF fate and transport models, the third-order, total-variation-diminishing (TVD) solver of MT3DMS was initially employed because it is characterized as being mass conservative and typically produces an accurate solution, free of numerical dispersion. However, the TVD solver "minimizes numerical dispersion at the expense of introducing spurious oscillations" (Zheng and Wang, 1999), which proved to be the case with the HPIA and HPLF models. The artificial oscillations produced negative simulated concentrations, especially along areas of sharp concentration fronts, indicative of an advection-dominated system. To alleviate the oscillation problem, the standard finite-difference solution method was used, which, not unexpectedly, produced a solution characterized by increased numerical dispersion. To assess the quality of the results, the HPIA and HPLF models were run using different solvers. Well HP-651 reconstructed concentrations from the calibrated model, which use the finite-difference solver, were compared with results of simulations obtained by using the TVD solver and the method of characteristics (MOC) solver (Figure S6.21).

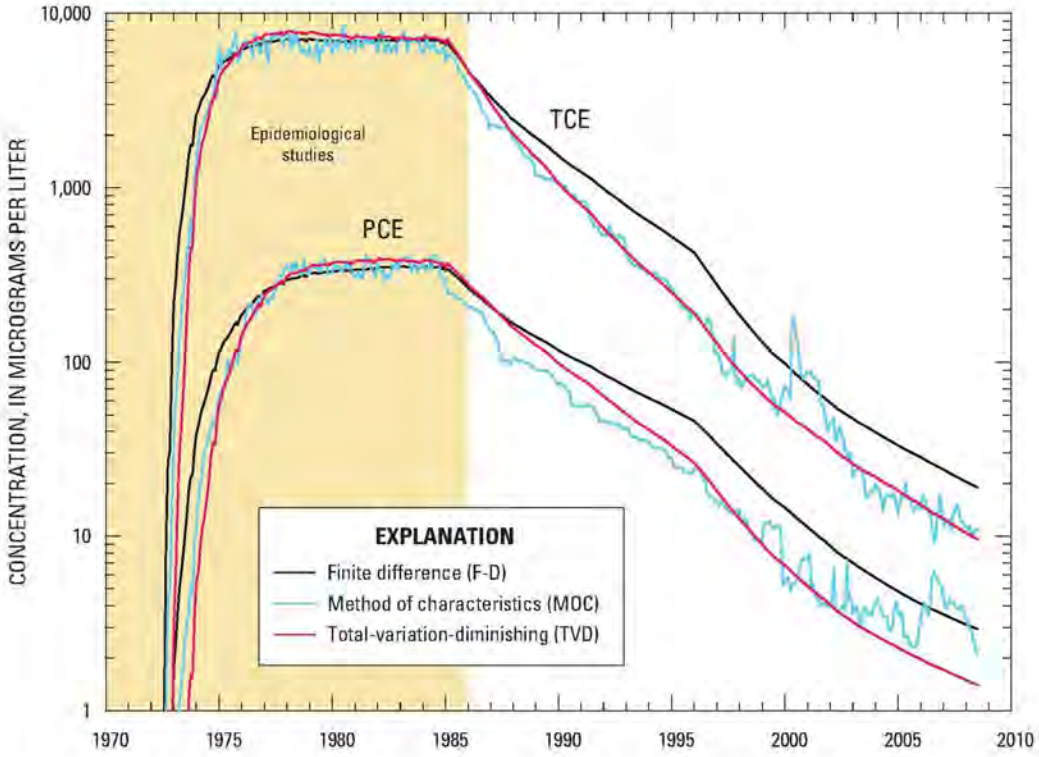

Figure S6.21. Simulated tetrachloroethylene (PCE) and trichloroethylene (TCE) concentrations at water-supply well HP-651 using MT3DMS finite-difference solver (F-D, calibrated model), method of characteristics solver (MOC) and total-variation-diminishing (TVD) solver, Hadnot Point–Holcomb Boulevard study area, U.S. Marine Corps Base Camp Lejeune, North Carolina.

Trichloroethylene Source-Release Date

Historical records delineating the timing and volume of inadvertent releases of solvents during routine operations, from leaking UST systems, or from disposal of solvent waste, spent dry cleaning filters, or other materials were not available for the HPHB study area. For modeling purposes, a median source-release date of 9 years from the date of UST system installation or site development (in the case of the HPLF area) was used in the contaminant fate and transport models. This source-release date formulation is consistent with empirical data indicating that the median timeframe for leak development in UST systems (typically in piping and joint components) is 9 years from installation date (USEPA 1986, 1987; Gangadharan et al. 1987). UST systems were not the source of contaminants in the HPLF area. However, given the lack of historical information, a similar source-release time frame, in this case 7 years from site development, was applied to HPLF-area sources within the model. The shorter source-release time frame acknowledges that landfill disposal likely encompassed a range of contained and uncontained source materials, in contrast to the engineered tank and piping system sources discussed previously.

To assess the effect of source-release-date variation on TCE concentrations in finished water at the HPWTP, a sensitivity analysis was conducted whereby the source-release date was modified from the calibrated source-release date. For example, a decrease of 5 years from the calibrated median of 9 years indicates a source-release date of 4 years from the estimated installation date for a UST system. Conversely, an increase of 5 years from the calibrated median of 9 years indicates a source-release date of 14 years from the estimated UST installation date.

Four sensitivity analysis simulations were conducted using the HPIA and HPLF area TCE contaminant source-release dates (Table S6.5). For these sensitivity analyses, the calibrated source-release date (9 years for suspected UST system sources and 7 years for HPLF area sources) was decreased by 5 and 9 years and increased by 5 and 9 years (7 years for the HPLF area sources) (Figure S6.22). In the case of the HPLF area sources, the calibrated source-release date was decreased by 7 years, to coincide with Base development in 1941. Results indicate that reconstructed TCE concentrations of finished-water for the HPWTP at the start of the epidemiological studies (January 1968) display little variation, except for a source-release-date increase of 9 years. The maximum reconstructed TCE concentration during the time frame (1968–1985) of the epidemiological studies varies by about 5 percent or less from the calibrated maximum value of 783 µg/L (Figure S6.22). Decreasing the source-release date by 9 years from its calibrated value (Figure S6.22) implies that contaminant leakage in the HPLF area would have started during or immediately following the onset of construction (1941/1942) of USMCB Camp Lejeune, which is not an unrealistic scenario given landfill-construction technologies that existed during the 1940s and 1950s. Results from this scenario indicate that the MCL for TCE in finished water at the HPWTP would have been exceeded during November 1948, compared to the calibrated exceedance date of August 1953. Variations in source-release dates of ±9 years show MCL exceedance-date variations of about 5 years earlier to 14 years later than the calibrated TCE MCL exceedance date (August 1953). In terms of historical reconstruction results of interest to the ATSDR epidemiological studies (finished-water concentrations of TCE during the period 1968–1985), the variation (and uncertainty due to a lack of data) in source-release dates does not appear to have a substantial effect..

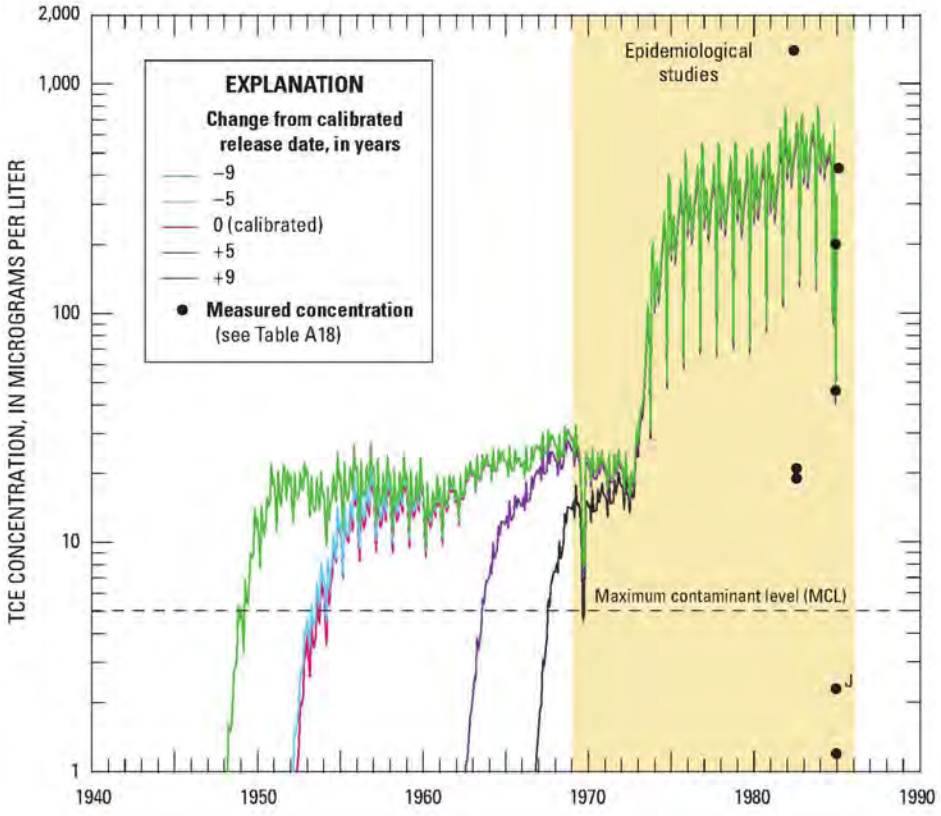

[1]Change from calibrated release date, in years	First month exceeding MCL	Concentration at start of epidemiological study (January 1968), in micrograms per liter	Maximum concentration during epidemiological study period (January 1968–December 1985), in micrograms per liter
−9	November 1948	26	800
−5	April 1953	26	798
0 (calibrated)	August 1953	27	783
+5	August 1963	23	748
+9	August 1967	7	740

[1]Calibrated release date varies by source location (Table S6.5)

Note:
−9 years means 9 years earlier than calibrated-source release date
+9 years means 9 years after calibrated-source release date

Figure S6.22. Reconstructed (simulated) finished-water concentrations of trichloroethylene (TCE) derived from variations in contaminant-source release dates, Hadnot Point water treatment plant, Hadnot Point–Holcomb Boulevard study area, U.S. Marine Corps Base Camp Lejeune, North Carolina.
[J, estimated concentration]

Uncertainty Analysis

In order to demonstrate the effect of uncertainty in the pumping schedules of water-supply wells, a Latin hypercube sampling (LHS) methodology was used. LHS is a useful tool for generating a limited number of random samples that are evenly distributed over a multidimensional random field. In this respect, LHS is an ideal approach to overcome the computational expense posed by the Monte Carlo (MC) simulation by reducing the number of simulations required. The LHS technique was first introduced by McKay et al. (1979). Helton and Davis (2003) provide a summary on LHS used for uncertainty analyses of complex systems. LHS was used to model spatial uncertainty in forest landscape simulations by Xu et al. (2005). Lahkim et al. (1999) applied LHS methodology to reduce the number of simulations required for the uncertainty analysis for the exposure and risk analyses in a polluted aquifer.

For this analysis, MATLAB® (version R2012b, 2012) was used to generate the Latin hypercube samples for the pumping schedules of the wells providing groundwater to the HPWTP and the HBWTP (Figure S6.23). The default criterion for LHS is to maximize the minimum distance between points. For this analysis, the number of random variables can be calculated as the product of the number of wells and number of months (i.e., 72 wells×792 months=57,024 for HPWTP, and 24 wells×792 months=19,008 for HBWTP). Replicating the approach described in Maslia et al. (2007, 2009) for conducting a similar uncertainty analysis for the HPHB study area was not computationally feasible even when using the LHS methodology. Therefore, a limited analysis with 10 Latin hypercube samples was conducted. The MATLAB® LHS function that was used generates 10 Latin hypercube samples for the monthly flow produced by all 96 wells included in the analysis. Initially, the values assigned to each well for each month range from 0 to 1. These normalized samples are then

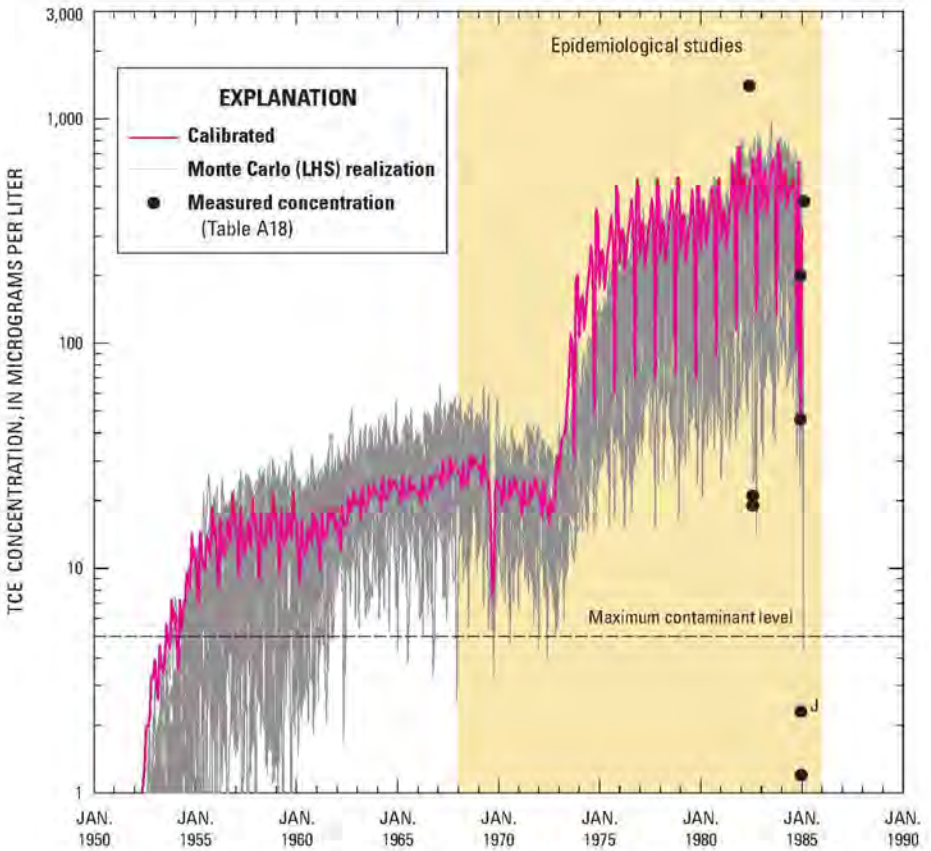

Figure S6.23. Variations in reconstructed (simulated) finished-water concentrations of trichloroethylene (TCE) derived using Latin hypercube sampling (LHS) methodology on water-supply well monthly operational schedules, Hadnot Point water treatment plant, Hadnot Point–Holcomb Boulevard study area, U.S. Marine Corps Base Camp Lejeune, North Carolina. [J, estimated]

scaled to the actual monthly flows reported by Telci et al. (2013) by multiplying with a range of flows for each well and each month. These flow ranges were determined by finding the difference between the maximum and minimum flows generated for 1,000 MC Markov Chain scenarios that satisfy conservation of mass at WTP water treatment plant within an error range of ±40 percent. The revised pumping schedules (relative to the calibrated schedules reported in Telci et al. (2013) were used as an input to the contaminant fate and transport models of the HPIA and HPLF area to reconstruct TCE concentrations delivered to the HPWTP by each well. Reconstructed TCE concentrations at the HPWTP derived from applying the LHS methodology to water-supply well monthly operational schedules are shown in Figure S6.23. In this figure, the red line indicates the TCE concentration obtained from the calibrated models. The gray lines indicate the TCE concentration variation over time for the 10 random scenarios obtained by LHS methodology. Results shown in Figure S6.23 indicate that observed data exhibit substantially greater variation than reconstructed concentrations generated by using the LHS-MC uncertainty analysis.

Discussion and Limitations

The purpose of this section is to provide readers with some additional thoughts pertinent to historical reconstruction results and application of models presented herein. All of the limitations that are presented in the Discussion section of Faye (2008) in reference to the TT study area fate and transport model are by extension applicable to the HPIA and HPLF area fate and transport models. Specifically, the water-quality sample records from the HPHB study area, on which assessment of model calibration results are substantially dependent, are subject to the same level of uncertainty and variability as discussed in Faye (2008). The water-quality data used in developing and calibrating the HPIA and HPLF area fate and transport models are tabulated in Faye et al. (2010, 2012), where there is further discussion of water-quality data. The reader is referred to those discussions for a better understanding of the complex nature of the water-quality data for the HPHB study area.

Results of the historical reconstruction process—concentrations at water-supply wells—should be interpreted as the most likely estimate representing monthly mean concentrations. These results represent the last day of the month. For example, for January 1968, the simulated TCE concentration at water-supply well HP-602 of 463 µg/L (Appendix A3) should be interpreted as occurring on January 31, 1968. For groundwater-flow model calibration (Suárez-Soto et al. 2013), sufficient water-level data are documented to apply statistical methods to assess the calibration fit.

For contaminant fate and transport modeling reported herein, however, insufficient water-quality data existed to conduct a statistical analysis for assessment of model calibration fit. In addition, specific data pertinent to the timing of initial deposition of contaminants to the ground or subsurface, chronologies of waste-disposal operations, such as dates and times when contaminants were deposited in the HPLF, or descriptions of the temporal variation of contaminant concentrations in the subsurface generally are not available. Determining these types of source identification and characterization data became part of the historical reconstruction process, whereby the contaminate fate and transport model was used to test source locations, varying concentrations, and beginning and ending dates for leakage and migration of source contaminants to the subsurface and the underlying groundwater-flow system.

Conducting a robust uncertainty analysis using Monte Carlo analysis (e.g., Maslia et al. 2009) requires simulating thousands of realizations. When using available computational equipment, the HPIA and HPLF models have a simulation time of about 6–8 hours for each simulation. The lengthy simulation times and the substantial data limitations therefore make a comprehensive uncertainty analysis computationally prohibitive based on available resources and time limitations. Thus, the ranges of values presented in the sensitivity analysis section of this report assess a limited number of input and output model parameters. The results (i.e., range of concentration) presented in the sensitivity analysis reported herein should not be considered or interpreted as the results of a robust and comprehensive uncertainty analysis, but do provide insight into parameter sensitivity and uncertainty in a qualitative sense.

References[27]

Agency for Toxic Substances and Disease Registry. Toxicological Profile for Benzene. Atlanta, GA: U.S. Department of Health and Human Services, Public Health Service, Agency for Toxic Substances and Disease Registry; 2007. [cited 2012 October 31]; Available from *http://www.atsdr.cdc.gov/ToxProfiles/tp3.pdf.*

Alvarez-Cohen L, and Speitel GE. Kinetics of Aerobic Cometabolism of Chlorinated Solvents. Biodegradation. 2001;12(2)105–126.

Aronson D, and Howard PH. Anaerobic Biodegradation of Organic Chemicals in Groundwater: A Summary of Field and Laboratory Studies. Final report prepared for the American Petroleum Institute by Environmental Science Center, Syracuse Research Corporation. North Syracuse, NY; 1997.

Baker Environmental, Inc. Final Remedial Investigation/ Feasibility Study Work Plan for Sites 6, 9, 48 and 69, Marine Corps Base Camp Lejeune, North Carolina; 1992. Contract Task Order 0024, Contract No.: N62470-89-D-4814 (CERCLA Administrative Record File #2802).

Baker Environmental, Inc. Final Record of Decision for Operable Unit No. 2 (Sites 6, 9, and 82), Marine Corps Base Camp Lejeune, North Carolina; 1993. Contract Task Order 0133, Contract No.: N62470-89-D-4814 (CERCLA Administrative Record File #1248).

Baker Environmental, Inc. Final Feasibility Study for Operable Unit No.1 (Sites 21, 24, and 78), Marine Corps Base Camp Lejeune, North Carolina; 1994. Contract Task Order 0177, Contract No.: N62470-89-D-4814 (CERCLA Administrative Record File #1256).

Baker Environmental, Inc. Final Basewide Remediation Assessment, Groundwater Study (BRAGS), Marine Corps Base Camp Lejeune, North Carolina, 1998a. Contract Task Order 0140, Contract No.: N62470-89-D-4814 (CERCLA Administrative Record File #02013).

Baker Environmental, Inc. Groundwater Modeling Report, Operable Unit No. 9, Site 73—Amphibious Vehicle Maintenance Facility, Marine Corps Base Camp Lejeune, North Carolina, 1998b. Contract Task Order 0312, Contract No.: N62470-89-D-4814 (CERCLA Administrative Record File #0258la2).

Catlin Engineers and Scientists, Leaking Underground Storage Tank Site Assessment Workplan, Building 1601, Marine Corps Base Camp Lejeune, North Carolina, 1996. Contract No.: N62470-93-D-4020 (Leaking Underground Storage Tank file #172).

CH2M HILL. Final Site Management Plan, Fiscal Year 2006, Marine Corps Base (MCB) Camp Lejeune, North Carolina. Norfolk, VA: Naval Facilities Engineering Command, Atlantic Division; 2006. Contract No.: N62470-03-D-4186.

CH2M HILL, Inc. Pilot Study Report, Operable Unit No. 2 (Site 82), Marine Corps Base Camp Lejeune, Jacksonville, North Carolina; 2008. Contract Task Order 0105, Contract No. N62470-02-D-3052, Navy Clean III (CERCLA Administrative Record File #3341).

CH2M HILL, Inc. Hadnot Point Industrial Area Groundwater Evaluation Report, Marine Corps Base Camp Lejeune, Jacksonville, North Carolina; 2010. Contract Task Order 040, Contract No. N62470-08-D-1000, NAVFAC Clean 1000 Program (e-mail August 2011).

Cozzarelli IM, Bekins BA, Eganhouse RP, Warren E, and Essaid HI. In Situ Measurements of Volatile Aromatic Hydrocarbon Biodegradation Rates in Groundwater. Journal of Contaminant Hydrology. 2010;111(1–4):48–64.

Daus AD, and Frind EO. An Alternating Direction Galerkin Technique for Simulation of Contaminant Transport in Complex Groundwater Systems. Water Resources Research. 1985; 21(5):653–664.

Engineering and Environment, Inc. and Michael Bantal Jr., Inc. Annual Monitoring Report, Operable Unit No. 2, Sites 6 and 82, Marine Corps Base Camp Lejeune, North Carolina; 2004. Contract Task Order 0004, Contract No.: N62470-03-D-4000 (CERCLA Administrative Record File #03637).

Environmental Science and Engineering, Inc. Characterization Step Report for Hadnot Point Industrial Area, Confirmation Study to Determine Existence and Possible Migration of Chemicals In Situ. Marine Corps Base Camp Lejeune, North Carolina; 1988. Contract No. N62470-83-C-6106 (CERCLA Administrative Record File #258).

Faye RE. Analyses of Groundwater Flow, Contaminant Fate and Transport, and Distribution of Drinking Water at Tarawa Terrace and Vicinity, U.S. Marine Corps Base Camp Lejeune, North Carolina: Historical Reconstruction and Present-Day Conditions—Chapter F: Simulation of the Fate and Transport of Tetrachloroethylene (PCE). Atlanta, GA: Agency for Toxic Substances and Disease Registry; 2008.

[27] Certain documents have been provided to ATSDR by the Department of the Navy (Headquarters Marine Corps, Eastern Area Counsel Office, and Marine Corps Base Camp Lejeune) under the terms of "For Official Use Only" (FOUO) documents. Some of these documents are not releasable by ATSDR under the terms of FOUO.

Faye RE. Analyses and Historical Reconstruction of Groundwater Flow, Contaminant Fate and Transport, and Distribution of Drinking Water Within the Service Areas of the Hadnot Point and Holcomb Boulevard Water Treatment Plants and Vicinities, U.S. Marine Corps Base Camp Lejeune, North Carolina—Chapter B: Geohydrologic Framework of the Brewster Boulevard and Castle Hayne Aquifer Systems and the Tarawa Terrace Aquifer. Atlanta, GA: Agency for Toxic Substances and Disease Registry; 2012.

Faye RE, Anderson BA, Suárez-Soto RJ, and Sautner JB. Analyses and Historical Reconstruction of Groundwater Flow, Contaminant Fate and Transport, and Distribution of Drinking Water Within the Service Areas of the Hadnot Point and Holcomb Boulevard Water Treatment Plants and Vicinities, U.S. Marine Corps Base Camp Lejeune, North Carolina—Chapter C: Occurrence of Selected Contaminants in Groundwater at Installation Restoration Program Sites. Atlanta, GA: Agency for Toxic Substances and Disease Registry; 2010.

Faye RE, Jones LE, and Suárez-Soto RJ. Descriptions and Characterizations of Water-Level Data and Groundwater Flow for the Brewster Boulevard and Castle Hayne Aquifer Systems and the Tarawa Terrace Aquifer—Supplement 3. In: Maslia ML, Suárez-Soto RJ, Sautner JB, Anderson BA, Jones LE, Faye RE, Aral MM, Guan J, Jang W, Telci IT, Grayman WM, Bove FJ, Ruckart PZ, and Moore SM. Analyses and Historical Reconstruction of Groundwater Flow, Contaminant Fate and Transport, and Distribution of Drinking Water Within the Service Areas of the Hadnot Point and Holcomb Boulevard Water Treatment Plants and Vicinities, U.S. Marine Corps Base Camp Lejeune, North Carolina—Chapter A: Summary and Findings. Agency for Toxic Substances and Disease Registry; 2013.

Faye RE, Suárez-Soto RJ, and Maslia ML. Analyses and Historical Reconstruction of Groundwater Flow, Contaminant Fate and Transport, and Distribution of Drinking Water Within the Service Areas of the Hadnot Point and Holcomb Boulevard Water Treatment Plants and Vicinities, U.S. Marine Corps Base Camp Lejeune, North Carolina—Chapter D: Occurrence of Selected Contaminants in Groundwater at Above-Ground and Underground Storage Tank Sites. Atlanta, GA: Agency for Toxic Substances and Disease Registry; 2012.

Freeze RA, and Cherry JA. Groundwater. Englewood Cliffs, NJ: Prentice-Hall, Inc.; 1979.

Gangadharan AC, Narayanan TV, Raghavan R, and Amoruso G. Leak Prevention in Underground Storage Tanks: A State-of-the-Art Survey. Cincinnati, OH: U.S. Environmental Protection Agency, Hazardous Waste Engineering Research Laboratory, Office of Research and Development; 1987. Report No.: EPA/600/2-87/018.

Geraghty and Miller. Final Report: Phase I LUST Study (Tables), Marine Corps Base Camp Lejeune, North Carolina; 1990. Contract No. N62470-86-C-8746. (UST Management Web Portal File #504).

Harbaugh AW. MODFLOW-2005: The U.S. Geological Survey Modular Ground-Water Model—The Ground-Water Flow Process. U.S. Geological Survey Techniques and Methods 6-A16; 2005.

Helton JC, and Davis FJ. Latin Hypercube Sampling and the Propagation of Uncertainty in Analyses of Complex Systems. Reliability Engineering & System Safety. 2003; 81(1): 23-69.

Jang W, Anderson BA, Suárez-Soto RJ, Aral MM, and Maslia ML. Source Characterization and Simulation of the Migration of Light Nonaqueous Phase Liquids (LNAPLs) in the Vicinity of the Hadnot Point Industrial Area—Supplement 7. In: Maslia ML, Suárez-Soto RJ, Sautner JB, Anderson BA, Jones LE, Faye RE, Aral MM, Guan J, Jang W, Telci IT, Grayman WM, Bove FJ, Ruckart PZ, and Moore SM. Analyses and Historical Reconstruction of Groundwater Flow, Contaminant Fate and Transport, and Distribution of Drinking Water Within the Service Areas of the Hadnot Point and Holcomb Boulevard Water Treatment Plants and Vicinities, U.S. Marine Corps Base Camp Lejeune, North Carolina—Chapter A: Summary and Findings. Atlanta, GA: Agency for Toxic Substances and Disease Registry; 2013.

Jang W, and Aral MM. Modeling of Co-Existing Anaerobic-Aerobic Biotransformations of Chlorinated Ethenes in the Subsurface. Presented at: The Third International Conference on Environmental Science and Technology, American Academy of Science; 2007, Houston.

Jang W, and Aral MM. Analyses of Groundwater Flow, Contaminant Fate and Transport, and Distribution of Drinking Water at Tarawa Terrace and Vicinity, U.S. Marine Corps Base Camp Lejeune, North Carolina: Historical Reconstruction and Present-Day Conditions—Chapter G: Simulation of Three-Dimensional Multispecies, Multiphase Mass Transport of Tetrachloroethylene (PCE) and Associated Degradation By-Products. Atlanta, GA: Agency for Toxic Substances and Disease Registry; 2008.

Jang W, and Aral MM. Physical and Chemical Properties and Biological Transformation of Chlorinated Volatile Organic Compounds and BTEX. Multimedia Environmental Simulations Laboratory. Atlanta, GA: Georgia Institute of Technology; 2009.

Konikow LF, Goode DJ, and Hornberger GZ. A Three-Dimensional Method-of-Characteristics Solute-Transport Model (MOC3D). U.S. Geological Survey Water-Resources Investigations Report 96-4267. Reston, VA: U.S. Geological Survey; 1996.

References

Lahkim MB, Garcia LA, and Nuckols JR. Stochatic Modeling of Exposure and Risk in a Contaminated Heterogenous Aquifer. 2: Application of Latin Hypercube Sampling. Environmental Engineering Science. 1999; 16(5):329-343.

Law Engineering and Environmental Services, Inc. Leaking Underground Storage Tank Site Assessment Report, Building SLCH-4019, Marine Corps Base Camp Lejeune, North Carolina; 1996. Job No.: 30740-5-0500-0055 (Leaking Underground Storage Tank File # 0346).

Lawrence SJ. Analyses of Groundwater Flow, Contaminant Fate and Transport, and Distribution of Drinking Water at Tarawa Terrace and Vicinity, U.S. Marine Corps Base Camp Lejeune, North Carolina: Historical Reconstruction and Present-Day Conditions—Chapter D: Properties and Degradation Pathways of Common Organic Compounds in Groundwater. Atlanta, GA: Agency for Toxic Substances and Disease Registry; 2007.

Mackay D, Shiu WY, Ma KC, and Lee SC. Handbook of Physical-Chemical Properties and Environmental Fate for Organic Chemicals. Boca Raton, FL: CRC Press; 2006.

Madigan MT, Martinko JM, and Parker J. Biology of Microorganisms. Upper Saddle River, NJ: Pearson Education, Inc.; 2003.

Maslia ML, and Aral MM. ACTS—Analytical Contaminant Transport Analysis System (ACTS)—Multimedia Environmental Fate and Transport. ASCE Practice Periodical of Hazardous, Toxic, and Radioactive Waste Management. 8(3):181–198; 2004.

Maslia ML, Sautner JB, Faye RE, Suárez-Soto RJ, Aral MM, Grayman WM, Jang W, Wang J, Bove FJ, Ruckart PZ, Valenzuela C, Green JW Jr, and Krueger AL. Analyses of Groundwater Flow, Contaminant Fate and Transport, and Distribution of Drinking Water at Tarawa Terrace and Vicinity, U.S. Marine Corps Base Camp Lejeune, North Carolina: Historical Reconstruction and Present-Day Conditions—Chapter A: Summary of Findings. Atlanta, GA: Agency for Toxic Substances and Disease Registry; 2007.

Maslia ML, Suárez-Soto RJ, Sautner JB, Anderson BA, Jones LE, Faye RE, Aral MM, Guan J, Jang W, Telci IT, Grayman WM, Bove FJ, Ruckart PZ, and Moore SM. Analyses and Historical Reconstruction of Groundwater Flow, Contaminant Fate and Transport, and Distribution of Drinking Water Within the Service Areas of the Hadnot Point and Holcomb Boulevard Water Treatment Plants and Vicinities, U.S. Marine Corps Base Camp Lejeune, North Carolina—Chapter A: Summary and Findings. Atlanta, GA: Agency for Toxic Substances and Disease Registry; 2013.

Maslia ML, Suárez-Soto RJ, Wang J, Aral MM, Faye RE, Sautner JB, Valenzuela C, and Grayman WM. Analyses of Groundwater Flow, Contaminant Fate and Transport, and Distribution of Drinking Water at Tarawa Terrace and Vicinity, U.S. Marine Corps Base Camp Lejeune, North Carolina: Historical Reconstruction and Present-Day Conditions—Chapter I: Parameter Sensitivity, Uncertainty, and Variability Associated with Model Simulations of Groundwater Flow, Contaminant Fate and Transport, and Distribution of Drinking Water. Atlanta, GA: Agency for Toxic Substances and Disease Registry; 2009.

Masters GM. Introduction to Environmental Engineering and Science. 2nd ed: Prentice Hall; 1998.

MATLAB®, version R2012b (computer software), The MathWorks Inc., Natick, MA: 2012. [cited 2013 Janaury 23]; Available from *http://www.mathworks.com/*.

McDonald MG, and Harbaugh AW. A Modular Three-Dimensional Finite-Difference Groundwater Flow Model. U.S. Geological Survey Open-File Report 83-875; 1984.

McKay MD, Beckman RJ, and Conover WJ. A Comparison of Three Methods for Selecting Values of Input Variables in the Analysis of Output from a Computer Code. Technometrics. 1979; 21(2): 239-245.

Mississippi Department of Environmental Quality. Cleanup Definitions; 2007. [cited 2012 October 15]; available from *http://www.deq.state.ms.us/mdeq.nsf/page/GARD_definitions/*.

OHM Remediation Services Corporation, Final Closeout Report for Removal & Abandonment of Underground Fuel Oil Pipelines, Hadnot Point Industrial Area, Marine Corps Base Camp Lejeune, North Carolina, 2001. Contract No.: N62470-97-D-5000 (Leaking Underground Storage Tank file #744).

Peele's Pump and Tank Company. Initial site Assessment Report, UST Closure by Removal, 1-1,500 Gallon Used Oil Tank, Bldg 1601, Camp Lejeune, Jacksonville, NC; 1993. (Leaking Underground Storage Tank Program File #624).

Richard Catlin & Associates. Leaking Underground Storage Tank Site Assessment Workplan. Building 1601, Marine Corps Base Camp Lejeune, North Carolina, 1996. Contract No. N62470-93-D-4020. (UST Management Web Portal File #172).

Sautner JB, Anderson BA, Suárez-Soto RJ, and Maslia ML. Descriptions and Characterizations of Data Pertinent to Water-Supply Well Capacities, Histories, and Operations—Supplement 1. In: Maslia ML, Suárez-Soto RJ, Sautner JB, Anderson BA, Jones LE, Faye RE, Aral MM, Guan J, Jang W, Telci IT, Grayman WM, Bove FJ, Ruckart PZ, and Moore SM. Analyses and Historical Reconstruction of Groundwater Flow, Contaminant Fate and Transport, and Distribution of Drinking Water Within the Service Areas of the Hadnot Point and Holcomb Boulevard Water Treatment Plants and Vicinities, U.S. Marine Corps Base Camp Lejeune, North Carolina—Chapter A: Summary and Findings. Atlanta, GA: Agency for Toxic Substances and Disease Registry; 2013.

Schmidt SK, Simkins S, and Alexander M. Models for the Kinetics of Biodegradation of Organic Compounds Not Supporting Growth. Applied and Environmental Microbiology. 1985;50(2)323–331.

Semprini L, Kitanidis PK, Kampbell DH, and Wilson JT. Anaerobic Transformation of Chlorinated Aliphatic Hydrocarbons in a Sand Aquifer Based on Spatial Chemical Distributions. Water Resources Research. 1995;31(4)1051–1062.

Sovereign Consulting Inc. Final Annual Groundwater Monitoring Report 2006–2007 (Building 900). Marine Corps Base Camp Lejeune, North Carolina. 2007. Contract Number: N62470-04-D-0205 (UST Management Web Portal File #900AMRFINAL2007).

Suárez-Soto RJ, Jones LE, and Maslia ML. Simulation of Three-Dimensional Groundwater Flow—Supplement 4. In: Maslia ML, Suárez-Soto RJ, Sautner JB, Anderson BA, Jones LE, Faye RE, Aral MM, Guan J, Jang W, Telci IT, Grayman WM, Bove FJ, Ruckart PZ, and Moore SM. Analyses and Historical Reconstruction of Groundwater Flow, Contaminant Fate and Transport, and Distribution of Drinking Water Within the Service Areas of the Hadnot Point and Holcomb Boulevard Water Treatment Plants and Vicinities, U.S. Marine Corps Base Camp Lejeune, North Carolina—Chapter A: Summary and Findings. Atlanta, GA: Agency for Toxic Substances and Disease Registry; 2013.

Telci IT, Sautner JB, Suárez-Soto RJ, Anderson BA, Maslia ML, and Aral MM. Development and Application of a Methodology to Characterize Present-Day and Historical Water-Supply Well Operations—Supplement 2. In: Maslia ML, Suárez-Soto RJ, Sautner JB, Anderson BA, Jones LE, Faye RE, Aral MM, Guan J, Jang W, Telci IT, Grayman WM, Bove FJ, Ruckart PZ, and Moore SM. Analyses and Historical Reconstruction of Groundwater Flow, Contaminant Fate and Transport, and Distribution of Drinking Water Within the Service Areas of the Hadnot Point and Holcomb Boulevard Water Treatment Plants and Vicinities, U.S. Marine Corps Base Camp Lejeune, North Carolina—Chapter A: Summary and Findings. Atlanta, GA: Agency for Toxic Substances and Disease Registry; 2013.

U.S. Environmental Protection Agency. Underground Motor Fuel Storage Tanks: A National Survey. Washington, DC: U.S. Environmental Protection Agency; 1986. Report No.: EPA-560/5-86-013.

U.S. Environmental Protection Agency. Causes of release from UST systems. Washington, DC: U.S. Environmental Protection Agency; 1987. Report No.: EPA 510-R-92-702.

U.S. Environmental Protection Agency. Soil Screening Guidance—Technical Background Document. Washington, DC: U.S. Environmental Protection Agency, Superfund Program; July 1996. Report No.: EPA/540/R-96/018.

U.S. Environmental Protection Agency. Anaerobic Biodegradation Rates of Organic Chemicals in Groundwater: A Summary of Field and Laboratory Studies. Washington, DC: U.S. Environmental Protection Agency; 1999.

U.S. Environmental Protection Agency. EPA On-Line Tools for Site Assessment Calculation. Athens, GA: U.S. Environmental Protection Agency, Ecosystems Research; 2011. [cited 2011 October 24]; Available from *http://www.epa.gov/athens/learn2model/part-two/onsite/es.html*.

U.S. Geological Survey. Toxic Substances Hydrology Program; 2013. [cited February 4, 2013]; Available from *http://toxics.usgs.gov/*.

Vogel TM, Criddle CS, and McCarty PL. Transformations of Halogenated Aliphatic Compounds. Environmental Science & Technology. 1987;21(8)722–736.

References

Wiedemeier TH, Swanson MA, Wilson JT, Kampbell DH, Miller RN, and Hansen JE. Patterns of Intrinsic Bioremediation at Two United States Air Force Bases. In: Hinchee RE, Wilson JT, and Downey DC, editors. Intrinsic Bioremediation. Columbus, OH: Battelle Press; 1995. p. 31–51.

Wiedemeier TH. Technical Protocol for Evaluating Natural Attenuation of Chlorinated Solvents in Ground Water. Cincinnati, Ohio: National Risk Management Research Laboratory Office of Research and Development; 1998.

Wilson JT, Kampbell DH, and Armstrong J. Natural Bioreclamation of Alkylbenzenes (BTEX) from a Gasoline Spill in Methanogenic Groundwater. In: Hinchee RE, Miller RN, and Hoeppel RE, editors. Hydrocarbon Bioremediation. Boca Raton, FL: Lewis Publishers; 1994. p. 201–218.

Witt ME, Klecka GM, Lutz EJ, Ei TA, Grosso NR, and Chapelle FH. Natural Attenuation of Chlorinated Solvents at Area 6, Dover Air Force Base: Groundwater Biogeochemistry. Journal of Contaminant Hydrology. 2002;57(1–2)61–80.

Xu CG, He HS, Hu YM, Chang Y, Li XZ, and Bu RC. Latin Hypercube Sampling and Geostatistical Modeling of Spatial Uncertainty in a Spatially Explicit Forest Landscape Model Simulation. Ecological Modelling. 2005; 185 (2-4):255-269.

Yu S and Semprini L. Kinetics and Modeling of Reductive Dechlorination at High PCE and TCE Concentrations. Biotechnology and Bioengineering. 2004;88(4)451–464.

Zheng C, and Bennett GD. Applied Contaminant Transport Modeling, Second Edition. Wiley-Interscience; 2002.

Zheng C, and Wang PP. MT3DMS, A Modular Three-Dimensional Multispecies Transport Model for Simulation of Advection, Dispersion, and Chemical Reactions of Contaminants in Groundwater Systems. Department of Geology and Mathematics, University of Alabama; 1999.

Appendix S6.1. Biological Reactions of Selected Contaminants of Concern, Hadnot Point–Holcomb Boulevard Study Area

[28] Chlorinated volatile organic carbons (VOCs) and benzene, toluene, ethylbenzene, and xylenes (BTEX) were detected in groundwater that was extracted at Installation Restoration Program Sites 6 and 82 (Figure S6.3), Hadnot Point–Holcomb Boulevard study area, U.S. Marine Corps Base Camp Lejeune. Sites 6 and 82 adjoin one another and together comprise over 200 acres. Site 6 is composed of equipment staging and open storage areas, including Storage Lots 201 and 203. Site 82 is a mostly wooded area that borders Site 6 to the north. Prior to the late 1980s, much of the northern portion of Storage Lot 203 and Site 82 was used for storage, disposal, and handling of hazardous waste and materials. Located in the central and southern portions of Site 6, Storage Lot 201 has been used to stage equipment and material since the 1940s. Lot 201 was also reportedly used to store pesticides and polychlorinated biphenyls until the late 1980s.

At Sites 6 and 82, the measured maximum concentrations of contaminants are 6,500, 180,000, 18,000, 8,070, 187, and 800 micrograms per liter (µg/L) for tetrachlorotheylene (PCE), trichloroethylene (TCE), *cis*-1,2-dichloroethylene (1,2-cDCE), *trans*-1,2-dichloroethylene (1,2-tDCE), 1,1-dichloroethylene (1,1-DCE), and vinyl chloride (VC), respectively (refer to Faye et al. 2010 for measured concentrations at Sites 6 and 82). When considering potential biological processes of PCE and TCE, shown in Figure S6.1.1, the presence of the high concentration of three DCE isomers (1,2-cDCE, 1,2-tDCE, and 1,1-DCE) strongly suggests that the anaerobic biological transformation of PCE and TCE into DCEs occurred in the subsurface at both Sites 6 and 82. The biological dechlorination processes of PCE and TCE have been reported at contaminated sites (Vogel et al. 1987; Semprini et al. 1995; Witt et al. 2002; Jang and Aral 2008).

Aerobic and anaerobic bioreactions of chlorinated VOCs are complicated, and bioreaction rates are difficult to measure in the environment. A first-order kinetic model is often used to express the reductive dechlorination of chlorinated VOCs at contaminated sites (Schmidt et al. 1985; Wiedemeier 1998; Alvarez-Cohen and Speitel 2001; Jang and Aral 2007). In this study, a first-order kinetic model is applied to describe the dechlorination of chlorinated VOCs: PCE, TCE, 1,2-cDCE, 1,2-tDCE, 1,1-DCE, and VC. A first-order kinetic model can be written as:

$$\frac{dC_i}{dt} = -kC_i \qquad \text{(S6.1.1)}$$

where

C_i is the concentration of a target contaminant (M/L^3],
t is time [T], and
k is a first-order rate [T^{-1}].

Typically, the temporal profiles of concentrations of contaminants (i.e., contaminant concentration vs. time) are used to estimate the biodegradation of contaminants. However, the temporal variation of measured contaminant concentrations (or measured concentration data of chlorinated VOCs) at Sites 6 and 82 are the outcome of multiple processes, including advection (or groundwater flow), diffusion and dispersion, dilution, sorption, and biotic and abiotic reactions. In this study, we use a simplified analytical solution, derived from Equation S6.1.1, to estimate the attenuation rates[29] of chlorinated VOCs. Some of the field data and fitted curves used herein are illustrated in Figure S6.1.1, and the calculated attenuation rates of PCE, TCE, 1,2-cDCE, 1,2-tDCE, 1,1-DCE, and VC are presented in Table S6.1.1.

[28] Discussion presented in this appendix was obtained from the Biological Reactions of Target Chlorinated VOCs at Hadnot Point section in Jang and Aral 2009.

[29] Attenuation and bioreaction rates are sometimes used synonymously; however, calculated rates in this appendix should be considered attenuation rates because the calculated rate comprises multiple processes (e.g., advection, dispersion).

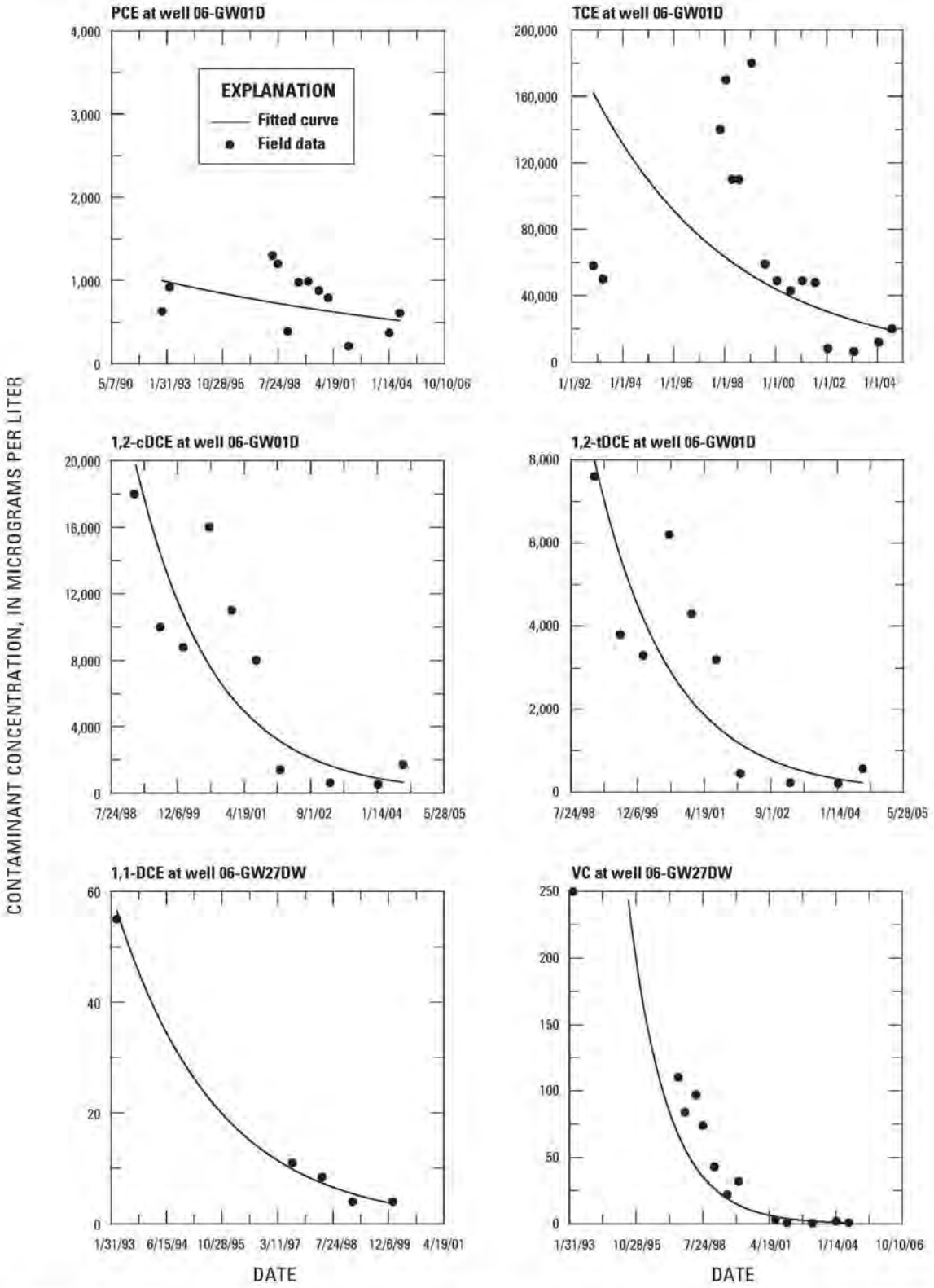

Figure S6.1.1. Field data and fitted curves for tetrachlorotheylene (PCE), trichloroethylene (TCE), *cis*-1,2-dichloroethylene (1,2-cDCE), *trans*-1,2-dichloroethylene (1,2-tDCE), 1,1-dichloroethylene (1,1-DCE), and vinyl chloride (VC). The fitted curves are for a first-order dechlorination kinetics, Hadnot Point–Holcomb Boulevard study area, U.S. Marine Corps Base Camp Lejeune, North Carolina.

Table S6.1.1. Calculated attenuation rates at selected monitor wells in the Hadnot Point landfill area, Hadnot Point–Holcomb Boulevard study area, U.S. Marine Corps Base Camp Lejeune, North Carolina.

Well number	Attenuation rates (day^{-1})	Half-life, in days	R^2 (root mean square)
Tetrachloroethylene (PCE)			
06-GW01D	1.54×10^{-4}	4,501	0.15
06-GW27DW	9.75×10^{-4}	711	0.84
Trichloroethylene (TCE)			
06-GW01D	3.59×10^{-4}	1,931	0.37
06-GW01DA	6.14×10^{-4}	1,129	0.23
06-GW27DW	1.50×10^{-3}	462	0.93
cis-1,2-dichloroethylene (1,2-cDCE)			
06-GW01D	1.70×10^{-3}	408	0.73
06-GW27DW	2.26×10^{-3}	307	0.67
trans-1,2-dichloroethylene (1,2-tDCE)			
06-GW01D	1.76×10^{-3}	394	0.75
06-GW27DW	2.47×10^{-3}	281	0.63
1,1-dichloroethylene (1,1-DCE)			
06-GW01D	7.36×10^{-4}	942	0.61
06-GW27DW	1.10×10^{-3}	630	0.97
Vinyl chloride (VC)			
06-GW01D	1.22×10^{-3}	568	0.72
06-GW27DW	1.72×10^{-3}	403	0.84

Appendix S6.2. Results for Sensitivity Analysis for Selected Water-Supply Wells

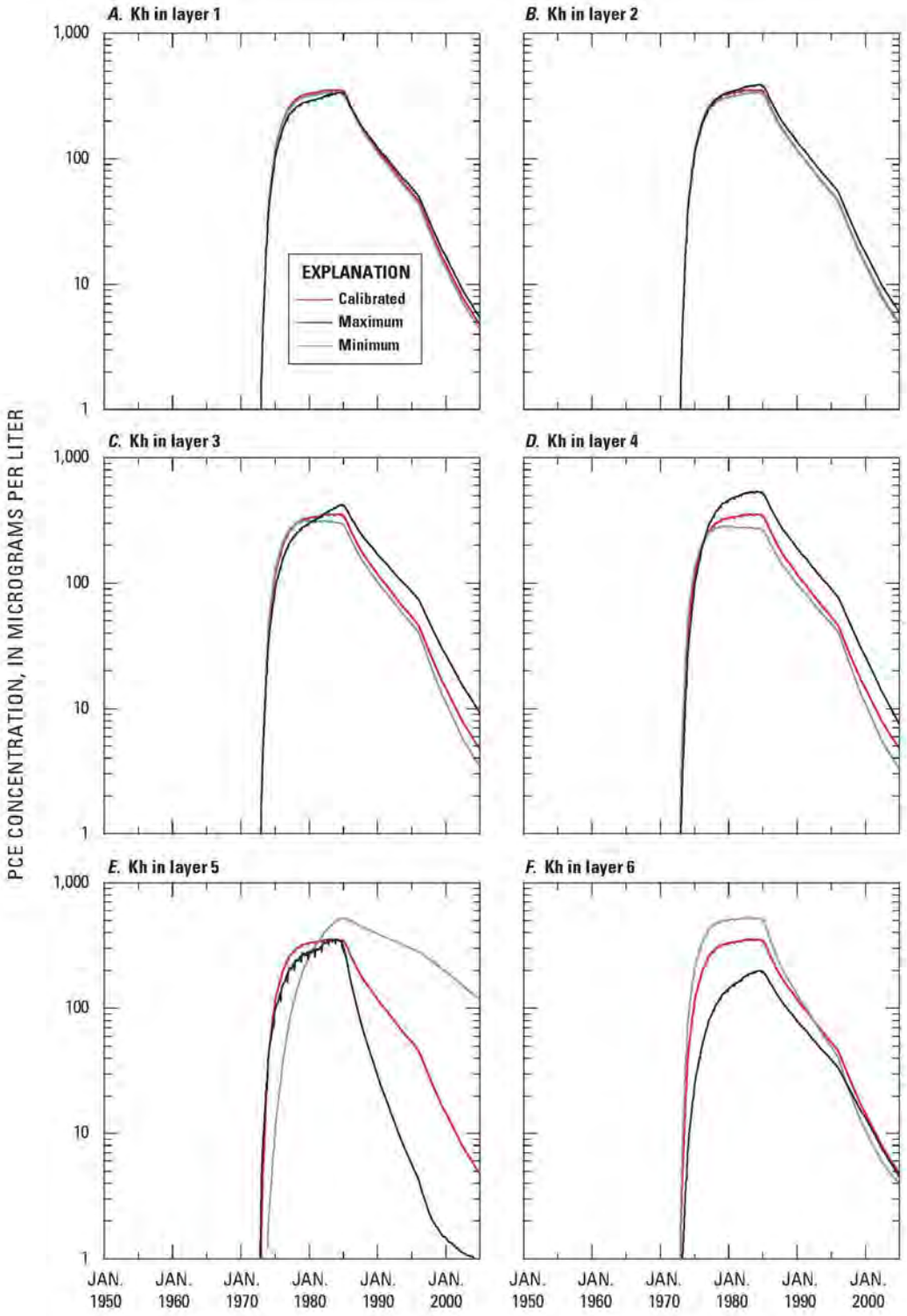

Figure S6.2.1. Tetrachloroethylene (PCE) concentrations at well HP-651 for calibrated value and minimum and maximum calibration-constrained values of K_h in *(A)* layer 1, *(B)* layer 2, *(C)* layer 3, *(D)* layer 4, *(E)* layer 5, and *(E)* layer 6, Hadnot Point landfill area fate and transport model, Hadnot Point–Holcomb Boulevard study area, U.S. Marine Corps Base Camp Lejeune, North Carolina.

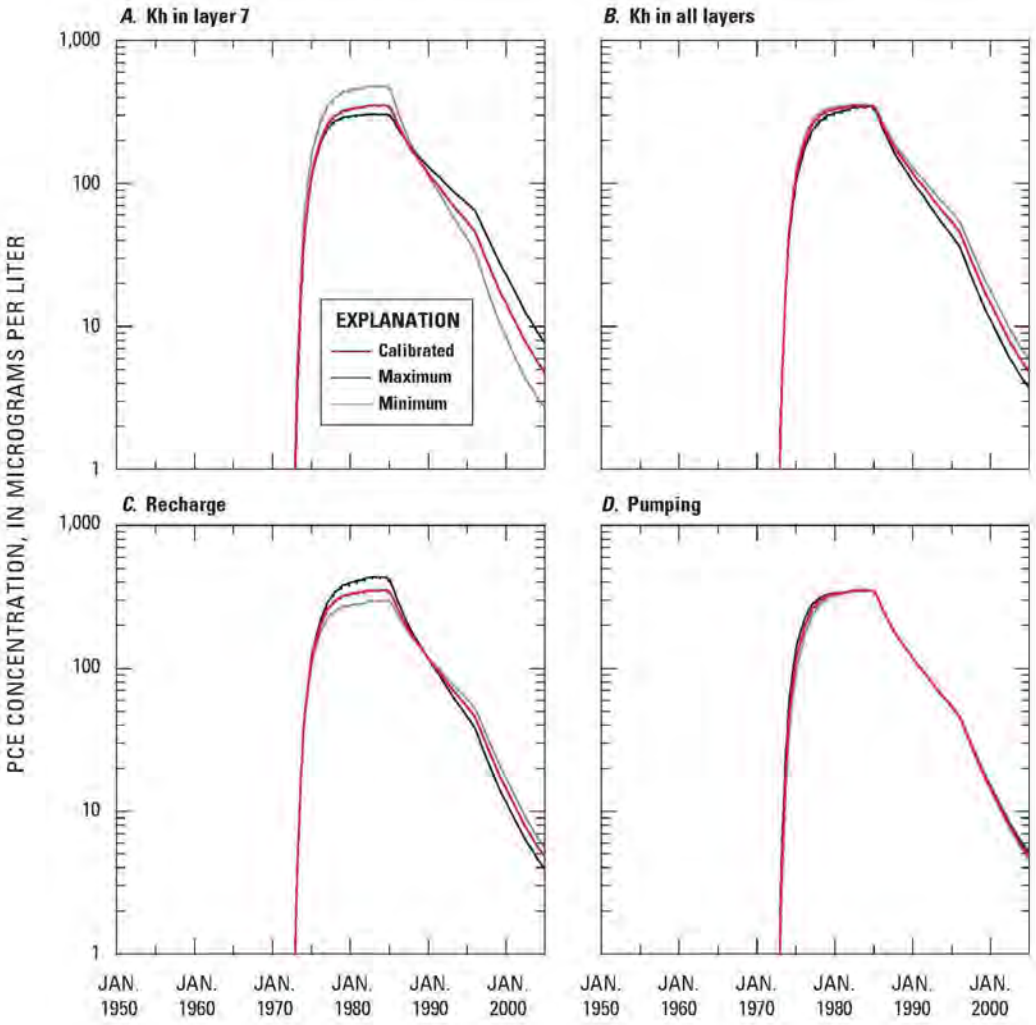

Figure S6.2.2. Tetrachloroethylene (PCE) concentrations at well HP-651 for calibrated value and minimum and maximum calibration-constrained values of *(A)* K_h in layer 7, *(B)* K_h in all layers, *(C)* recharge, and *(D)* water-supply well pumping, Hadnot Point landfill area fate and transport model, Hadnot Point–Holcomb Boulevard study area, U.S. Marine Corps Base Camp Lejeune, North Carolina.

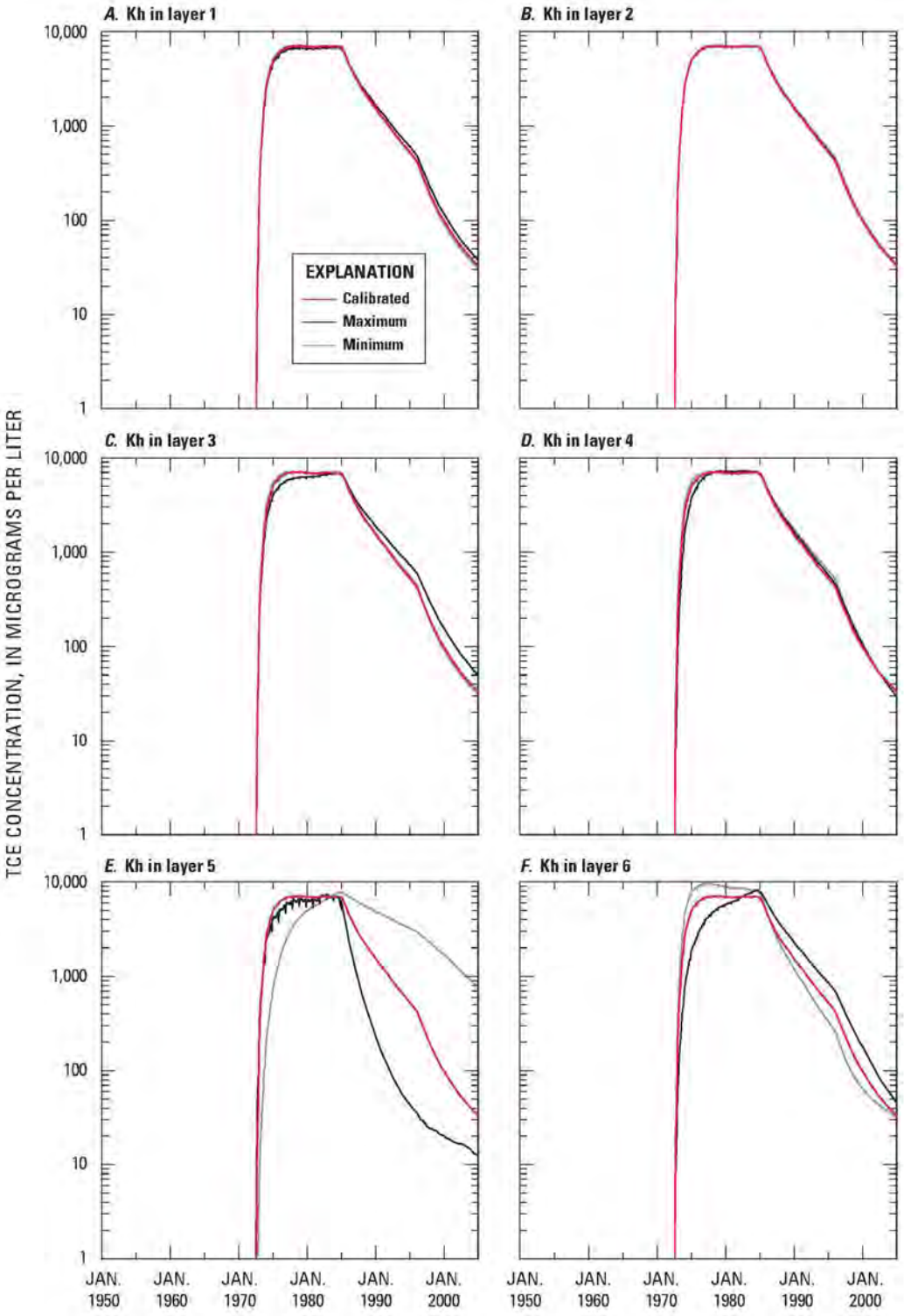

Figure S6.2.3. Trichloroethylene (TCE) concentrations at well HP-651 for calibrated value and minimum and maximum calibration-constrained values of K_h in *(A)* layer 1, *(B)* layer 2, *(C)* layer 3, *(D)* layer 4, *(E)* layer 5, and *(E)* layer 6, Hadnot Point landfill area fate and transport model, Hadnot Point–Holcomb Boulevard study area, U.S. Marine Corps Base Camp Lejeune, North Carolina.

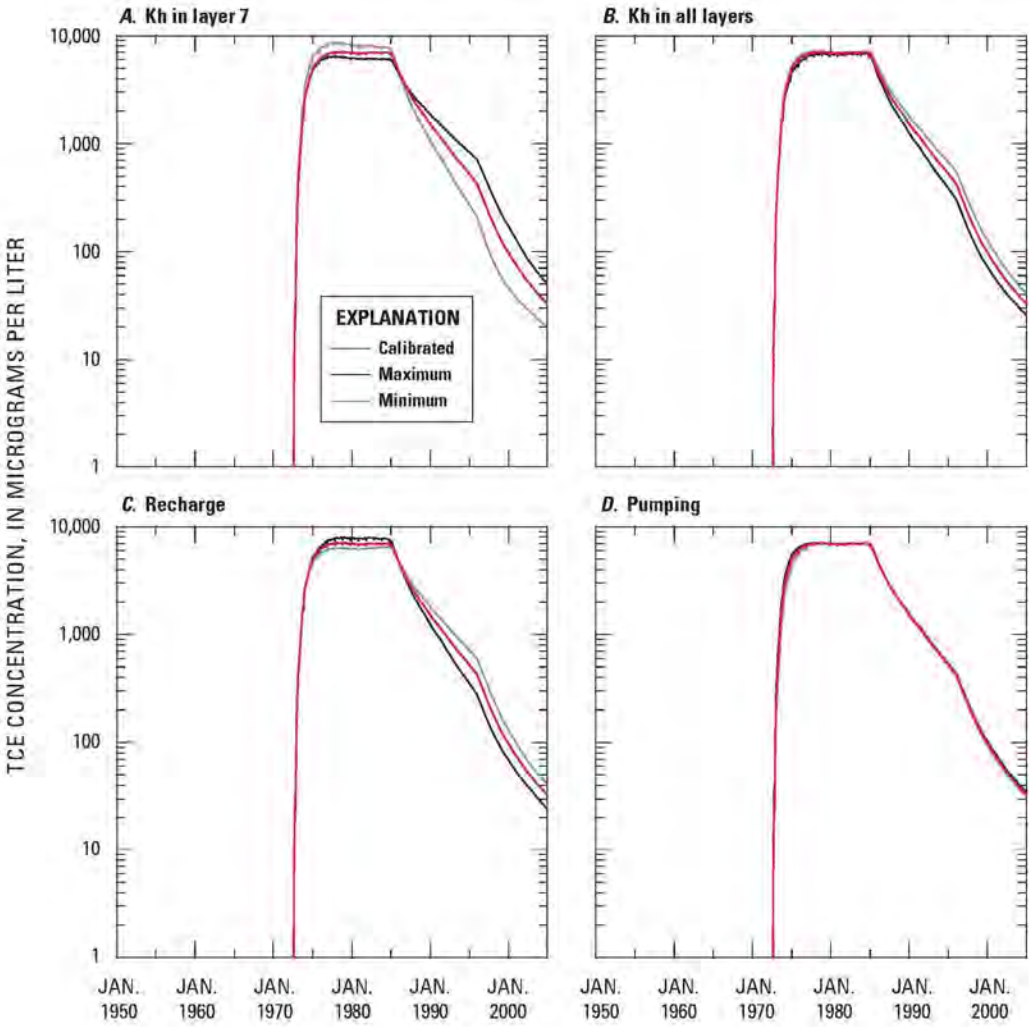

Figure S6.2.4. Trichloroethylene (TCE) concentrations at well HP-651 for calibrated value and minimum and maximum calibration-constrained values of *(A)* K_h in layer 7, *(B)* K_h in all layers, *(C)* recharge, and *(D)* water-supply well pumping, Hadnot Point landfill area fate and transport model, Hadnot Point–Holcomb Boulevard study area, U.S. Marine Corps Base Camp Lejeune, North Carolina.

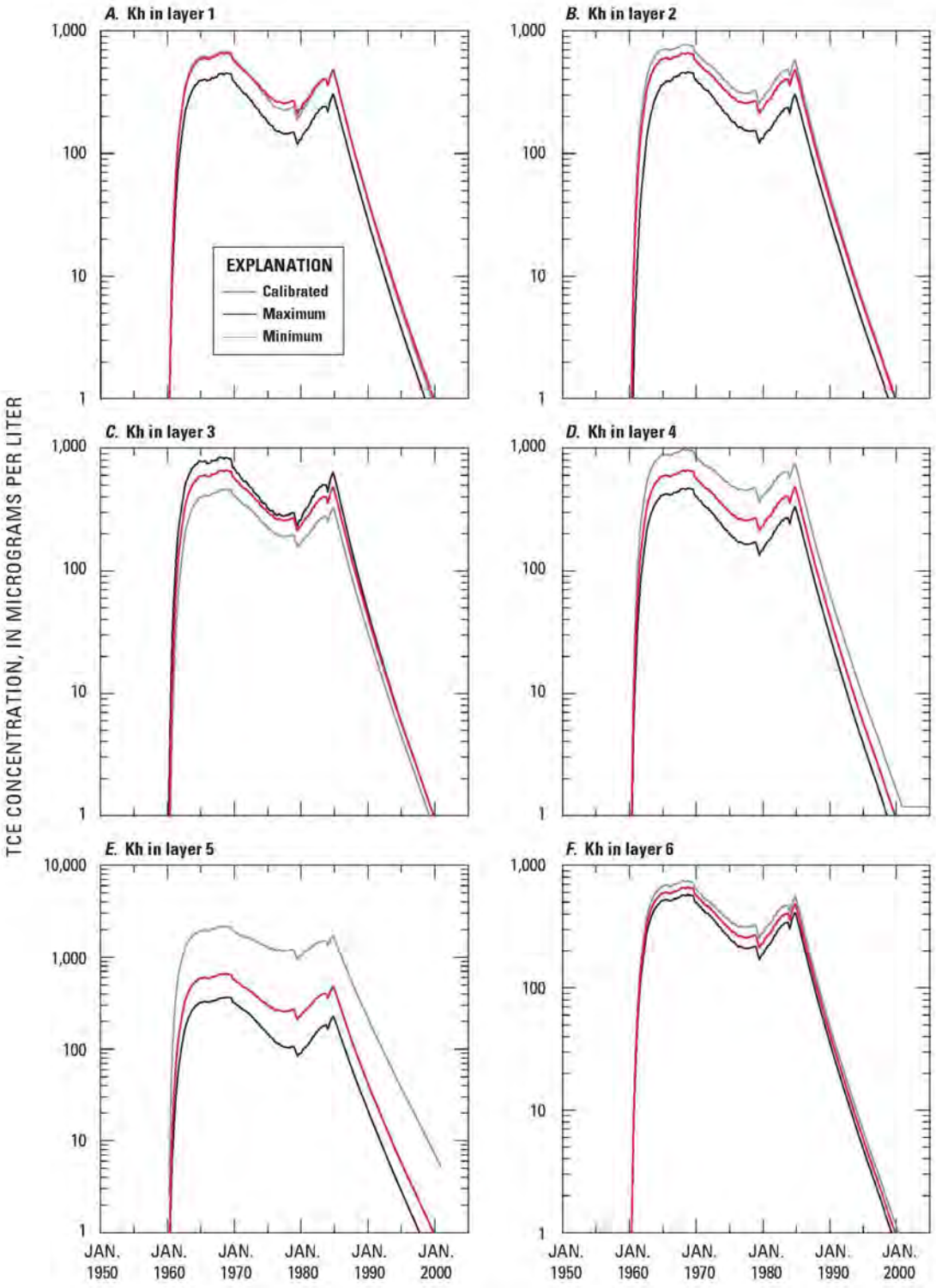

Figure S6.2.5. Trichloroethylene (TCE) concentrations at well HP-634 for calibrated value and minimum and maximum calibration-constrained values of K_h in *(A)* layer 1, *(B)* layer 2, *(C)* layer 3, *(D)* layer 4, *(E)* layer 5, and *(F)* layer 6, Hadnot Point landfill area fate and transport model, Hadnot Point–Holcomb Boulevard study area, U.S. Marine Corps Base Camp Lejeune, North Carolina.

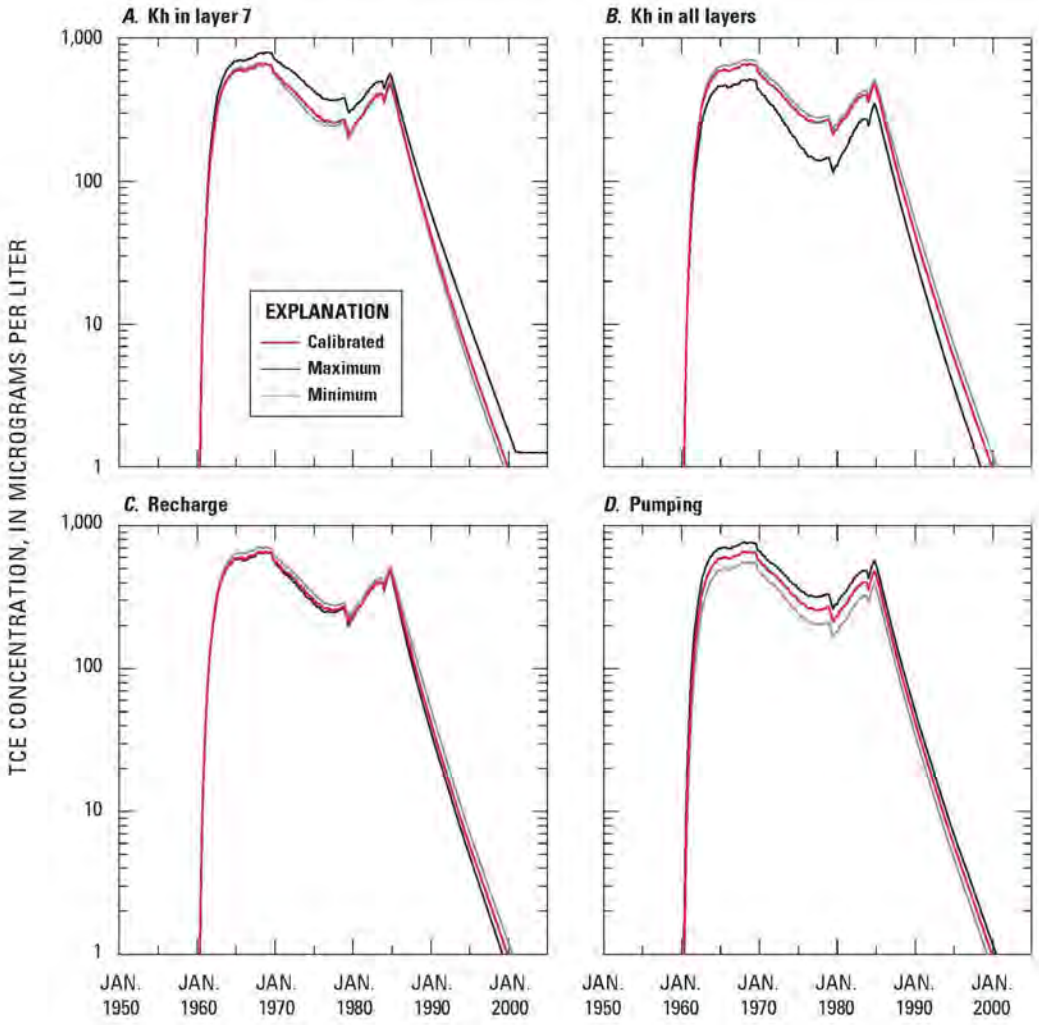

Figure S6.2.6. Trichloroethylene (TCE) concentrations at well HP-634 for calibrated value and minimum and maximum calibration-constrained values of *(A)* K_h in layer 7, *(B)* K_h in all layers, *(C)* recharge, and *(D)* water-supply well pumping, Hadnot Point landfill area fate and transport model, Hadnot Point–Holcomb Boulevard study area, U.S. Marine Corps Base Camp Lejeune, North Carolina.

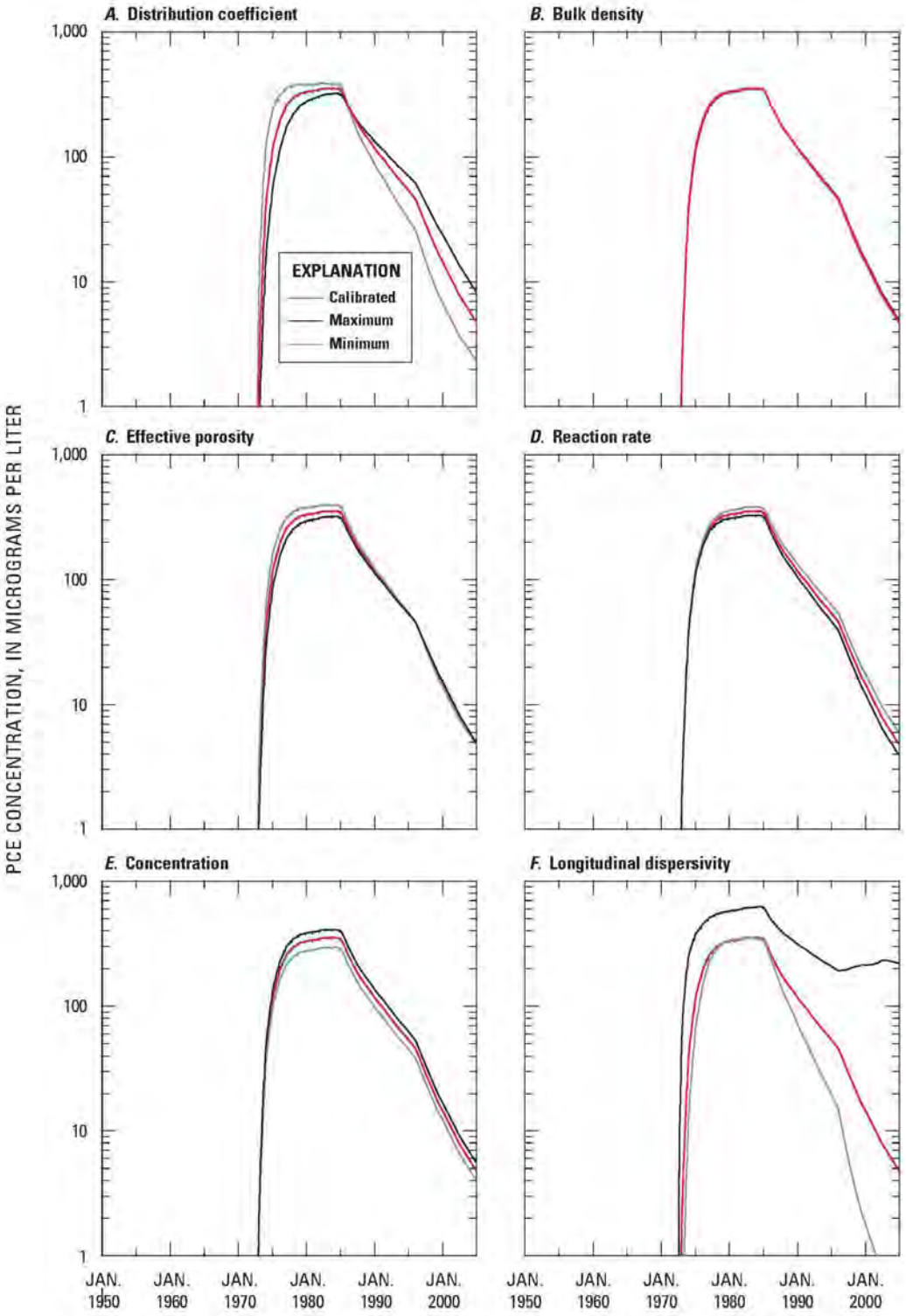

Figure S6.2.7. Tetrachloroethylene (PCE) concentrations at well HP-651 for calibrated value and minimum and maximum values of *(A)* distribution coefficient, K_d; *(B)* bulk density, ρ_b; *(C)* effective porosity, n_E; *(D)* reaction rate, r; *(E)* concentration, C; and *(F)* longitudinal dispersivity, α_L; Hadnot Point landfill area fate and transport model, Hadnot Point–Holcomb Boulevard study area, U.S. Marine Corps Base Camp Lejeune, North Carolina.

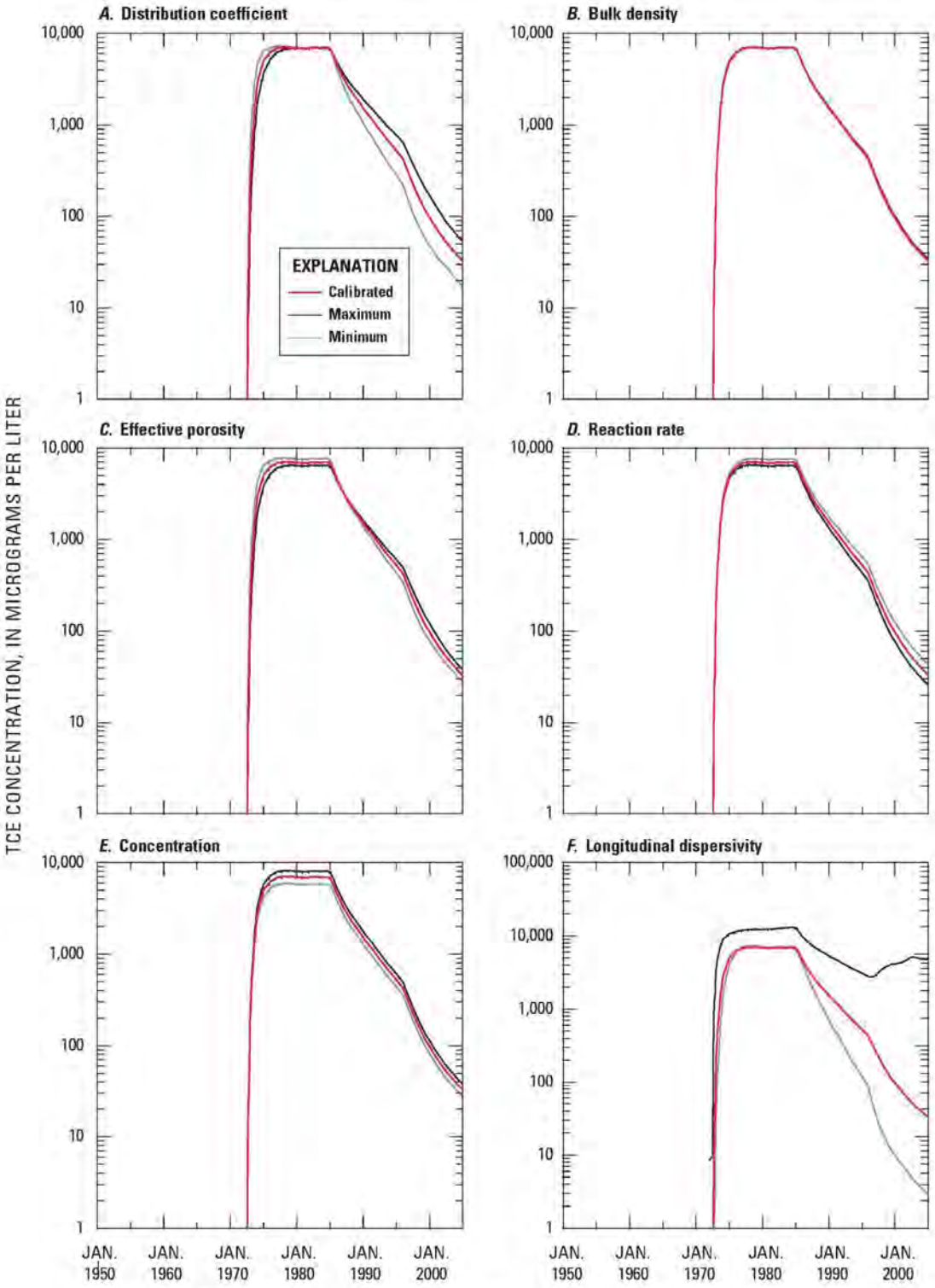

Figure S6.2.8. Trichloroethylene (TCE) concentrations at well HP-651 for calibrated value and minimum and maximum values of *(A)* distribution coefficient, K_d; *(B)* bulk density, ρ_b; *(C)* effective porosity, n_E; *(D)* reaction rate, r; *(E)* concentration, C; and *(F)* longitudinal dispersivitiy, α_L; Hadnot Point landfill area fate and transport model, Hadnot Point–Holcomb Boulevard study area, U.S. Marine Corps Base Camp Lejeune, North Carolina.

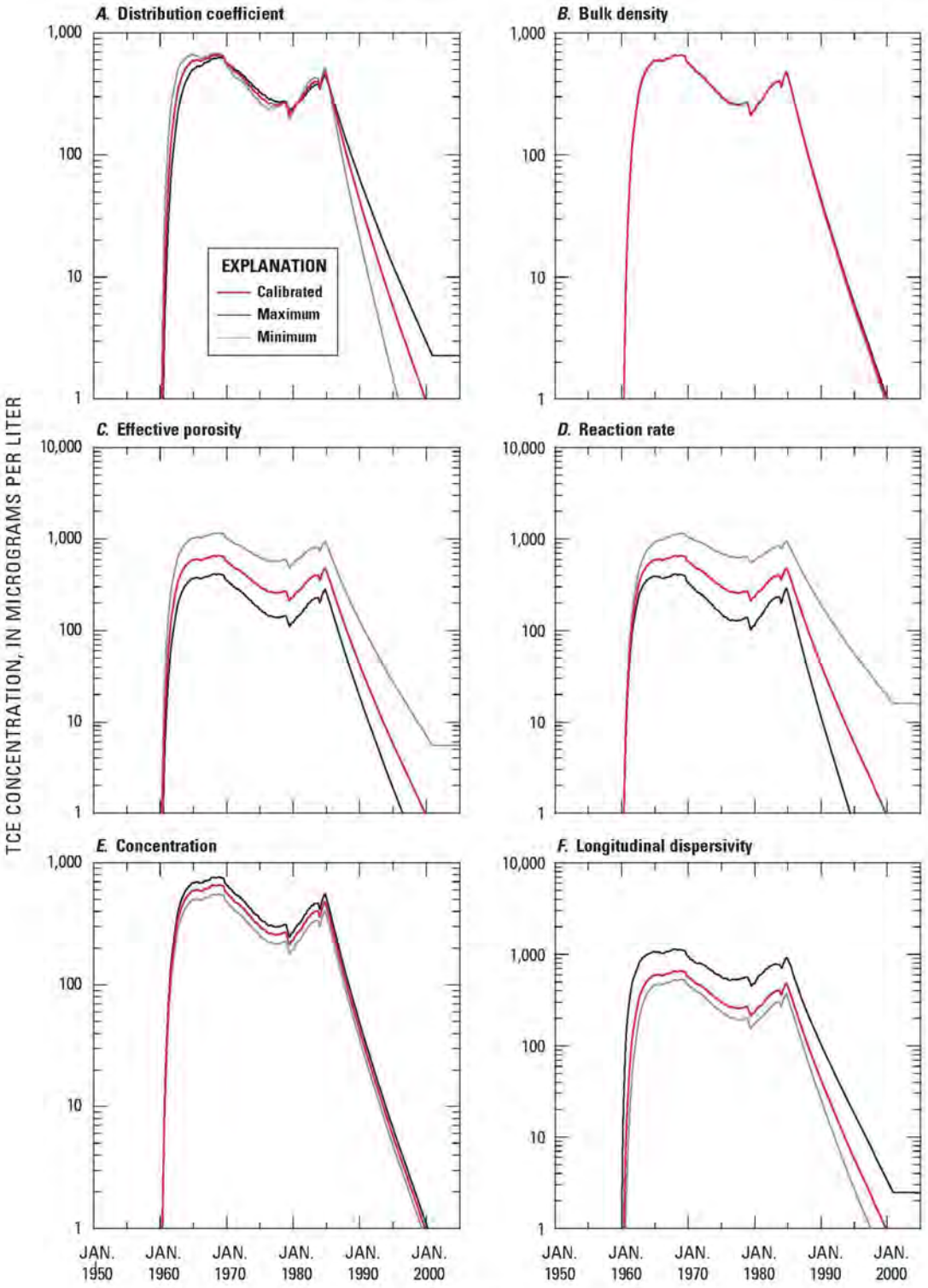

Figure S6.2.9. Trichloroethylene (TCE) concentrations at well HP-634 for calibrated value and minimum and maximum values of *(A)* distribution coefficient, K_d; *(B)* bulk density, ρ_b; *(C)* effective porosity, n_E; *(D)* reaction rate, r; *(E)* concentration, C; and *(F)* longitudinal dispersivity, α_L; Hadnot Point landfill area fate and transport model, Hadnot Point–Holcomb Boulevard study area, U.S. Marine Corps Base Camp Lejeune, North Carolina.

ATSDR
AGENCY FOR TOXIC SUBSTANCES AND DISEASE REGISTRY

Analyses and Historical Reconstruction of Groundwater Flow, Contaminant Fate and Transport, and Distribution of Drinking Water Within the Service Areas of the Hadnot Point and Holcomb Boulevard Water Treatment Plants and Vicinities, U.S. Marine Corps Base Camp Lejeune, North Carolina—Chapter A–Supplement 6: Characterization and Simulation of Fate and Transport of Selected Volatile Organic Compounds in the Vicinities of the Hadnot Point Industrial Area and Landfill